ISOPRENE FLUX MEASUREMENTS ABOVE A NORTHERN HARDWOOD FOREST

By

SHELLEY NOELLE PRESSLEY

A dissertation submitted in partial fulfillment of the
requirements for the degree of

DOCTOR OF PHILOSOPHY

WASHINGTON STATE UNIVERSITY
Department of Civil and Environmental Engineering

DECEMBER 2004

To the Faculty of Washington State University:

The members of the Committee appointed to examine the dissertation of SHELLEY NOELLE PRESSLEY find it satisfactory and recommend that it be accepted.

_____
Chair

_____

_____

_____

ACKNOWLEDGMENT

There have been so many people involved with this project that I would like to acknowledge, so please bear with me. First and foremost I would like to acknowledge the support and guidance of my primary advisor Dr. Brian Lamb, and the rest of the Civil and Environmental Engineering faculty that have been a part of my academic experience. Brian has provided excellent mentorship not only through his words, but also more importantly through his actions. Other advisors and committee members, Drs. Hal Westberg, George Mount, John Bassman, and Candis Claiborn, have all been instrumental in helping with my research and providing excellent teaching. Gene Allwine and Lee Bamesberger have both helped tremendously with my research, and instruments would have ceased to work without their expertise. Also, a great thanks to those that keep things running: Lola Gillespie, Tom Weber, Kathy Cox, Maureen Clausen, Larissa Morton, and Vicki Ruddick. Other WSU students that helped in front of the computer; Julia Flaherty and Jessica Aumanji; and Tara Strand and Susan O'Neill for providing the inspiration to run that extra mile or swim that extra 500 yards.

In addition to the support provided by WSU personnel, there have been numerous people involved with the NSF IGERT/BART program that I would like to acknowledge. My BART mentors Drs. Peter Curtis (Ohio State University) and Hans Peter Schmid (Indiana University) have both been very supportive and encouraging during the summer field seasons in Michigan. Drs. Diana Newman, David Karowe (Western Michigan University) and Steven Bertman (Western Michigan University) were instrumental in developing the BART program and pouring all of their energy into creating such a dynamic and wonderful experience. In addition to the BART personnel, I owe a huge

thanks to the great UMBS staff: Bob Vande Kopple, Michael Grant, Tony Sutterley, Sherry Webster, and again those in the front office that keep things running, Lisa Readmond and Diana Taylor. The one that I relied on the most during the field season (and still rely on for data) is Christoph Vogel, the UMBS~Flux expert. Others that helped tremendously during the field season include other BART students: Jennifer Hutton, Michael Reiskind, Alan Hogg, Lucas Neil, Doug Martins, and Erika Williams. Several Research Experience for Undergraduates (REU) students helped; especially Cheryl Gilbert and Grant Hatten.

Other researchers that were helpful during the field seasons include those involved with PROPHET. A special thanks to Troy Thornberry, Mark Lilly, Margaret Pippin, Mary Anne Carroll, Paul Shepson, and all the other Propheteers. Significant technical advice was also provided by Dr. Alan Hills of Hills Scientific, Inc.

Lastly, for the emotional support, I would like to thank my family and Dr. David White for continuing to stand by me.

ATTRIBUTION

The research presented in this dissertation is a result of the work completed during a 2-year fellowship called the biosphere-atmosphere research training (BART) under the National Science Foundation (NSF) integrated graduate education and research training (IGERT) program. Funding was also provided under the U.S. Environmental Protection Agency (USEPA) project entitled "Measurements and Modeling of Isoprene Fluxes in PROPHET 2000-01". Support for field measurements from 2000 through 2003 was also provided through an NSF grant (ATM-0074535).

The research contained in this dissertation is a compilation of many ideas, and data collection efforts from many people. Drs. Brian Lamb and Hal Westberg prepared the initial proposal for research to the USEPA, and Shelley Pressley, Drs. Brian Lamb, Hal Westberg, Hans Peter Schmid, and Peter Curtis prepared the NSF IGERT fellowship proposal.

This dissertation contains two separate manuscripts that have been submitted for publication. Multiple authors have contributed to both papers; however, S. Pressley is the primary author of both papers. S. Pressley was responsible for essentially all of the data analysis and had primary responsibility for operation of the field measurement system during 2000-2002. Christoph Vogel, Bob Vande Kopple, Alan Hogg, Lucas Neil, Jennifer Hutton, and Michael Reiskind provided invaluable on-site assistance with maintenance of the system during these years, while Brian Lamb, Hal Westberg, Gene Allwine, and Rae Hafer maintained the field measurement system in the years prior to 2000. Additional on-site support was also provided by two Research Experience for Undergraduate (REU) students: Grant Hatten (2000) and Cheryl Gilbert (2001). Various

equipment was borrowed for this research from several supporters including Dr. Pat Zimmerman, South Dakota School of Mines, and Alex Guenther, National Center for Atmospheric Research. Equipment and exceptional technical support was also provided by Dr. Alan Hills, Hills Scientific, Inc.

ISOPRENE FLUX MEASUREMENTS ABOVE A NORTHERN HARDWOOD FOREST

Abstract

By Shelley Noelle Pressley, PhD
Washington State University
December 2004

Chair: Brian Lamb

Long-term measurements of above canopy isoprene emissions are reported for a mixed hardwood forest in northern lower MI, USA. Eddy covariance techniques were used to obtain fluxes of sensible heat (H), latent heat (LE), momentum, CO_2, and isoprene. Results presented here include years 1999 – 2002. Measurements were made in collaboration with the AmeriFlux site located at the University of Michigan Biological Station (UMBS) and the Program for Research on Oxidants: PHotochemistry, Emissions and Transport (PROPHET). This work provides a unique long-term dataset useful for verifying canopy scale models and to help us better understand the dynamics of the biosphere atmosphere exchange of isoprene.

In general, isoprene emissions increased throughout the day with increasing temperature and light levels, peaked at mid-afternoon, and declined to zero by night. Average midday isoprene fluxes were 2.8, 3.2, and 2.9 mg C m^{-2} h^{-1} for 2000 through 2002 respectively. Last frost and full leaf out were significantly delayed in 2002 compared to the other years, however, total accumulated isoprene emissions for each year varied by less than 10%. Fully developed isoprene emissions occurred between 400 and

500 heating degree days, roughly half those required at other sites. Using long-term net ecosystem exchange measurements from the UMBS~Flux group, isoprene represents between 1.7 to 3.1% of the net carbon uptake at this site.

Seasonally averaged LE fluxes were reduced in 2000 as a result of reduced rainfall, and average isoprene fluxes were 1.5 times greater in 2000 compared to years 2001 and 2002. Daytime fluxes of isoprene and both H and LE flux were linearly correlated on a daily basis, but the slopes of these relationships varied from one day to the next. The strong correlation between isoprene fluxes and associated energy fluxes is an important relationship that should be accurately reflected in canopy models used for estimating biogenic emissions. Observations were compared with the BEIS3 emission model and to a canopy scale biogenic emission model (WSU-BEIS). Estimates of isoprene agree well with observations during the mid-summer period, but BEIS3 overestimates observations during the spring and the fall. Estimates of sensible heat flux with WSU-BEIS were larger than observed, and the estimates of LE were within approximately 50% of observations.

TABLE OF CONTENTS

LIST OF TABLES

CHAPTER 4

LIST OF FIGURES

LIST OF ABBREVIATIONS

ATI	Applied Technologies, Inc.
ATP	adenosine triphosphate
BART	Biosphere Atmosphere Research Training
BEIS	biogenic emission inventory system
BELD3	Biogenic Emissions Land cover Database (version 3)
BHC	biogenic hydrocarbon
BVOC	biogenic volatile organic compound
C	carbon
CH_4	methane
CH_2O	formaldehyde
C_L	light correction term
CMAQ	Community Multiscale Air Quality Modeling System
CO	carbon monoxide
CO_2	carbon dioxide
C_T	temperature correction term
C_5H_8	isoprene (2-methyl-1,3-butadiene)
d	zero-plane displacement height
°D	heating degree day
D	molecular diffusion
DMAPP	dimethylallyl pyrophosphate
DOE	U.S. Department of Energy
DOY	day of year
E	measured emission rate
Es	standard emission rate
F_{iso}	isoprene flux
FB	fractional bias
FE	fractional error
FIS	fast isoprene sensor
G	soil heat flux
GA-3-P	glyceraldehyde 3-phosphate
GLOBEIS	GLObal Biogenic Emissions and Interactions System
H	sensible heat flux
h_c	canopy height
H_2	hydrogen
H_2O	water
H_2O_2	hydrogen peroxide
HC	hydrocarbon
HCOCHO	glyoxal
HNO_3	nitric acid
HO_2	hydroperoxyl radical
Hz	hertz
ID	inside diameter
IGERT	Integrated graduate education and research training

IPP	isopentenyl pyrophosphate
IRGA	infrared gas analyzer
LAI	leaf area index
LE	latent heat flux
m	meter
mg	milligrams
M	mass
MACR	methacrolein
MB	mean bias
ME	mean error
MBO	2-methyl-3-buten-2-ol
MEP	2-deoxyxylulose 5-phosphate/2-methylerythritol 4-phosphate
MPAN	peroxy-methacrylic nitric anhydride
MVA	mevalonic acid
MVK	methyl vinyl ketone
NEE	net ecosystem exchange
NIGEC	National Institute for Global Environmental Change
NMHC	non-methane hydrocarbon
nmol	nanomol
NMSE	normalized mean square error
NO	nitric oxide
NO_2	nitrogen dioxide
NO_3	nitrate radical
NOx	nitric oxides (NO and NO_2)
NSF	National Science Foundation
OH	hydroxyl radical
OLS	ordinary least squares
O_2	oxygen
O_3	ozone
PAN	peroxyacetyl nitrate
PAR	photosynthetic active radiation
PMT	photomultiplier tube
PPN	peroxypropionic nitric anhydride
PROPHET	Program for Research: Oxidation, PHotochemistry, Emissions and Transport
PPFD	photosynthetic photon flux density
PpbC	part per billion carbon
ppbv	part per billion volume
ppmv	part per million volume
pptv	part per trillion volume
Q	additional energy sources and sinks
REA	relaxed eddy accumulation
REU	Research Experience for Undergraduates
RH	relative humidity
R_n	net radiation
RO	alkoxy radical

RO_2	alkyl peroxy radical
slpm	standard liters per minute
S	heat storage
SLW	specific leaf weight
SMOKE	Sparse Matrix Operator Kernel Emissions
Tg	terragram
u*	friction velocity
μmol	micromol
UMBS	University of Michigan Biological Station
USEPA	United States Environmental Protection Agency
VAI	vegetation area index
VOC	volatile organic compound
W	Watt
WSU	Washington State University
z	measurement height

CHAPTER 1

INTRODUCTION

1.1. Overview and Objectives

Why do plants spend energy and resources to produce the compound isoprene? This has been a question researchers have been asking for years. Isoprene (2-methyl-1,3-butadiene) is a reactive compound that is oxidized quickly in the atmosphere by the hydroxyl radical (OH), ozone (O_3) and, at night, by the nitrate radical (NO_3) (Fehsenfeld et al., 1992). The oxidation products can contribute to the formation of tropospheric ozone, and other photochemical smog constituents if the correct mix of NOx and sunlight are available (Andreae & Crutzen 1997). The large abundance of isoprene from natural sources, along with other biogenic emissions, easily outweighs any anthropogenic sources of volatile organic compounds (VOCs) on a global level (Guenther et al., 2000) and in many regions (Geron et al., 1994; Guenther et al., 1995). Thus, air pollution control strategies must be developed that take into account the role of isoprene and other biogenic emissions in ozone formation within and downwind of urban areas. Isoprene plays a critical role in the air quality of our troposphere, it is emitted from a vast and widespread source of vegetation, and we have little understanding about what ultimately controls the emission rate of isoprene.

In order to improve our understanding of isoprene emissions, measurements of isoprene fluxes above a northern hardwood forest were made using the eddy covariance technique. The site is located in the northern lower peninsula of Michigan at the University of Michigan Biological Station (UMBS). Multiple towers have been

constructed at this site including a 46-m AmeriFlux tower (Baldocchi et al., 2001) and a 31.5-m atmospheric chemistry tower used for the Program for Research on Oxidants, PHotochemistry, Emissions and Transport (PROPHET) (Carroll et al., 2001). Flux measurements of isoprene, CO_2, sensible heat (H), latent heat (LE), and momentum have been collected continuously during the summer growing seasons since 1999, with some limited flux measurements made in 1997 and 1998 (Westberg et al., 2001). The research summarized in this dissertation presents a description of the flux measurement data collection, post-processing and analyses of the long-term dataset. Seasonal and annual trends are presented and there is some comparison between the measurements and current biogenic emission inventory models.

Using the long-term dataset, there are several hypotheses we addressed in the following body of work. We hypothesize there are long-term controls on the emission of isoprene, such as historical temperatures, water stress, and seasonal "switches". Since the biosynthesis of isoprene is enzymatic and is dependent on precursor materials, increasing temperatures (over the past 3-5 days) should produce increased isoprene emissions. Similarly, drought stress can result in reduced latent heat fluxes, or a loss of cooling capacity, which in turn causes elevated leaf temperatures and increased isoprene emissions. Lastly, the delay between leaf emergence and isoprene emissions should be a function of cumulative degree-days, and based on previous studies should fall around 1000 °H (heating degree days). In addition, given the similarities of the biosphere drivers for both isoprene and energy fluxes, we hypothesize that correlations between these fluxes are consistent, and they could be a useful tool both for testing existing canopy emission models and to guide the development of improved isoprene emission models.

More specifically, we anticipate that canopy models, which accurately estimate energy fluxes, will perform better in predicting isoprene emissions, since they are inherently linked by environmental drivers (temperature and light) and canopy dynamics (turbulence and transport of mass and energy).

The primary objectives of this research are to improve our ability to model isoprene emissions and fate in the atmosphere. The primary approach for this objective involves making long-term isoprene flux measurements above the forest canopy using eddy covariance techniques, and using the long-term dataset to better understand specific aspects of isoprene emissions. The specific objectives include; 1) analyzing the multi-year dataset for seasonal and/or annual trends of isoprene emissions; 2) analyzing multiple datasets (AmeriFlux, PROPHET) in order to better understand biological/environmental conditions that may affect isoprene emissions; 3) evaluating current emission inventory models; and 4) determining the correlation between isoprene and associated energy fluxes and using this to improve current canopy scale models.

The dissertation is divided into five chapters. The Introduction chapter provides a summary of some of the most recent research in this field, providing a brief overview of biogenic hydrocarbons with an emphasis on isoprene. The second chapter, Experimental Methods and Materials, provides the details regarding the collection, processing and analysis of the dataset. The next two chapters are manuscripts that have been submitted for publication. The first manuscript entitled "Long term Isoprene Flux Measurements Above a Northern Hardwood Forest" presents the long-term dataset along with seasonal and annual trends of isoprene fluxes, H and LE. This manuscript was submitted to Journal of Geophysical Research and it is currently in review. The fourth chapter is a

manuscript entitled "Relationships among canopy scale energy fluxes and isoprene flux using eddy covariance measurements over multiple growing seasons". This manuscript was submitted and accepted to Agricultural and Forest Meteorology as part of a special edition in remembrance of the late Marv Wesely. The version included in this dissertation is the final draft and it is currently in press. Lastly chapter five contains a brief summary and some discussion on the "lessons learned" during this research. A supplemental CD contains some of the details such as source codes for data acquisition and processing, the entire dataset (the 30-minute averaged fluxes), logbook notes and calibration data.

1.2. Tropospheric Chemistry of Isoprene

Primary emission of isoprene has no known adverse health effects, however, this short-lived and highly reactive volatile is an important factor in controlling the chemistry of the troposphere (Fehsenfeld et al., 1992; Paulson et al., 1990; Monson & Holland 2001). Isoprene contains an olefinic double bond that makes the compound very reactive in the atmosphere and easily oxidized by OH, O_3, or NO_3 (Seinfeld and Pandis, 1998). This leads to the production of peroxy radicals (RO_2), which may lead to the formation of organic acids, or depending on the level of nitric oxides present, to either production or consumption of tropospheric O_3 (Brasseur et al., 1999; Fehsenfeld et al., 1992; Atkinson 2000). Overall, since isoprene is one of the more reactive biogenic VOCs (BVOCs), isoprene plays an important role in regulating the oxidative capacity of the troposphere, which in turn determines the lifetime of numerous atmospheric constituents such as

methane (CH_4) and CO. By increasing the lifetimes of greenhouse gases such as CH_4, isoprene emissions may potentially influence the global climate (Constable et al., 1999). In fact, work by Collins et al., (2002) has shown that isoprene has a positive secondary global warming potential. Lastly, the emissions of biogenic VOCs also affect the spatial distribution of NOx and its transport and deposition to remote areas (Monson & Holland 2001).

Some of the earliest work done in this area is the well-known paper by Went (1960) entitled "Blue Hazes in the Atmosphere". Went proposed that the blue haze seen in areas such as the Great Smoky Mountains is caused by natural hydrocarbon emissions and not anthropogenic emissions. This hypothesis along with Haagen-Smit's (1952) work touched off study of biogenic hydrocarbons (BHCs) that is still ongoing today. It became apparent that the role BHCs play in tropospheric chemistry is very complex and very important.

1.2.1. Isoprene Chemistry Details

The production of excess O_3 in the troposphere requires NOx, VOCs, and sunlight. Under normal atmospheric conditions, the photodecomposition of NO_2 creates O_3 (equations 1 and 2), and the cycle is balanced because NO and O_3 react to regenerate NO_2 (equation 3):

$$NO_2 + h\nu \rightarrow NO + O(^3P) \quad (1)$$

$$O(^3P) + O_2 + M \rightarrow O_3 + M \quad (2)$$

$$NO + O_3 \rightarrow NO_2 + O_2 \quad (3)$$

However, if NO can be converted to NO_2 without scavenging O_3, excess O_3 will be generated. The conversion of NO to NO_2 can occur with biogenic VOCs as the fuel, as illustrated in the following equations:

$$VOC + OH + O_2 \rightarrow RO_2 + \text{residual products} \quad (4)$$

$$RO_2 + NO \rightarrow NO_2 + RO \quad (5)$$

$$RO + O_2 \rightarrow HO_2 + \text{aldehyde} \quad (6)$$

$$HO_2 + NO \rightarrow NO + OH \quad (7)$$

The primary removal pathway for isoprene emitted into the atmosphere is oxidation by the OH radical (equation 4), but similar reactions can occur by O_3 and NO_3 oxidation. Various recent reviews describe in great detail the reaction pathways for the degradation of the VOCs, both biogenic and anthropogenic (Atkinson 1997; Atkinson 2000; Finlayson-Pitts and Pitts 2000). Equations 4-7 show the generalized reaction pathway for VOCs in the troposphere, where the important intermediate products are alkyl radicals (R·), which quickly combine with O_2 to form alkyl peroxy radicals ($RO\cdot_2$), and alkoxy radicals (RO·) (Atkinson 2000). Specifically for isoprene, the major reaction pathway is radical addition by OH to a carbon atom of either carbon-carbon-double bond.

Atmospheres with low NOx levels (typically less than 5-10 pptv) are termed "clean" atmospheres, and those with significant NOx (in the ppb range) are termed "dirty" (Finlayson-Pitts and Pitts 2000). The rates of reactions are related to the concentration of NOx in a very complex manner. When NOx is low, nitric acid (HNO_3) and hydrogen peroxide are formed, both important in acid rain formation (Gaffney &

Marley 1991). However, when NOx levels are high, the reaction steps outlined above occur creating excess O_3. The formation of O_3 is a very nonlinear process that is a function of the (HC/NOx) ratio, temperature, and sunlight, (Fehsenfeld et al., 1992; Logan 1985).

Other isoprene oxidation products include organic nitrates, (i.e. peroxyacetyl nitrate (PAN), peroxymethacryloyl nitrate (MPAN)), methyl vinyl ketone (MVK), methacrolein (MACR), formaldehyde (CH_2O), and HO_2. Organic nitrates are less reactive than the other HCs, thus they act to sequester NOx and transport it to other regions. One of the better-understood organic nitrates, PAN, is an organic reservoir of reactive nitrogen, which is very stable in cold air masses but quickly decomposes in warmer environments. The transport of PAN to "clean" areas accounts for a substantial portion of nitrogen in rural environments that can react with HCs to form O_3 (Atherton & Penner 1990). The intermediate compounds MVK and MACR are typically oxidized to form formaldehyde, which is then either quickly photo-dissociated or oxidized by OH, producing CO, HO_2 radicals, and H_2 (Finlayson-Pitts and Pitts 2000). Carbon monoxide plays an important role in the atmosphere by controlling the oxidative capacity of the atmosphere, thus acting indirectly as a greenhouse gas. CO does not absorb significantly in the infrared spectra like other greenhouse gases, but it is a sink for the OH radical and therefore it affects the atmospheric CH_4 concentration. Increased CO levels reduce the OH levels which increases levels of the greenhouse gas CH_4 (Daniel & Solomon 1998). As previously mentioned, HO_2 is a precursor for H_2O_2 and RO_2H which also play an important role in the oxidant balance. Lastly, the formation of secondary aerosols specifically from isoprene emissions is negligible (Pandis et al., 1991).

1.2.2. Atmospheric Lifetime of Isoprene

A considerable number of smog chamber studies have been conducted to determine rate constants for the oxidation of isoprene with photochemical oxidants and to investigate the products of the oxidation reactions (for example, Juuti et al., 1990; Hoffmann et al., 1997). Atmospheric concentrations of OH can vary depending on solar radiation, local meteorological conditions, latitude, and season. Ozone, on the other hand, varies less with changes in the environmental parameters than OH (Altshuller 1983). For typical tropospheric daylight concentrations, isoprene will react more rapidly with OH than with O_3. Isoprene also has a relatively large rate constant, therefore, isoprene emissions are not transported great distances (Calvert & Madronich 1987).

By combining the rate constant with measured or estimated ambient tropospheric concentrations of the reactants, tropospheric lifetimes for the reaction processes can be derived. Table 1.1 presents lifetimes for isoprene, and for comparison two monoterpenes, and some oxidation products (Atkinson & Arey 1998; Atkinson 2000). These lifetimes were determined assuming average concentrations (as listed in the table) for each of the reactants, (OH, O_3, and NO_3) which are typical of a relatively clean atmosphere for OH and O_3, however, the NO_3 concentrations presented are typical of an urban area. Table 1.1 indicates the oxidation of isoprene by the OH radical as the major pathway of reaction during the daylight hours.

1.2.3. Ambient Measurements of Isoprene

Some of the confusion regarding the importance of BHCs in tropospheric chemistry is due to the fact that ambient levels of BHCs rarely exceed 5% of the total non-methane hydrocarbon (NMHC) level, even in rural, heavily forested areas (Arnts &

Meeks 1981). Therefore, many researchers have concluded that the BHCs do not contribute significantly to the formation of O_3 or aerosols in the troposphere (Altshuller 1983; Arnts & Meeks 1981). However, understanding their photochemical reactions and relative reactivities is necessary in order to understand their potential impact upon ambient air quality. Reaction rates for the specific BHCs and anthropogenic hydrocarbons are different and each compound can interact differently with the local environment.

Ambient concentrations of BHCs and their primary and secondary oxidation products have been measured at a variety of sites such as forests, croplands, and grasslands. Ambient concentrations of isoprene ranged from 0 to more than 30 ppbv during the day above a central Pennsylvania deciduous forest, with midday isoprene levels typically between 5-10 ppbv (Martin et al., 1991). In northern Italy, average monthly concentrations of isoprene, MACR, and MVK ranged from 10 ppbC in June, July and September to 20 ppbC in August, with maximum concentrations of isoprene reaching up to 70 ppbC (Duane et al., 2002). Limited measurements have been made in the tropics, but Kuhn et al., (2002) made some measurements during the wet season in the forests of Brazil. They saw ambient isoprene concentrations peak at 8 ppbv inside the forested canopy. Lastly, airborne measurements of isoprene and oxidation products can be used for monitoring biogenics. Williams et al., (1997) made some of the first measurements of peroxy-methacrylic nitric anhydride (MPAN), PAN, and peroxypropionic nitric anhydride (PPN), all products formed from isoprene-NOx photochemistry. Measurements were made over the central and southeastern U.S., where

background levels of PAN were measured at 325 pptv, and maximum levels reached near 5000 pptv.

1.3. Biosynthetic Pathways for Isoprene

The biosynthesis of isoprenoids occurs in plant organelles, or plastids, and it originates with the production of 5-carbon building blocks called isopentenyl pyrophosphate (IPP) (Figure 1.1). It was thought that IPP and its isomer dimethylallyl pyrophosphate (DMAPP) were derived from the well-known mevalonic acid (MVA) pathway (McGarvey & Croteau 1995). However, recent research with ^{13}C labeled glucose has shown that higher plants have two distinct routes for the biosynthesis of DMAPP; the MVA pathway and the 2-deoxyxylulose 5-phosphate/2-methylerythritol 4-phosphate (MEP) pathway (Lichtenthaler et al., 1997). In the MEP route, DMAPP is formed from glyceraldehyde 3-phosphate and pyruvate, as opposed to the mevalonate precursor (Sharkey & Yeh 2001). The mevalonate-independent isoprenoids (such as isoprene, carotenoids, and phytol) are those formed in the chloroplasts. Sesquiterpenes and triterpenes are synthesized from mevalonic acid in nonplastid compartments and isoprene, monoterpenes, phytol (C_{20}) and carotenoids (C_{40}) are synthesized from IPP generated from the MEP pathway (Lichtenthaler et al., 1997; Zeidler et al., 1997). The IPP is isomerized into DMAPP, which is the precursor for the synthesis of isoprene; however, this pathway is not well understood. The final step of isoprene synthesis is the elimination of pyrophosphate from DMAPP by the enzyme isoprene synthase (Silver & Fall 1991; Wildermuth & Fall 1996). Research recently has focused on understanding

the isoprene synthase, and it appears to be a membrane bound, light activated enzyme. In addition, changes with its activity are correlated with changes in isoprene emission (Kuzma & Fall 1993; Monson et al., 1992). This light activated enzyme is one of the reasons that light is a primary factor in controlling isoprene emissions.

It is known that ATP, produced during photosynthesis, is required for the synthesis of isoprene (Monson & Fall 1989). This agrees well with the experimental evidence that isoprene production (and emission) is closely linked to photosynthesis (Tingey et al., 1979; Monson & Fall 1989; Loreto & Sharkey 1990). With a better understanding of the biosynthetic pathway, the energy cost associated with isoprene emission can be determined. Sharkey and Yeh (2001) report that the MEP pathway is more efficient than the MVA pathway, but it is still substantial, and benefits associated with isoprene emission must be compared to the cost of carbon and energy given up by the plant.

1.4. Requirements for Isoprene Synthesis

The discovery of the MEP pathway for isoprene has resolved some inconsistencies in the literature when it was assumed that all isoprene biosynthesis occurred in the MVA pathway. For example, inhibitors used to block the MVA pathway did not block the production of isoprene (Bach & Lichtenthaler 1983). The discovery of the light activated isoprene synthase and its link with isoprene emissions indicates that isoprene emissions are not related to volatility (like monoterpene emissions) but rather to its metabolism (Sharkey & Yeh 2001). Thus, the primary requirements for isoprene

synthesis are light, warm temperatures, and availability of MEP pathway precursors from photosynthetic processes.

1.4.1. Temperature and light

Isoprene emissions clearly depend on both light and temperature (Tingey et al., 1979; Tingey et al., 1981; Monson & Fall 1989; Karl et al., 2001; Monson et al., 1992). The effects due to temperature are enzymatic, and two distinct phases can be observed in the increase of isoprene emissions. For small rate changes in temperature, the isoprene emission changes as quickly as the leaf temperature changes (average time constant of 8.2 s). For larger rate changes, the plant must make metabolic adjustments and activate enzymes to increase isoprene emissions, all of which occur with a time constant of 116 s (Singsaas & Sharkey 1998; Singsaas & Sharkey 2000).

Not only have short-term effects of temperature and light intensity on isoprene emission rates been observed, but also leaves that develop in full sun emit isoprene at a higher rate than leaves that develop in the shade (Sharkey et al., 1991; Sharkey et al., 1996; Harley et al., 1994; Harley et al., 1997). For example, isoprene emissions measured in a deciduous oak canopy at two heights were significantly higher for sun leaves compared to shade leaves when expressed on a leaf area basis (51 versus 31 nmol m^{-2} s^{-1}; $P < 0.01$) (Harley et al., 1997). Recent studies have shown that the light and/or temperature environment over several days can influence the isoprene emission rate (Sharkey et al., 1999; Geron et al., 2000; Petron et al., 2001). One approach to characterizing these variations in isoprene emissions is to determine emissions as a function of thermal degree units (Monson et al., 1995; Fuentes et al., 1999; Geron et al., 2000; Hakola et al., 2000).

However, the dependence on temperature is very different for isoprene emissions versus photosynthesis. A maximum photosynthesis rate for most C3 plants occurs around 30°C (Sharkey & Yeh 2001), whereas isoprene emissions continue at temperatures above 30°C. Most plants studied cease to emit isoprene at temperatures above approximately 40°C where it is assumed that biosynthetic enzymes are denatured (Guenther et al., 1993; Lerdau & Keller 1997; Fall 1999). Another effect of this temperature dependence is the ratio of fixed carbon emitted as isoprene increases rapidly with temperature, in particular with temperatures above 30°C (Sharkey et al., 1996).

1.4.2. Photosynthesis

The two primary environmental controls on the emission of isoprene are temperature and light. Light is important because it drives photosynthesis, which is the supplier of precursor materials. So the increase in the rate of isoprene emission is caused by either of these two effects or some combination of the two (Monson et al., 1995; Wildermuth & Fall 1996). Early researchers determined the light saturation point for isoprene emissions is very similar to the light saturation point for photosynthesis (Rasmussen 1973), however, in some cases isoprene emissions will continue with increased light intensity above the photosynthetic saturation point (Harley et al., 1996; Lerdau & Keller 1997; Sharkey & Loreto 1993). Plants do have the capability to draw on carbon reserves for isoprene production. This has been shown to happen during long-term drought stress where photosynthesis shuts down, stomata are closed; yet isoprene continues to be produced (Sharkey & Loreto 1993; Loreto & Sharkey 1993).

However, there are cases where isoprene emissions do not follow photosynthesis rates closely. For example, the temperature dependencies of photosynthesis and isoprene

emission are different (Monson et al., 1992), and in newly emerging leaves the developmental onset of photosynthesis and isoprene emissions are different (Grinspoon et al., 1991; Sharkey & Loreto 1993; Harley et al., 1994; Monson et al., 1994).

1.5. Benefits of Isoprene Production

The function of isoprene is still not completely understood. Although isoprene synthesis is typically 2% of photosynthesis, it is by far the dominant product of the MEP pathway with carotenoid synthesis only accounting for 0.02% of photosynthesis (Schulze-Siebert et al., 1987). So why do plants spend energy to produce isoprene? Theories include thermotolerance, protection from oxidants, and as a means to shunt excess carbon.

1.5.1. Thermotolerance

Research within the past 10 years indicates that isoprene may serve to protect the leaf and plant during high heat episodes (Sharkey 1996; Singsaas et al., 1997). It is known that with isoprene present there is less damage to the intercellular membranes during short high-temperature episodes (Singsaas et al., 1999; Singsaas & Sharkey 1998; Sharkey et al., 2001; Loreto et al., 1998), but the way in which isoprene protects the leaf is not well understood. The thylakoid membranes, which surround the chloroplast structures, are known to become leaky at moderately high temperatures (Bukhov et al., 1999; Pastenes & Horton 1996). Since isoprene is hydrophobic, it is capable of partitioning into the interior layers of the thylakoid membrane (Logan & Monson 1999),

thus protecting the membranes from denaturing by either enhancing hydrophobic interactions within the thylakoid, or due to the large size of the C-C double bonds blocking the formation of water channels. Other ideas also include enhancing hydrophobic interactions within protein complexes, such as the photosystem II, in order to prevent fragmentation or separation into non-bilayer structures (Gounaris et al., 1984). Regardless of the mechanism, the thermotolerance affects may serve as a defense against climate warming (Penuelas & Llusia 2003).

1.5.2. Anti-oxidant

Chamber studies have shown that in leaves where isoprene was inhibited by fosmidomycin, photosynthesis, stomatal conductance, and chloroplast fluorescence parameters were significantly affected by ozone. Exogenous isoprene (i.e. isoprene not produced by the leaf) offered protection to the leaf that was more evident during long time (8 hours) and low (100 ppb) ozone levels then with short (3 hours) and acute (300 ppb) ozone levels (Loreto & Velikova 2001). But is the protection by radical quenching, or membrane strengthening, similar to that explained in the thermotolerance theory? Ozone can damage plant materials by directly inducing stomatal closure (Heath 1994) and ozone can reduce either the amount or the activity of Rubisco, which lowers the carboxylation efficiency and therefore photosynthesis (Farage et al., 1991; Pell et al., 1994; Pell et al., 1997). In addition, ozone can react rapidly with cellular structures creating toxic active oxygen species (O_2•, OH•, H_2O_2) that cause peroxidation and denaturation of membrane lipids. However, according to Loreto and Velikova (2001), more oxidative products were formed when isoprene was not present, thus isoprene stabilizes the membrane lipid bilayer by quenching oxidative products (in particular

H_2O_2). Contrary to this theory, since isoprene reacts so quickly with O_3 and OH radicals, it is thought that isoprene propagates radicals instead of quenching them because isoprene-emitting plants were found to be more sensitive to ozone damage due to the formation of hydroperoxides on the plants (Hewitt et al., 1990; Stokes et al., 1998).

1.5.3. Pathway to shunt excess carbon

Another theory that has been proposed, however it is very unlikely, is that isoprene acts as a safety valve to release excess carbon and energy (Logan et al., 2000). The problem with this theory is that the amount of energy lost through the production of isoprene is very small. In addition, plants already have a mechanism of deactivating Rubisco to more effectively handle situations of excess carbon.

1.6. Regulation of Isoprene Emissions

The role of factors other than temperature or light in the control of BHC emissions is very complex. Laboratory and field studies have been conducted to measure relationships between BHC emissions and a multitude of environmental and physiological effects such as plant water stress, relative humidity, leaf nitrogen levels, ambient ozone and carbon dioxide concentrations, wounding/needle damage, etc. As Penuelas and Llusia (2001) point out, there is considerable complexity in the interactions and the different responses to these factors that can control the emission rate of isoprene.

1.6.1. Environmental Controls

Environmental conditions control the plant's ability to acquire important nutrients such as water and nitrogen. The effects of nitrogen and water limitations on isoprene emissions have been studied, with most of the work being conducted in greenhouse studies. The impact of water stress is difficult to quantify because even though isoprene emissions are reduced when water is scarce (Lerdau & Keller 1997; Fang et al., 1996; Sharkey & Loreto 1993), transpiration is also reduced causing the leaf temperature to rise. And when leaf temperature rises, isoprene emissions increase (Singsaas et al., 1997). The correlation of isoprene emissions and leaf nitrogen levels were observed to be different during various stages of development. During the initial leaf development stage, isoprene emission rates were negatively correlated with leaf nitrogen concentrations, however, during the autumnal decline in isoprene emissions they were positively correlated (Litvak et al., 1996).

1.6.2. Biological controls

Other biological parameters that have a strong influence on isoprene emission rate include plant taxon, ontogeny, and growth history. At the leaf level, the capacity to emit isoprene is arbitrarily standardized by the rate of emission at 30°C and 1000 μmol m^{-2} s^{-1} photosynthetic active radiation (PAR). This is typically referred to as the basal emission rate, and it does vary based on species. The variation in isoprene emissions primarily occurs at the genera level, and there appears to be no real taxonomic pattern (Harley et al., 1999). Developmental stage of the leaf also affects the isoprene emission rate. Isoprene emission rates are delayed from bud break for up to 2 - 4 weeks in some cases, and most plants do not reach their basal emission rates until full leaf development and

expansion (Monson et al., 1994; Fuentes et al., 1999). Growth history refers to the developmental environment for a specific leaf, such as predominantly shade vs. full sun. As previously stated, leaves that develop in full sun emit isoprene at a higher rate than leaves that develop in the shade (Sharkey et al., 1991; Harley et al., 1994; Harley et al., 1997).

1.7. Emission algorithms

A leaf emission algorithm contains two parts: a mean or standard emission rate at a standard set of environmental conditions, and variations of the standard emission rate due to changes in environmental conditions (Guenther et al., 1991). Thus, mathematically, the instantaneous emission is the product of the standard emission rate and a correction factor that takes into account the prevailing environmental conditions.

Early attempts to model isoprene emission rates utilized an environmental control chamber to generate algorithms relating isoprene emissions to temperature and light intensities (Tingey et al., 1979). Since temperature and light effects were interdependent, Tingey and co-workers developed temperature dependent equations at four temperatures and light dependent equations at four different light intensities. The two sets of equations were inconsistent (depending on which set was used), and they were difficult to use at intermediate light and temperature levels (Guenther et al., 1991).

The initial work by Tingey et al., (1979) was simplified by Guenther et al., (1991), and two new correction terms were introduced into the isoprene emission algorithm. The light correction factor C_L, and the temperature correction factor C_T. In

addition to light and temperature, there were also correction terms for relative humidity and CO_2 concentrations. After a review of reported measurements, Guenther et al., (1993) simplified the isoprene emission equation even further by removing the RH and CO_2 terms. The result was equation (8), which is commonly used by researchers to standardize measured emission rates. For isoprene, the emission algorithm relates a measured emission rate to a standardized emission rate as a function of both temperature and light levels.

$$E = E_s \times C_T \times C_L \,, \tag{8}$$

In equation 8, E is the isoprene emission rate at temperature T and PAR, E_s is the standardized emission rate at standard temperature T_s (30°C) and PAR (1000 $\mu molm^{-2}s^{-1}$), and the scaling factors for light (C_L) and temperature (C_T) are defined by:

$$C_L = \frac{\alpha \times C_{L1} \times PAR}{\sqrt{1 + \alpha^2 \times PAR^2}} \; and \; C_T = \frac{\exp(C_{T1} \times (T - T_s)/(R \times T \times T_s))}{1 + \exp(C_{T2} \times (T - T_m)/(R \times T \times T_s))}\,, \tag{9}$$

where R is the gas constant (8.314 $JK^{-1}mol^{-1}$) and C_{T1} (95,000 $Jmol^{-1}$), C_{T2} (230,000 $Jmol^{-1}$), T_m (314 K or 41°C), α (0.0027) and C_{L1} (1.066) are empirical parameters derived from measurements on four isoprene emitting species; eucalyptus, sweet gum, aspen, and velvet bean (Guenther et al., 1993). The scaling factor for light (C_L) is similar to equations used to model the light dependency of photosynthesis and the scaling factor for

temperature (C_T) simulates the temperature response of enzymatic activity (Farquhar et al., 1980).

1.8. Biogenic Emission Inventories

Photochemical models used to predict tropospheric O_3 concentrations, particulate matter (PM), and other atmospheric pollutants require accurate estimates of biogenic emissions. The effects of biogenic emissions on regional pollution were initially explored in early studies by Trainer et al., (1987) and Pierce et al., (1998). More recently Hanna et al., (2001) showed that for the UAM-V photochemical model, biogenic VOCs ranked 6th out of 128 input variables that have significant correlations with predicted ozone concentrations. Jiang et al., (2003) showed that for the Puget Sound area of Washington state, isoprene was the 2nd most important VOC in terms of contribution to the peak ozone formed downwind during a specific episode. This is a somewhat surprising result given the abundance of conifer species in this region and the relatively sparse distribution of aspens, poplars and other isoprene emitting vegetation. However, it highlights the fact that isoprene is emitted in large amounts by aspens compared to the emission of monoterpenes from conifers, and it highlights the highly reactive nature of isoprene in the atmosphere. Work by Poisson et al., (2000) involving a global, three-dimensional chemistry transport model with detailed NMHC oxidation chemistry was used to quantify the impacts of NMHC emissions on tropospheric chemistry. Results indicate that NMHC oxidation contributes 40-60% additional CO to the surface layer over the continents; it almost doubles the net photochemical production of O_3 in the

troposphere with even higher O_3 concentrations in NOx-rich areas; and as a result of changes to the OH concentration, the tropospheric lifetime of CH_4 is increased by 15%. Similar findings indicating that NMHCs have the potential to markedly influence atmospheric photochemistry can be found in the following papers: Wang & Shallcross 2000; Houweling et al., 1998; Roelofs & Lelieveld 2000.

1.8.1. Development of BEIS

In the late '80s and early '90s the research and regulatory community developed the biogenic emission inventory system (BEIS) in order to quantify emissions at appropriate spatial and temporal resolution for input into models of atmospheric chemistry (Pierce & Waldruff 1991), and there have been steady improvements of the models over the last 15 years. For any biogenic emission model there are three components; 1) a land use dataset (Kinnee et al., 1997), 2) standard emission rates, or emission factors, for each land use category, and 3) algorithms to adjust the emissions to ambient environmental conditions (Guenther et al., 2000). In BEIS1, a simple scaled canopy model was employed to calculate leaf/needle temperatures within the canopy and emission algorithms were employed as a function of height within the canopy. In BEIS2, the canopy model was dropped, but light levels were attenuated as a function of height within the canopy. With BEIS1, emissions were calculated for isoprene, the sum of monoterpenes, and other VOCs. These were calculated for three forest types, several non-forested ecosystems, and a range of agricultural crops (Lamb et al., 1987; Lamb et al., 1993; Pierce & Waldruff 1991). In BEIS2, the same chemical species were estimated, but emissions were calculated using individual emission rate factors for approximately 40 different vegetation classes at the tree genus level (Geron et al., 1994).

The difference between BEIS1 and BEIS2 was significant, with isoprene emissions increased by a factor of 5 (Pierce et al., 1998).

Inaccurate land use and species composition data were determined to be a large source of uncertainty in the model results, and consequently, BEIS3 was released using the Biogenic Emissions Land cover Database version 3 (BELD3) for the entire United States. The BELD3 database resolves forest canopy coverage by tree species and it incorporates 1-km horizontal resolution for 230 different land use types. In addition, BEIS3 has been implemented into the Sparse Matrix Operator Kernel Emissions (SMOKE) model (Pierce et al., 2002) and the Community Multiscale Air quality Modeling System (CMAQ) (Pierce et al., 2002). Additional improvements over BEIS2 include normalized emission factors for 34 chemical species (including 14 monoterpenes and methanol), a soil nitric oxide (NOx) emissions algorithm that accounts for soil moisture, canopy coverage, and fertilizer applications, and lastly the chemical speciation algorithms for the CBIV, RADM2, and SAPRC99 chemical mechanisms, which are some of the most widely used chemical mechanisms in air quality modelling (Pierce et al., 2002).

Inputs for the BEIS3 model include spatially and temporally resolved meteorological data including temperature, incoming short wave radiation, and surface pressure. Other necessary inputs (which are included with BEIS3) are spatially resolved species-specific vegetation, species-specific biogenic emissions factors, and leaf area index (LAI). Emissions factors are the species-specific and compound specific standard flux-rates that are emitted under standard environmental conditions of 30°C and 1000 μmol m^{-2} s^{-1} PAR. For each of the 230-land use types in the BELD3 database, emission

factors exist for isoprene, monoterpene, NOx and other VOCs. LAI is used to adjust the isoprene emissions for the attenuation of PAR through the leaf canopy, but there is no adjustment currently in BEIS3 for the change in temperature through the canopy (Pierce et al., 2002).

Biogenic processing within SMOKE is a true simulation model, which is driven by the ambient meteorology (SMOKE user's manual, 2003). Beginning with the land use data, normalized emissions for each grid cell and land use category are computed. Next the normalized emissions are adjusted based on gridded, hourly meteorology data, and lastly the chemical species are classified into the appropriate profile depending on the chosen chemical mechanism (SMOKE user's manual, 2003).

A more complex and flexible modeling framework referred to as GLObal Biogenic Emissions and Interactions System (GLOBEIS) allows the user to select individual model components and to treat the canopy as a series of layers that each have different light and temperature environments (Guenther et al., 1999; Guenther et al., 2000). Input parameters for GLOBEIS are more extensive than BEIS3, including above-canopy temperature, radiation, wind speed, and relative humidity (RH). The above canopy parameters of temperature, RH, and wind speed are scaled for each layer using simple functions (Lamb et al., 1993). Radiation is attenuated through the canopy using a model described in Guenther et al., (1995) with the exception that the average diffuse radiation is attenuated through the canopy as an exponential function of LAI.

A comparison between GLOBEIS, BEIS2, and BEIS revealed that total predicted annual US fluxes of NMHCs were within 15% of each other, however, the temporal and spatial emission rates can vary by more than a factor of 5 (Guenther et al., 2000). In the

most recent climate modeling systems, biogenic emission models are dynamic in nature and are truly coupled land surface-atmosphere models. BVOCs are calculated within a land surface and dynamic vegetation model that simulates physiological processes that affect BVOC emissions (Levis et al., 2003). The land surface model then operates as a component of a climate system model that includes atmosphere (atmospheric chemistry and transport included), ocean, and sea ice components. Coupling processes are favored in particular when nonlinear interactions are involved (i.e. isoprene emissions, or tropospheric chemical reactions), when surface characteristics change (i.e. vegetation) (Levis et al., 2003) and when one is interested in climate feedbacks, which could significantly affect isoprene emissions (Wang & Shallcross 2000).

1.8.2. Model Results

Using biogenic emission models, various estimates have been proposed for global natural VOC emissions ranging for example, from 692 Tg C yr^{-1} (Levis et al., 2003) to 1150 Tg C yr^{-1} (Guenther et al., 1995). The discrepancy between these two results is primarily for compounds other than isoprene since the respective isoprene emission estimates are 507 and 503 Tg C yr^{-1} (Levis et al., 2003; Guenther et al., 1995). Other annual global isoprene emission estimates are 559 (Potter et al., 2001), 530 (Wang & Shallcross 2000), and 456 Tg C (Naik et al., 2000).

Overall, current biogenic emission models estimate isoprene emission within approximately 50% of measured fluxes (Geron et al., 1997). This estimate of the uncertainty generally applies to midday summer isoprene emissions from selected locations. Uncertainty with other natural emission estimates can be as high as a factor of 10 for various landscapes and compounds. Model verification is primarily dependent on

flux measurements. Various field measurements of isoprene fluxes have been made around the world, and measurements indicate that our model estimated emissions are within the right order of magnitude (Levis et al., 2003). A few of the field measurements are summarized in Table 1.2 along with a brief description of the ecosystem and measurement system.

1.9. References

Altshuller, A. 1983. Review: Natural volatile organic substances and their effect on air quality in the US. *Atmospheric Environment* 17, 2131-2166.

Andreae, M. O. and Crutzen, P. J. 1997. Atmospheric aerosols: Biogeochemical sources and role in atmospheric chemistry. *Science* 276, 1052-1058.

Arnts, R. and Meeks, S. 1981. Biogenic hydrocarbon contribution to the ambient air of selected areas. *Atmospheric Environment* 15, 1643-1651.

Atherton, C. and Penner, J. 1990. The effects of biogenic hydrocarbons on the transformation of nitrogen oxides in the troposphere. *Journal of Geophysical Research* 95, 14027-14038.

Atkinson, R. 1997. Gas-phase tropospheric chemistry of volatile organic compounds. 1. Alkanes and alkenes. *J. Phys. Chem. Ref. Data* 26, 215-290 .

Atkinson, R. 2000. Atmospheric chemistry of VOCs and NOx. *Atmospheric Environment* 34, 2063-2101.

Atkinson, R. and Arey, J. 1998. Atmospheric Chemistry of Biogenic Organic Compounds. *Acc. Chem. Res.* 31, 574-583.

Bach, T. J. and Lichtenthaler, H. K. 1983. Inhibition by mevilonin of plant growth, sterol formation and pigment accumulation. *Physiological Plant* 59, 50-60.

Baldocchi, D., Falge, E., Gu, L., Olson, R., Hollinger, D., Running, S., Anthoni, P., Bernhofer, C., Davis, K., Evans, R., Fuentes, J., Goldstein, A., Katul, G., Law, B., Lee, X., Malhi, Y., Meyers, T., Munger, W., Oechel, W., Paw U., K. T., Pilegaard, K., Schmid, H. P., Valentini, R., Verma, S., Vesala, T., Wilson, K., Wofsy, S. 2001. FLUXNET: a new tool to study the temporal and spatial variability of ecosystem-scale carbon dioxide, water vapor and energy flux

densities. *Bulletin of the American Meteorological Society* 82, 2415-2434.

Brasseur, G. P., Orlando, J. J., Tyndall, G. S. 1999. *Atmospheric chemistry and global change*, New York: Oxford Univ. Press.

Bukhov, N. G., Wiese, C., Neimanis, S., Heber, U. 1999. Heat sensitivity of chloroplasts and leaves: leakage of protons from thylakoids and reversible activation of cyclic electron transport. *Photosynth. Res.* 59, 81-93.

Calvert, J. and Madronich, S. 1987. Theoretical study of the initial products of the atmospheric oxidation of hydrocarbons. *Journal of Geophysical Research* 92, 2211-2220.

Carroll, M. A., Bertman, S. B., Shepson, P. B. 2001. Overview of the program for research on Oxidants: PHotochemistry, Emissions, and Transport (PROPHET) summer 1998 measurements intensive. *Journal of Geophysical Research* 106, 24275-24288.

Collins, W. J., Derwent, R. G., Johnson, C. E., Stevenson, D. S. 2002. The Oxidation of Organic Compounds in the Troposphere and Their Global Warming Potentials. *Climatic Change* 52, 453-479 .

Constable, J. V. H., Guenther, A. B., Schimel, D. S., Monson, R. K. 1999. Modelling changes in VOC emission in response to climate change in the continental United States. *Global Change Biology* 5, 791-806.

Daniel, J. and Solomon, S. 1998. On the climate forcing of carbon monoxide. *Journal of Geophysical Research* 103, 13249-13260.

Duane, M., Poma, B., Rembges, D., Astorga, C., Larsen, B. R. 2002. Isoprene and its degradation products as strong ozone precursors in Insubria, northern Italy. *Atmospheric Environment* 36, 3867-3879.

Fall R. 1999. Biogenic Emissions of Volatile Organic Compounds from Higher Plants. In *Reactive Hydrocarbons in the Atmosphere*, ed. Hewitt, C. N.,41-96 pp. San Diego, CA: Academic Press.

Fang, C., Monson, R. K., Cowling, E. B. 1996. isoprene emissions, photosynthesis, and growth in sweetgum (Liquidambar styraciflua) seedlings exposed to short- and long-term drying cycles. *Tree Physiology* 16, 441-446.

Farage, P., Long, S. P., Lechner, E. G., Baker, N. R. 1991. The sequence of change within the photosynthetic apparatus of wheat following short-term exposure to ozone. *Plant Physiol.* 95, 529-535.

Farquhar, G., von Caemmerer, S., Berry, J. 1980. A biochemical model of

photosynthetic CO2 assimilation in leaves of C3 species. *Planta* 149, 78-90.

Fehsenfeld, F., Calvert, J., Fall, R., Goldan, P., Guenther, A., Hewitt, C. N. 1992. Emissions of volatile organic compounds from vegetation and the implications for atmospheric chemistry. *Global Biogeochemical Cycles* 6, 389-430.

Finlayson-Pitts B. J., and Pitts, J. N. 2000. *Chemistry of the upper and lower atmosphere.* New York: Academic Press.

Fuentes, J. D., Wang, D., Gu, L. 1999. Seasonal variations in isoprene emissions from a Boreal Aspen forest. *Journal of Applied Meteorology* 38, 855-869.

Gaffney, J., and Marley, N. 1991. Tropospheric chemistry of natural hydrocarbons and energy-related pollutants: biosphere/climate feedbacks? In *Atmospheric Chemistry: Models and predictions for climate and air quality*, ed. Sloane, C., Tesche, T., Chelsea, MI: Lewis Publishers, Inc.

Geron, C., Guenther, A., Sharkey, T., Arnts, R. R. 2000. Temporal variability in basal isoprene emission factor. *Tree Physiology* 20, 799-805.

Geron, C. D., Guenther, A. B., Pierce, T. E. 1994. An Improved model for estimating emissions of volatile organic compounds from forests in the eastern United-States. *Journal of Geophysical Research* 99, 12773-12791.

Geron, C. D., Nie, D., Arnts, R. R., Sharkey, T. D., Singsaas, E. L., Vanderveer, P. J., Guenther, A., Sickles, J. E., Kleindienst, T. E. 1997. Biogenic isoprene emission: model evaluation in a southeastern United States bottomland deciduous forest. *Journal of Geophysical Research* 102, 18889-18901.

Gounaris, K., Brain, A. P. R., Quinn, P. J., Williams, W. P. 1984. Structural reorganization of chloroplast thylakoid membranes in response to heat stress. *Biochim. Biophys. Acta* 766, 198-208.

Greenberg, J. P., Guenther, A. B., Madronich, S. , Baugh, W., Ginoux, P., Druilhet, A., Delmas, R., Delon, C. 1999. Biogenic Volatile Organic Compound Emissions in Central Africa During the Experiment for the Regional Sources and Sinks of Oxidants (EXPRESSO) Biomass Burning Season. *Journal of Geophysical Research* 104, 30659-30671.

Grinspoon, J., Bowman, W., Fall, R. 1991. Delayed onset of isoprene emission in developing velvet bean (*Mucuna sp.*) leaves. *Plant Physiol.* 97, 170-174.

Guenther, A., Baugh, B., Brasseur, G., Greenberg, J., Harley, P., Klinger, L., Serca, D., Vierling, L. 1999. Isoprene Emission Estimates and Uncertainties for the Central African EXPRESSO Study Domain. *Journal of Geophysical Research* 104, 30625-30639.

Guenther, A., Geron, C., Pierce, T., Lamb, B., Harley, P., Fall, R. 2000. Natural emissions of non-methane volatile organic compounds; carbon monoxide, and oxides of nitrogen from North America. *Atmospheric Environment* 34, 2205-2230.

Guenther, A., Greenberg, J., Harley, P., Helmig, D., Klinger, L., Vierling, L., Zimmerman, P., Geron, C. 1996. Leaf, Branch, Stand and Landscape Scale Measurements of Volatile Organic Compound Fluxes From Us Woodlands. *Tree Physiology* 16, 17-24.

Guenther, A., Hewitt, C. N., Erickson, D., Fall, R., Geron, C., Graedel, T., Harley, P., Klinger, L., Lerdau, M., Mckay, W. A., Pierce, T., Scholes, B., Steinbrecher, R., Tallamraju, R., Taylor, J., Zimmerman, P. 1995. A Global model of natural volatile organic compound emissions. *Journal of Geophysical Research* 100, 8873-8892.

Guenther, A. B., Monson, R. K., Fall, R. 1991. Isoprene and monoterpene emission rate variability - observations with Eucalyptus and emission rate algorithm development. *Journal of Geophysical Research* 96, 10799-10808.

Guenther, A. B., Zimmerman, P. R., Harley, P. C., Monson, R. K., Fall, R. 1993. Isoprene and monoterpene emission rate variability - model evaluations and sensitivity analyses. *Journal of Geophysical Research* 98, 12609-12617.

Haagen-Smit, A. J. 1952. Chemistry and physiology of Los Angeles smog. *Industrial Engineering and Chemistry* 44, 1342-1346.

Hakola, H., Laurila, T., Rinne, J., Puhto, K. 2000. The ambient concentrations of biogenic hydrocarbons at a northern European boreal site. *Atmospheric Environment* 34, 4971-4982.

Hanna, S. R., Lu, Z. G., Frey, H. C., Wheeler, N., Vukovich, J., Arunachalam, S., Fernau, M., Hansen, D. A. 2001. Uncertainties in predicted ozone concentrations due to input uncertainties for the UAM-V photochemical grid model applied to the July 1995 OTAG domain. *Atmospheric Environment* 35, 891-903.

Harley, P., Guenther, A., Zimmerman, P. 1996. Effects of light, temperature and canopy position on net photosynthesis and isoprene emission from Sweetgum (Liquidambar Styraciflua) leaves. *Tree Physiology* 16, 25-32.

Harley, P., Guenther, A., Zimmerman, P. 1997. Environmental Controls Over Isoprene Emission in Deciduous Oak Canopies. *Tree Physiology* 17, 705-714.

Harley, P. C., Litvak, M. E., Sharkey, T. D., Monson, R. K. 1994. Isoprene emission from Velvet Bean-leaves - interactions among nitrogen availability, growth

photon flux-density, and leaf development. *Plant Physiol.* 105, 279-285.

Harley, P. C., Monson, R. K., Lerdau, M. T. 1999. Ecological and Evolutionary Aspects of Isoprene Emission From Plants. *Oecologia* 118, 109-123.

Heath, R. L. 1994. Possible mechanisms for the inhibition of photosynthesis by ozone. *Photosynth. Res.* 39, 439-451.

Hewitt, C. N., Kok, G. L., Fall, R. 1990. Hydroperoxides in plants exposed to ozone mediate air pollution damage to alkene emitters. *Nature* 344, 56-58.

Hoffmann, T., Odum, J. R., Bowman, F., Collins, D., Klockow, D., Flagan, R., Seinfeld, J. H. 1997. Formation of organic aerosols from the oxidation of biogenic hydrocarbons. *Journal of Atmospheric Chemistry* 26, 189-222.

Houweling, S., Dentener, F., Lelieveld, J. 1998. The impact of nonmethane hydrocarbon compounds on tropospheric photochemistry. *Journal of Geophysical Research* 103, 10673-10696.

Jiang, G., Lamb, B., Westberg, H. 2003. Using back trajectories and process analysis to investigate photochemical ozone production in the Puget Sound region. *Atmospheric Environment* 37, 1489-1502.

Juuti, S., Arey, J., Atkinson, R. 1990. Monoterpene emission rate measurements from a Monterey pine. *Journal of Geophysical Research* 95, 7515-7519.

Karl, T., Crutzen, P. J., Mandl, M., Staudinger, M., Guenther, A., Jordan, A., Fall, R., Lindinger, W. 2001. Variability-lifetime relationship of VOCs observed at the Sonnblick Observatory 1999 - estimation of HO-densities. *Atmospheric Environment* 35, 5287-5300.

Kinnee, E., Geron, C., Pierce, T. 1997. United States land use inventory for estimating biogenic ozone precursor emissions. *Ecological Applications* 7, 46-58.

Kuhn, U., Rottenberger, S., Biesenthal, T., Wolf, A., Schebeske, G., Ciccioli, P., Brancaleoni, E., Frattoni, M., Tavares, T. M., Kesselmeier, J. 2002. Isoprene and monoterpene emissions of Amazonian tree species during the wet season:direct and indirect investigations on controlling environmental functions. *Journal of Geophysical Research* 107, art. no.-8071.

Kuzma, J. and Fall, R. 1993. Leaf isoprene emissions rate is dependent on leaf development and the level of isoprene synthase. *Plant Physiol.* 101, 435-440.

Lamb, B., Gay, D., Westberg, H., Pierce, T. 1993. A Biogenic hydrocarbon emission inventory for the USA using a simple forest canopy model. *Atmospheric Environment* 27, 1673-1690.

Lamb, B., Guenther, A., Gay, D., Westberg, H. 1987. A national inventory of biogenic hydrocarbon emissions. *Atmospheric Environment* 21, 1695-1705.

Lerdau, M. and Keller, M. 1997. Controls on Isoprene Emission From Trees in a Subtropical Dry Forest. *Plant, Cell Environ.* 20, 569-578.

Levis, S., Wiedinmyer, C., Bonan, G. B., Guenther, A. 2003. Simulating biogenic volatile organic compound emissions in the community climate system model. *Journal of Geophysical Research* 108, 4659.

Lichtenthaler, H. K., Schwender, J., Disch, A., Rohmer, M. 1997. Biosynthesis of isoprenoids in higher plant chloroplasts proceeds via a mevalonate-independent pathway. *FEBS Lett.* 400, 271-274.

Litvak, M. E., Loreto, F., Harley, P. C., Sharkey, T. D., Monson, R. K. 1996. The response of isoprene emission rate and photosynthetic rate to photon flux and nitrogen supply in Aspen and White Oak trees. *Plant, Cell Environ.* 19, 549-559 .

Logan, B. A. and Monson, R. K. 1999. Thermotolerance of Leaf Discs from Four Isoprene-Emitting Species is Not enhanced by Exposure to Exogenous Isoprene. *Plant Physiol.* 120, 821-825.

Logan, B. A., Monson, R. K., Potosnak, M. J. 2000. Biochemistry and physiology of foliar isoprene production. *Trends in Plant Science* 5, 477-481.

Logan, J. A. 1985. Tropospheric ozone: Seasonal behavior, trends, and anthropogenic influence. *Journal of Geophysical Research* 90, 10463-10482.

Loreto, F. and Sharkey, T. D. 1990. A Gas-Exchange Study of Photosynthesis and Isoprene Emission in Quercus-Rubra L. *Planta* 182, 523-531.

Loreto, F. and Sharkey, T. D. 1993. On the Relationship Between Isoprene Emission and Photosynthetic Metabolites Under Different Environmental- Conditions. *Planta* 189, 420-424.

Loreto, F., Ciccioli, P., Brancaleoni, E., Valentini, R., Lillis, M. D., Csiky, O., Seufert, G. 1998. A hypothesis on the evolution of isoprenoid emission by oaks based on the correlation between emission type and Quercus taxonomy. *Oecologia* 115, 302-305.

Loreto, F. and Velikova, V. 2001. Isoprene produced by leaves protects the photosynthetic apparatus against ozone damage, quenches ozone products, and reduces lipid peroxidation of cellular membranes. *Plant Physiol.* 127, 1781-1787.

Martin, R. S., Westberg, H., Allwine, E., Ashman, L., Farmer, J. C., Lamb, B. 1991.

Measurement of Isoprene and Its Atmospheric Oxidation-Products in a Central Pennsylvania Deciduous Forest. *Journal of Atmospheric Chemistry* 13, 1-32.

McGarvey, D. J. and Croteau, R. 1995. Terpenoid metabolism. *Plant Cell* 7, 1015-1026.

Monson, R. and Fall, R. 1989. Isoprene emission from Aspen leaves: Influence of environment and relation to photosynthesis and photorespiration. *Plant Physiol.* 90, 267-274.

Monson, R., Jaeger, C., Adams, W., Driggers, E., Silver, G., Fall, R. 1992. Relationships among isoprene emission rate, photosynthesis, and isoprene synthesis, as influenced by temperature. *Plant Physiol.* 92, 1175-1180.

Monson, R. K., Harley, P. C., Litvak, M. E., Wildermuth, M., Guenther, A. B., Zimmerman, P. R., Fall, R. 1994. Environmental and developmental controls over the seasonal pattern of isoprene emission from aspen leaves. *Oecologia* 99, 260-270.

Monson, R. K. and Holland, E. A. 2001. Biospheric trace gas fluxes and their control over tropospheric chemistry. *Annual Review of Ecology and Systematics* 32, 547-576.

Monson, R. K., Lerdau, M. T., Sharkey, T. D., Schimel, D. S., Fall, R. 1995. Biological aspects of constructing volatile organic compound emission inventories. *Atmospheric Environment* 29, 2989-3002.

Naik, V., Delire, C., and Wuebbles, D. J. 2000. Modeling the climate variability of biogenic isoprene and monoterpenes. Suppli Abstract A61B-0076 Eos Trans. AGU 83(47).

Pandis, S. N., Paulson, S. E., Seinfeld, J. H., Flagan, R. C. 1991. Aerosol Formation in the Photooxidation of Isoprene and Beta-Pinene. *Atmospheric Environment* 25, 997-1008.

Pastenes, C. and Horton, P. 1996. Effect of high temperature on photosynthesis in beans 1. Oxygen evolution and chlorophyll fluorescence. *Plant Physiol.* 112, 1245-1251.

Pattey, E., Desjardins, R. L., Westberg, H., Lamb, B., Zhu, T. 1999. Measurement of Isoprene Emissions Over a Black Spruce Stand Using a Tower-Based Relaxed Eddy-Accumulation System. *Journal of Applied Meteorology* 38, 870-877.

Paulson, S., Pandis, S., Baltensberger, U., Seinfeld, J., Flagan, R. 1990. Characterization of photochemical aerosols from biogenic hydrocarbons. *J. Aerosol Sci.* 21S, 245-248.

Pell, E. J., Eckardt, N. A., Glick, R. E. 1994. Biochemical and molecular basis for impairment of photosynthetic potential. *Photosynthesis Research* 39, 453-462.

Pell, E. J., Schlagnhaufer, C. D., Arteca, R. N. 1997. Ozone-induced oxidative stress: mechanisms of action and reactioni. *Physiological Plant* 100, 264-273.

Penuelas, J. and Llusia, J. 2001. The Complexity of Factors Driving Volatile Organic Compound Emissions by Plants. *Biologia Plantarum* 44, 481-487.

Penuelas, J. and Llusia, J. 2003. BVOCs: Plant Defense Against Climate Warming? *Trends in Plant Science* 8, 105-109.

Petron, G., Harley, P., Greenberg, J., Guenther, A. 2001. Seasonal temperature variations influence isoprene emission. *Geophys. Res. Lett.* 28, 1707-1710.

Pierce, T., Geron, C., Bender, L., Dennis, R., Tonnesen, G., Guenther, A. 1998. Influence of increased isoprene emissions on regional ozone modeling. *Journal of Geophysical Research* 103, 25611-25629.

Pierce, T., Geron, C., Pouliot, G., Kinnee, E., and Vukovich, J. 2002. Integration of the Biogenic Emissions Inventory System (BEIS3) into the Community Multiscale Air Quality modeling system. The 25th Agricultural and Forest Meteorology/12th Air Pollution/4th Urban Environment Meeting. Norfolk, VA

Pierce, T. and Waldruff, P. 1991. PC-BEIS: A Personal computer version of the biogenic emissions inventory system. *Journal of Air and Waste Management Association* 41, 937-941.

Poisson, N., Kanakidou, M., Crutzen, P. J. 2000. Impact of non-methane hydrocarbons on tropospheric chemistry and the oxidizing power of the global troposphere: 3-dimensional modelling results. *Journal of Atmospheric Chemistry* 36, 157-230.

Potter, C. S., Alexander, S. E., Coughlan, J. C., Klooster, S. A. 2001. Modeling Biogenic Emissions of Isoprene: Exploration of Model Drivers, Climate Control Algorithms, and Use of Global Satellite Observations. *Atmospheric Environment* 35, 6151-6165.

Rasmussen, R. A. 1973. Emission of isopene from leaf discs of *Hamamelis*. *Phytochemistry* 12, 15-19.

Roelofs, G.-J. and Lelieveld, J. 2000. Tropospheric ozone simulation with a chemistry-general circulation model:influence of higher hydrocarbon chemistry. *Journal of Geophysical Research* 105, 22697-22712.

Schulze-Siebert D., Heintze, A., Schultz G. 1987. Substrate flow from photosynthetic carbon metabolism to chloroplast isoprenoid synthesis in spinach evidence for a

plastidic phosphoglycerate mutase. *Z. Naturforsch* 42 Teil C, 570-580.

Seinfeld, J. and Pandis, S. 1998. *Atmospheric chemistry and physics: from air pollution to climate change*, New York, NY: Jon Wiley and Sons, Inc.

Sharkey, T. D. 1996. Emission of Low Molecular Mass Hydrocarbons From Plants. *Trends in Plant Science* 1, 78-82.

Sharkey, T. D., Chen, X. Y., Yeh, S. 2001. Isoprene Increases Thermotolerance of Fosmidomycin-Fed Leaves. *Plant Physiol.* 125, 2001-2006.

Sharkey, T. D. and Loreto, F. 1993. Water-stress, temperature, and light effects on the capacity for isoprene emission and photosynthesis of kudzu leaves. *Oecologia* 95, 328-333.

Sharkey, T. D., Loreto, F., Delwiche, C. F. 1991. High-Carbon Dioxide and Sun Shade Effects on Isoprene Emission From Oak and Aspen Tree Leaves. *Plant, Cell Environ.* 14, 333-338.

Sharkey, T. D., Singsaas, E. L., Lerdau, M. T., Geron, C. D. 1999. Weather Effects on Isoprene Emission Capacity and Applications in Emissions Algorithms. *Ecological Applications* 9, 1132-1137.

Sharkey, T. D., Singsaas, E. L., Vanderveer, P. J., Geron, C. 1996. Field Measurements of Isoprene Emission From Trees in Response to Temperature and Light. *Tree Physiology* 16, 649-654.

Sharkey, T. D. and Yeh, S. S. 2001. Isoprene emission from plants. *Annual Review of Plant Physiology and Plant Molecular Biology* 52, 407-436.

Silver, G. M. and Fall, R. 1991. Enzymatic synthesis of isoprene from dimethylallyl diphosphate in aspen leaf extracts. *Plant Physiol.* 97, 1588-1591.

Singsaas, E. L., Laporte, M. M., Shi, J. Z., Monson, R. K., Bowling, D. R., Johnson, K., Lerdau, M., Jasentuliytana, A., Sharkey, T. D. 1999. Kinetics of Leaf Temperature Fluctuation Affect Isoprene Emission From Red Oak (Quercus Rubra) Leaves. *Tree Physiology* 19, 917-924.

Singsaas, E. L., Lerdau, M., Winter, K., Sharkey, T. D. 1997. Isoprene increases thermotolerance of isoprene-emitting species. *Plant Physiol.* 115, 1413-1420.

Singsaas, E. L. and Sharkey, T. D. 1998. The Regulation of Isoprene Emission Responses to Rapid Leaf Temperature Fluctuations . *Plant, Cell Environ.* 21, 1181-1188.

Singsaas, E. L. and Sharkey, T. D. 2000. The Effects of high temperature on isoprene synthesis in Oak leaves. *Plant, Cell Environ.* 23, 751-757.

SMOKE User's Manual *version 2.0*. report. 2003.

Stokes, N. J., Terry, G. M., Hewitt, C. N. 1998. The impact of ozone, isoprene and propene on antioxidant levels in two leaf classes of velvet bean (*Mucuna pruriens L.*). *J. Exp. Bot.* 49, 115-123.

Tingey, D., Manning, M., Grothaus, L., Burns, W. 1979. The influence of light and temperature on isoprene emission rates from live Oak. *Physiol. Plant.* 47, 112-118.

Tingey, D. T., Evans, R., Gumpertz, M. 1981. Effects of environmental conditions on isoprene emission from live oak. *Planta* 152, 565-570.

Trainer, M., Williams, E., Parrish, D., Buhr, M., Allwine, E., Westberg, H., Fehsenfeld, H., Liu, S. 1987. Models and observations of the impact of natural hydrocarbons on rural ozone. *Nature* 329, 705-707.

Wang, K. Y. and Shallcross, D. E. 2000. Modeling terrestrial biogenic isoprene fluxes and their potential impact on global chemical species using a coupled LSM-CTM model. *Atmospheric Environment* 34, 2909-2925.

Went, F. 1960. Blue Hazes in the atmosphere. *Nature* 187, 641-643.

Westberg, H., Lamb, B., Hafer, R., Hills, A., Shepson, P., Vogel, C. 2001. Measurement of isoprene fluxes at the PROPHET site. *Journal of Geophysical Research* 106, 24347-24358.

Wildermuth, M. C. and Fall, R. 1996. Light-dependent isoprene emission-characterization of a thylakoid-bound isoprene synthase in Salix discolor chloroplasts. *Plant Physiol.* 112, 171-182.

Williams, J., Roberts, J. M., Fehsenfeld, F. C., Bertman, S. B., Buhr, M. P., Goldan, P. D., Hubler, G., Kuster, W. C., Ryerson, T. B., Trainer, M., Young, V. 1997. Regional ozone from biogenic hydrocarbons deduced from airborne measurements of PAN, PPN, and MPAN. *Geophys. Res. Lett.* 24, 1099-1102.

Zeidler, J. G., Lichtenthaler, H. K., May, H. U., Lichtenthaler, F. W. 1997. Is isoprene emited by plants synthesized via the novel isopentenyl pyrophosphate pathway? *Z. Naturforsch* 52, 15-23.

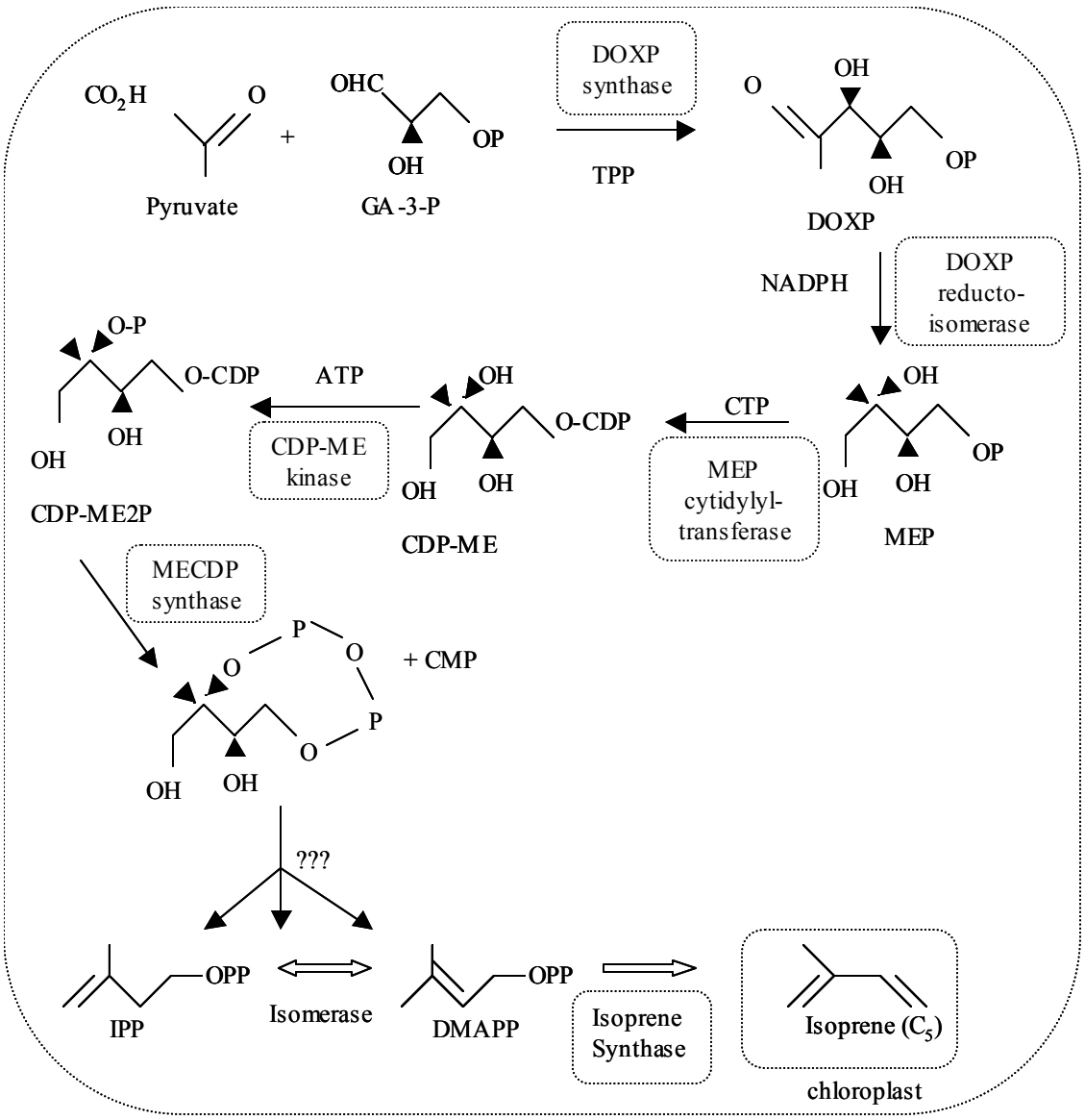

Figure 1.1: Biosynthetic pathway for isoprene. GA-3-P is glyceraldehydes 3-phosphate, MEP stands for the 2-deoxyxylulose 5-phosphate/2-methylerythritol 4-phosphate pathway, IPP is isopentenyl pyrophosphate, DMAPP is dimethylallyl pyrophosphate, CDP-ME is 4-(cytidine 5'-diphospho)-2-C-methyl-D-erythritol, CDP-ME2P is 2-phospho-4-(cytidine 5'-diphospho)-2-C-methyl-D-erythritol, DOXP is 1-deoxy-D-xylulose-5-phosphate, and MECDP is 2-C-methyl-D-erythritol 2,4-cyclodiphosphate.

Table 1.1: Lifetimes of some common biogenic hydrocarbons and their oxidation products (Atkinson & Arey 1998; Atkinson 2000).

	Lifetime		
Compound (Concentration)	OH radical 2×10^6 molec cm^{-3}	O_3 7×10^{11} molec cm^{-3}	NO_3 (night)* 5×10^8 molec cm^{-3}
Isoprene	1.4 h	1.3 day	1.6 h
α-pinene	2.6 h	4.6 h	11 min
β-pinene	1.8 h	1.1 day	25 min
Formaldehyde	1.2 day	> 4.5 yr	80 day
Methylvinylketone	6.8 h	3.6 day	>385 day
Methacrolein	4.1 h	15 day	11 day

* NO_3 levels presented are for an urban area

Table 1.2: Field measurements of isoprene fluxes from various ecosystems.

Location	Average isoprene flux	Ecosystem type	Reference
Central Africa	3930 μg C m^{-2} h^{-1}	Tropical rain forest	(Greenberg et al., 1999)
Central Africa	2520 μg C m^{-2} h^{-1}	Degraded woodland	(Greenberg et al., 1999)
Canada	2290 μg C m^{-2} h^{-1}	Boreal forest	(Pattey et al., 1999)
Southeastern US	3000-4000 μg C m^{-2} h^{-1}	Forested sites	(Guenther et al., 1996)

CHAPTER TWO

EXPERIMENTAL METHODS AND MATERIALS

2.1. Introduction

Large amounts of time and effort are involved with obtaining field measurements that are appropriate for answering scientific questions related to biogenic emissions. When designing a field study, there are many aspects to consider; such as choosing an appropriate site, choosing which sampling technique to employ, determining which instruments are best suited for the site and technique, resolving how to capture and store the data, determining what ancillary data is needed to support the primary data, deciding where to mount the instruments and how often to calibrate them, and calculating how to process the data to make sure the data are of the highest quality possible. Most of these decisions are best made in hindsight, and of course many of them are decided based on cost and availability of instruments and site locations. However, there are pros and cons associated with each decision, and understanding the repercussions is important. This section of the dissertation describes the entire measurement system in detail, much of which is too specific to be included in published journal articles, but nonetheless is important. Descriptions of the sampling site, micrometeorological technique (eddy covariance), instrumentation, data storage and processing, biological data collection, quality assurance/quality control, and measurement uncertainties are provided in the following sections.

2.2. Site Description

Measurements were made at the University of Michigan Biological Station (UMBS) located near Pellston, MI, in the northern portion of the lower peninsula (45°30'35.4"N, 84°42'46.8"W, and elevation 238 m) (Figure 2.1). Two towers were constructed at this site, the UMBS~Flux tower (part of the AmeriFlux program) (Baldocchi et al., 2001) and an atmospheric chemistry tower which is part of the Program for Research on Oxidants: PHotochemistry, Emissions, and Transport (PROPHET) (Carroll et al., 2001). The specific ecosystem studied at this site is in the transition zone between mixed hardwood and boreal forest on a high-outwash plain deposited by glacial drift (Schmid et al., 2003; Pearsall 1995). The towers are located on a level to gently sloping area in a secondary successional hardwood forest (over story age of the forest is approximately 75 years) with bigtooth aspen (*Populus grandidentata* Michx.) and quaking aspen (*P. tremuloides* Michx.) the predominant species within a 1 km radius of the tower (Schmid et al., 2003). Other species at the site include beech (*Fagus grandifolia* Ehrh.), paper birch (*Betula papyrifera* Marsh.), maple (*Acer rubrum* L.*, A. saccharum* Marsh.) and red oak (*Quercus rubra* L.), with an under story component of young eastern white pine (*Pinus strobus* L.) and bracken fern (*Pteridium aquilium*). Douglas Lake is located 1 km to the north and Burt Lake 3.5 km to the southeast.

Both towers are accessed via an unimproved driveway and gravel foot-path off of Bryant Road (east of the site), with the PROPHET tower located approximately 130 m to the south of the UMBS~Flux tower. The PROPHET tower is a 31 m high walk-up

scaffolding tower, rectangular in shape with 1.5 by 1.8 m platforms and a fall protection system. A 5 cm ID Pyrex sampling manifold brings air at a rate of ~3300 l min^{-1} to the large shelter at the base of the tower that houses the pump and sampling equipment (Carroll et al., 2001). The UMBS~Flux tower has a triangular cross section with a large base at the bottom (5.1 m sides) that tapers to 1.8 m sides at 30.5 m in height. From 30.5 to 46 m, the triangular cross sections are uniform with steel grid work platforms every 6 m. An interior ladder provides access to the top of the tower, and a shelter at the base of the tower houses data acquisition equipment and other instruments (Schmid et al., 2003).

The fetch is relatively flat with a maximum change in elevation of 20 m over 1 km distance in any direction from the tower (Schmid et al., 2003). The primary fetch is considered to be north, northwest, and west of the tower with winds from the east to southeast passing through the tower itself. Canopy height (h_c) is roughly 22 m and the zero-plane displacement height (d) during the foliated (summer) period was estimated to be 16.5 m ($d = 0.75\ h_c$) using the logarithmic wind profile and the sonic anemometer data from the 46 m and 34 m levels (Su et al., 2004).

2.3. Eddy Covariance Theory

Micrometeorological techniques for measuring trace gas emissions have proven to be the technique of choice for many reasons. Unlike enclosure techniques that alter the environment surrounding a leaf, branch, or small tree, micrometeorological techniques do not perturb the vegetation. Techniques such as gradient, relaxed eddy accumulation (REA), disjunct eddy covariance, and eddy covariance also measure fluxes from an areal

basis which eliminates the need to scale-up leaf level measurements. Instrumentation demands with micrometeorological techniques are often greater compared to enclosure methods and require compound specific, fast-response instruments (ideal response < 1s) that can provide the required sensitivity and withstand the weather for lengthy periods of time. Additional drawbacks include the need for a tall tower that extends above the canopy, and a large upwind fetch with uniform surface/vegetation characteristics. Regardless of these requirements, long-term eddy covariance measurements of CO_2 in particular are considered to be among the best available estimates of carbon sequestration above terrestrial ecosystems (Baldocchi et al., 2001).

Eddy covariance was selected for this work because unlike REA or other micrometeorological techniques, eddy covariance is a direct measure of the biosphere-atmosphere exchange of trace gases (Massman and Lee 2002). Eddy covariance (then referred to as eddy correlation) was first proposed and tested by Swinbank (1951), however, the instrumentation and data collection capabilities were not sufficient for eddy covariance until almost 3 decades later. The covariance of the chemical mixing ratio with vertical wind currents is the fundamental concept of eddy covariance, but there are certain criteria that need to be met in order for the technique to be valid. If measurements are made at sites where the assumptions are not met, then potential sources of uncertainty or bias must be accounted for.

More details on the corrections and errors associated with eddy covariance flux measurements are presented in the Data Acquisition, Storage and Processing Section (§2.5.) and the Quality Control and Flux Uncertainties Section (§2.7.). A brief description of the theory behind eddy covariance and the assumptions are presented here.

There is a considerable amount of literature available explaining micrometeorological techniques, and some of the more helpful references include: Stull 1989; Kaimal and Finnigan 1994; Baldocchi et al., 1988; Dabberdt et al., 1993; Massman and Lee 2002; Moncrieff et al., 1996.

Assuming the measurement point is fixed in space, and we are operating in an Eulerian framework, then the conservation equation of species mass is:

$$\underbrace{\frac{\partial \overline{c}}{\partial t}}_{I} + \underbrace{\overline{u}\frac{\partial \overline{c}}{\partial x} + \overline{v}\frac{\partial \overline{c}}{\partial y} + \overline{w}\frac{\partial \overline{c}}{\partial z}}_{II} + \underbrace{\frac{\partial \overline{u'c'}}{\partial x} + \frac{\partial \overline{v'c'}}{\partial y} + \frac{\partial \overline{w'c'}}{\partial z}}_{III} = D + S + R \qquad (1)$$

where u, v, and w are the wind velocity components (x: mean wind direction, y: lateral direction, and z: direction normal to the surface), D is molecular diffusion, S is the source/sink term, and R represents chemical reactions. This form of the conservation equation has already employed Reynolds decomposition such that the instantaneous scalar (c) and wind components (u, v, w) are comprised of the mean over some averaging time (denoted by an overbar) plus the turbulent fluctuation (indicated by the prime notation):

$$c = \overline{c} + c' \quad \text{and} \quad u = \overline{u} + u' \qquad (2)$$

The left-hand side of equation 1 contains three components: the time rate of change of the mass, or the storage term (*I*), the advection of material by the mean winds (*II*), and the flux of material due to turbulent diffusion (*III*). Assumptions made in order

to simplify equation 1 include; (1) there is no chemistry that occurs between the source of the flux and the measurement height ($R = 0$); (2) mean wind is in the u direction and thus the mean lateral and vertical winds are zero ($\overline{v}, \overline{w} = 0$); (3) molecular diffusion is much smaller than turbulent diffusion and thus it can be neglected ($D = 0$); (4) stationarity or the steady state assumption, such that over the designated averaging time (t) the statistical properties of the flow do not change ($\partial \overline{c} / \partial t = 0$); and lastly (5) horizontally homogeneous conditions based on flat and uniform site characteristics in all directions ($\overline{u}\frac{\partial \overline{c}}{\partial x} = 0, \frac{\partial \overline{u'c'}}{\partial x} = \frac{\partial \overline{v'c'}}{\partial y} = 0$). Thus, equation 1 is reduced to:

$$\frac{\partial \overline{w'c'}}{\partial z} = S \tag{3}$$

Integration of equation 3 with respect to height (z) provides the eddy covariance equation where Flux = $\overline{w'c'}$ measured at height z above the canopy.

$$\int_0^z S dz = \overline{w'c'} \Big|_0^z = \overline{w'c'} \tag{4}$$

Similarly, energy fluxes can also be measured by exchanging the mass (c) in the above equations with either temperature (T) for sensible heat flux (H), or water vapor concentration for latent heat flux (LE). The averaging time period for eddy covariance measurements ranges from 20 min to 1 hour. The time period must be long enough to

account for the range of eddy contributions to the flux, but short enough to avoid non-steady state changes due to diurnal variations.

2.4. Instrumentation Specifics

The choice of instrumentation and location for mounting the eddy covariance system varied slightly from year-to-year. Table 2.1 summarizes the details for each year, in terms of the instruments used, and where they were located, along with other measurement details. Measurements began in 1997 with a short trial period using the REA technique for isoprene (C_5H_8) fluxes from the PROPHET tower. Then in 1998 when the UMBS~Flux tower was operational, eddy covariance isoprene flux measurements were made for about 2 weeks at the 31m level of the UMBS~Flux tower (Westberg et al., 2001). Isoprene concentrations were determined using the Fast Isoprene Sensor (FIS, Hills Scientific, Inc.) (Guenther and Hills 1998; Hills and Zimmerman 1990). Additional fluxes of CO_2, H and LE were simultaneously measured using the Auble and Meyers open path Infrared gas analyzer (IRGA) (Auble and Meyers 1992) along with an Applied Technologies Inc., (ATI, Longmont, CO) sonic anemometer. Beginning in 1999, full growing season measurements of all of the fluxes (isoprene, CO_2, H, LE, and momentum) were made from the UMBS~Flux tower until 2002 when measurements were made from the PROPHET tower. After 1999, data was stored at 10 Hz frequency (2 Hz for 1999, and real time flux calculations in 1997 and 1998) and post processed off line. The following sections describe in more detail the specifics for each of the instruments used, a description of how each instrument works, some of the

positives and negatives associated with each one, and the inherent error or uncertainty related to each measurement.

2.4.1. Sonic Anemometer

The ATI K-configuration probe sonic anemometer was used for measuring the stream wise (*u*), lateral (*v*), and vertical (*w*) wind velocities along with the sonic temperature. The signal was logged using the ATI analog to digital converter (datapacker), which enabled 8 additional analog signals to be recorded at the same frequency as the sonic data. The sonic was mounted at the end of a 3.1 m horizontal boom directed into the prevailing wind direction (~300°) at a height of 31 m, and the datapacker was located at the same height on the tower platform (Figures 2.2 and 2.3). Serial RS-232 digital output was transmitted from the top of the tower to a computer located at the base of the tower.

Wind velocity can be computed by measuring the transit time for a sonic pulse to travel between two transducers. Sonic pulses are transmitted from one transducer and received by the opposite transducer located 15 cm apart in each of the three orthogonal axes. The sonic temperature is determined based on the speed of sound measurement in the vertical (W) axis, and software included with the sonic automatically corrects the temperature for crosswind contamination. The discrepancy between sonic temperature and absolute temperature is a function of the water vapor content in the air. Accuracy of output is reported to be ±0.03 m s^{-1} for wind speed and ±2°C for absolute temperature.

2.4.2. Open path Infrared Gas Analyzer (IRGA)

CO_2 and H_2O mixing ratios were measured using the Auble and Meyers open path fast response IRGA (Auble and Meyers 1992). The sensor was mounted at a slight angle from vertical to avoid water from pooling on the optical windows. The sensor was approximately 0.5 m downwind from the sonic on a perpendicular cross bar mounted to the sonic boom (Figures 2.2 and 2.3). Detection is based on the fact that CO_2 and H_2O absorb infrared radiation at specific wavelengths that are not greatly affected by other atmospheric gases (Auble and Meyers 1992). Thus the density of either CO_2 or H_2O can be determined by quantifying the attenuation of radiation at a specific wavelength (absorption band) between a source and a detector. Realizing the absorption coefficients are a function of pressure and temperature, that there are changes in source intensity and detector response, and that dust in the air or on the optics can affect the radiation absorbed and scattered, Beer's law is used as a close approximation for band absorption. By detecting radiation at a third absorption band (reference) that is different than the CO_2 and H_2O wavelengths, the adverse effects from the issues previously listed can be accounted for. Three narrow bandpass interference filters are used in this instrument with minimal cross-sensitivity and high absorption. The wavelengths are: reference 3.96 μm; H_2O 2.61 μm; and CO_2 4.22 μm. A chopper wheel rotates the three filters in front of the PbSe infrared detector and simultaneously chops the infrared source on and off so ambient light effects can be removed. The sensing volume is relatively small in order to reduce path averaging from small scale eddies, and a twice-folded path (80 cm) increases sensitivity within the 20 cm actual length.

The sensor is calibrated by placing a hood around the sensing volume and pumping calibration standards into the hood. Two CO_2 standards were used (~290 ppm and ~402 ppm) for calibration, and calibrations were performed roughly every two weeks. A constant dew point generator was not available for H_2O calibrations, so output voltages were corrected based on available, co-located relative humidity (RH) measurements. Typical noise levels reported by Auble and Meyers (1992) are less than 10 mg m^{-3} for H_2O and 300 μg m^{-3} for CO_2. Assuming noise levels similar to these, this sensor can measure scalar fluxes over a 30-minute period to an accuracy of 10%.

2.4.3. Fast Isoprene Sensor (FIS)

The fast isoprene sensor (FIS, Hills Scientific, Inc.) uses a chemiluminescent technique to measure isoprene concentrations. The reaction of isoprene (or any primary alkene) with ozone produces electronically excited formaldehyde and glyoxal:

$$C_5H_8 + O_3 \rightarrow HCHO^* + \text{products} \quad (5)$$

$$C_5H_8 + O_3 \rightarrow HCOCHO^* + \text{products} \quad (6)$$

When formaldehyde and glyoxal return to the ground state, they emit light at 490 nm and 550 nm respectively. A commercial photon detector (Hamamatsu) is used to detect and count individual photons. The required ozone for reactions 5 and 6 is produced by electronic discharge in oxygen from a commercially available O_3 generator (ClearWater Tech, Inc.). The FIS sensor operates at ambient pressure, and to reduce the diurnal temperature variations, the photomultiplier tube (PMT) housing is temperature

controlled. Photon counts from the detector are linearly proportional to isoprene concentration, so instrument response to an isoprene standard determines instrument sensitivity. Factors that affect sensitivity include O_3 concentration, reaction cell pressure, reaction cell flow rate, temperature, and reaction cell cleanliness.

The detection limit when operating the instrument at 10 Hz is 0.5 ppbv isoprene with 20% uncertainty. Calibrations were performed at a minimum of once per day to determine the zero and the slope, or sensitivity (photon counts per ppbv isoprene per time). In 2002 the FIS was upgraded with automated calibration capabilities, so calibrations were performed approximately every 7 hours or about 3 times per day. The FIS sensitivity varied slightly, with standard deviations of 27%, 25%, 28% and 19% for years 1999-2002 respectively. There was no discernable trend or drift with the FIS zero for any year. Guenther and Hills (1998) reported that instrument noise is primarily high frequency, random noise that is relatively independent of mixing ratio.

Since isoprene dominates other hydrocarbons in many environments, and the response for other hydrocarbons is less than the response for isoprene (Guenther and Hills 1998), this instrument is considered specific for isoprene in relatively clean forest environments. Guenther and Hills (1998) confirmed this by testing the FIS response to 18 compounds, including several isoprene oxidation products, methacrolein (MACR) and methyl vinyl ketone (MVK), and other biogenic compounds such as α-pinene, β-pinene, and 2-methyl-3-buten-2-ol (MBO). The only compound tested with a relative response of 1.0 (to isoprene) was propene. MVK and MACR had relative responses of 40% and 25% respectively, and the estimated net interference for eddy covariance isoprene flux measurements for all the compounds tested is less than 5% for most forested sites in

North America (Guenther and Hills 1998). Interference for the UMBS~Flux measurements are similar based on the fact that the combined concentration of MVK and MACR at this site was typically less than 500 pptv during midday and midday isoprene fluxes ranged from 4~8 ppbv on average (Westberg et al., 2001).

The sample inlet was attached to the horizontal boom (Figure 2.3) about 0.2 m behind the sonic array so that airflow near the sonic was not disturbed. Sample air was drawn through a 1.27 cm I.D. Teflon tube from the 31 m level to the FIS located at the base of the tower. Flow rates were sufficiently high enough to guarantee turbulent flow ($R_e \sim 18{,}839 >> 2030$) so that attenuation through the long sample line and high frequency loss was minimized (Massman 1991; Lenschow and Raupach 1991; Leuning and Moncrieff 1990). Flow rates averaged 30 slpm with a lag time due to transport through the sample line of ~10 s. The FIS pump drew a portion of the sample air, thus total FIS flow rates were controlled by the FIS and ranged between 3.5 and 4.5 slpm. FIS counts were output via a serial RS-232 connection directly to the computer used for data acquisition, and total FIS flow rate plus isoprene standard flow rate voltages were output to the datapacker.

Instrument response time is reported to be 0.4 s at 2 Hz (Guenther and Hills 1998). Prior to deployment in 2000, a frequency response test was performed in the laboratory using the same equipment that was installed in the field (Massman 1991; Munger et al., 1996). Response time of the instrument and attenuation of the sample through the Teflon tube reduces the response due to loss of high frequency fluxes. In order to determine the effective first-order time constant (τ) for the high frequency correction (discussed in §2.5.), isoprene standard was injected into the end of the sample

line at specific frequencies and the response from the FIS was recorded. The standard was controlled using a solenoid valve with the position of the valve recorded along with the FIS response. The test was performed 6 times with different frequencies (5, 2, 1, 0.5, 0.25, and 0.12 s) and each given frequency was measured 5 times. Figure 2.4 shows the valve response and the FIS response in photon counts. The average response for each test (n = 5) was plotted vs. the frequency (Figure 2.5) in order to determine the cut-off frequency (lowest frequency detected by the system). Based on Figure 2.5, system response begins to decline after 2 s. Thus, the time constant τ used for the high frequency loss correction was set to 2 s.

2.4.4. Relative Humidity and Temperature Probe

In 2001, a Vaisala (HMP45A, Vaisala Inc., Helsinki, Finland) relative humidity (RH) and temperature probe was added to the suite of instruments. This instrument was added to provide a slow sensor that would provide a stable measurement of RH and ambient temperature to augment the temperature measured by the sonic, and the H_2O mixing ratio measured by the IRGA. Humidity measurement is based on the capacitive thin film polymer sensor HUMICAP® 180. A resistive platinum sensor is used to measure temperature, and both sensors are located at the tip of the probe protected by a ventilated sun shield. The Vaisala probe was mounted at the same level as the sonic on the tower platform. Accuracy for humidity measurements made in the field at 20°C are ±2% RH between 0-90% RH and ±3% RH between 90-100% RH. Accuracy for the temperature measurements is reported to be ±0.2°C at 20°C.

2.5. Data Acquisition, Storage and Processing

Serial RS-232 data were transmitted from the top of the tower and from the FIS to a computer located in the shelter at the base of the tower. The data acquisition program was written in QuickBasic and the raw 10 Hz data were stored as ASCII files every 30 minutes. The computer used to acquire the data required two serial ports, one for the FIS counts, and one for the serial data stream from the datapacker. Synchronizing the two signals was important, otherwise the serial port buffers on the computer would overflow during the 30-minute period and the difference in time between the two signals would change. Thus, the QuickBasic code checked the buffer sizes and when necessary emptied the buffers in order to keep the two signals synchronized. Absolute synchronization wasn't necessary since there was a delay between the sonic signal and the FIS signal due to the time required to pump the air from the sonic to the FIS at the base of the tower. The delay between the two signals was accounted for using a cross-correlation analysis and assuming the lag was constant over the 30-minute period.

Depending on the instruments used each year, one 30-minute data file ranged in size from 218 Kbytes (Kb) in 1999 to 1,523 Kb in 2002. The files were written to the hard drive and to a CD or zip disk for duplication purposes. Approximately every week the files on the hard drive were saved to a CD and deleted from the hard drive. A standard PC computer with a relatively large hard drive (4 Giga-byte) was used for data acquisition.

The flux processing of the 10 Hz (or 2 Hz) raw data was done off line from the data acquisition system using programs written in IGOR (Wave Metrics, Inc.). There

were many steps involved in converting the raw data into 30-minute averaged fluxes, and each step is briefly described here.

(1) Calibration coefficients were determined, including FIS sensitivity and zero, and IRGA CO_2 and H_2O coefficients. Using the appropriate calibration factors, the raw 10 Hz data were converted from the digital signal into scientific units.

(2) Cross-correlations of vertical velocity and the isoprene mixing ratio were calculated during mid-day periods for a range of lag times (τ) between 0-30 s and the lag time corresponding to the maximum correlation for each 30-minute period was determined. A daily lag time between the sonic signal and the fast isoprene sensor was calculated by averaging the individual τ's for each period within one day. In 1999 when the FIS was located on the tower at the 31 m level, lag times were approximately 3 s. In 2000-2001 lag times ranged between 9-14 s, and in 2002 when the system was located on the PROPHET tower, lag times averaged 12-16 s.

(3) Hard spikes were removed from the raw data including instrumentation spikes and interference from weather such as rain. Unrealistic physical limits were selected for the hard spike filtering.

(4) Coordinate rotation was performed on the 3 wind components to orient u in the mean wind direction (Kaimal and Finnigan 1994).

(5) A second spike filter, referred to as a soft-spike filter was applied to the raw data. Data points were termed a soft spike if their magnitude exceeded the 30-minute standard deviation times a factor (k). The filter uses a 3-step pass-through with the factor k = 3.6,

3.9, and 4.2 for each pass respectively. The duration of the spike was also considered, and if the duration was greater than 2 time steps (0.2 s), then the event was considered realistic and not a spike. The soft-spike filter was developed based on Schmid et al., (2000).

(6) The 30-minute average and standard deviation for each parameter was calculated next using a recursive filter that simulates a running mean (Kaimal and Finnigan 1994; Massman and Lee 2002). There is discrepancy among researchers that collect flux data about the idea of detrending the dataset. The purpose for detrending is to remove trends that are close to but less than the timescale of the averaging period (i.e. 30 minutes). Many researchers apply a 3-minute running mean, however, that can be computationally expensive. Therefore a recursive filter is applied with a time constant (τ) of 3 minutes and the time step (t) of 0.1 s. The recursive filter (which also acts like a low-pass filter) is:

$$y_i = f1\ (y_{i-1}) + f2\ (x_i) \quad (7)$$

$$f1 = 1 - (t_s / \tau) \quad (8)$$

$$f2 = t_s / \tau \quad (9)$$

where x is the original time series, y is the filtered time series, τ is the time constant of the desired filter, and t_s is the time step.

(7) Deviations from the mean, also known as the prime quantities, were calculated by subtracting the average (determined by equation 7) from each instantaneous value.

(8) Instantaneous fluxes were calculated (taking into account appropriate lag times previously determined) as $w'c'$ where c is the scalar (or u' in the case of momentum) and w is the vertical wind.

(9) 30-minute average fluxes were determined for momentum, H, LE, CO_2, and isoprene.

(10) The Webb Pearmann and Leuning correction (Webb et al., 1980) was applied to the CO_2, LE, and isoprene fluxes to account for the simultaneous flux of heat and water vapor, which causes expansion of the air and thus affects the density of the trace gas of interest. If air is pre-dried prior to analysis, there is no need for a correction. If the measurement is in-situ, then there must be two corrections, one for moisture flux and one for heat flux. If air is drawn through a long sample line, temperature fluctuations are dampened and the correction for heat flux is not needed (Massman and Lee 2002). Thus, isoprene fluxes were not corrected for heat flux, only moisture flux.

(11) The last correction necessary was the isoprene flux high-frequency loss correction due to transport through the sampling line and the FIS response time (Leuning and Judd 1996; Jarvis et al., 1997). Since the sensible heat flux is calculated using the sonic temperature, it is assumed that sensible heat flux has negligible frequency loss. By applying a low-pass filter to the sensible heat flux (to simulate the attenuation through the tube for the isoprene flux), we can determine the ratio of the 30-minute averaged unfiltered/filtered sensible heat flux. The ratio for the sensible heat flux is multiplied by

the measured isoprene flux to determine the corrected isoprene flux (Westberg et al., 2001; Guenther and Hills 1998; Massman 2000; Massman and Lee 2002). The low-pass filter selected is the same recursive filter used in step 6, however, the time constant (τ = 2 s) was used based on the frequency response test described in §2.4.3.

Filtering effects due to the path length of the sonic and the IRGA were assumed negligible and there were no corrections applied to these signals. This assumption is based on the fact that the filtering effect due to path length is much smaller than the filtering effect due to a recursive filter provided that the height of the sensor above the surface level is much greater than the path length (Massman and Lee 2002). It was also assumed that the separation distance between sonic and IRGA contributed minimal flux loss (possible phase (time) shifts) to the CO_2 and latent heat fluxes. Phase differences are small for relatively low frequencies, but they can be important for larger frequencies. For all years considered in this report, the horizontal separation distance between the IRGA and the sonic was 0.5 m. Based on work done by Kristensen et al., (1997), a ratio of displacement (D) to measurement height (z), where D/z = 0.5/31 = 0.02 the measured flux is 98% of the "true" flux. Thus, there were no frequency loss corrections applied to other fluxes except isoprene.

2.6. Biomass Measurements and Meteorological Data

As part of the AmeriFlux program, the UMBS~Flux group performed various biomass measurements. A 60 m radius plot surrounding the UMBS~Flux tower was inventoried and all trees within the plot were identified and their diameter at breast height

(dbh) was measured. An additional 60 plots (each 16 m radius) are located at 100 m intervals along seven transect lines radiating from the tower between 255° and 15° azimuth (NW to N direction). All trees within the 61 plots with a dbh greater than 3 cm were used to estimate above ground biomass and distribution of biomass among species. Allometric equations were used to estimate both above and belowground biomass using dbh and tree height (Baldocchi et al., 2001). Table 2.2 summarizes the biomass inventory based on the forest inventory and standard allometric relationships. The isoprene emitting species at this site are bigtooth aspen, quaking aspen, and red oak.

The average canopy height is 22 m and the architecture of the canopy is considered to have a bimodal vertical profile (Baldocchi et al., 2001). There is a large amount of biomass between 14 and 18 m due to the aspen over story, and the understory eastern white pine creates a second biomass increase at approximately 4 m above ground. Figure 2.6 illustrates the vegetation area index (VAI) profile and the biomass density profile, and Figure 2.7 shows the seasonal total VAI for years 1999-2003. All VAI data were collected by the UMBS~Flux group using the leaf area index 2000 (LAI-2000) sensor (Li-Cor, Inc., Lincoln, NE) (Baldocchi et al., 2001).

Additional meteorological data recorded by the UMBS~Flux group were used for various analyses in the following chapters. Above canopy net Radiation (R_n) was recorded using an REBS Q*7.1 (REBS, Inc., Seattle, WA) net radiometer which measures radiation in the 0.25 to 60 μm range. Photosynthetically active photon flux density (PPFD) (0.4 – 0.7 μm) was measured using a Li-Cor LI-190SZ quantum sensor, and short wave radiation (0.4 – 1.1 μm) was measured using a Li-Cor LI-200SA pyranometer. Soil temperature (three locations, five depths: 2, 7.5, 20, 50, and 100 cm)

was continuously recorded, and soil moisture (five depths: 5, 10.2, 20.3, 50.8, and 101.6 cm) was also continuously logged using Vitel Hydra soil moisture probes (Stevens, Inc., Beaverton, OR). Details regarding the UMBS~Flux setup can be found in Schmid et al., (2003) and Curtis et al., (2002).

2.7. Quality Control and Flux Uncertainties

Fluxes can be measured, but the accuracy of these measurements can be difficult to assess because there is no standard method to calibrate any given flux measurement system. The assumptions used to derive the eddy covariance flux equation may be partially satisfied during different times of the day or under different meteorological conditions, and of course the site characteristics are very important. Due to these constraints, typical error analysis techniques cannot be used.

It is important to remember that due to the physical limitations of instrumentation, all eddy covariance systems lose the true turbulent signal at high and low frequencies (Massman and Lee 2002). Aspects that contribute to the loss of flux include the physical size of the instruments (i.e. path length for the sonic anemometer and the open-path IRGA), their separation distances, their placement on the tower and the flow distortion caused by the instruments and tower, the instrument time response (including time in the sample line), and any processing of the raw data such as detrending or mean removal (Massman 2000; Horst 1997; Massman and Lee 2002).

There are two general types of errors associated with eddy covariance measurements. Systematic errors are consistent over- or under- readings of fluxes, and

they can be the most detrimental. Some examples of systematic errors include: 1) incorrect calibrations, 2) under predicted nighttime fluxes due to drainage flow, 3) inadequate sensor response or flow distortion and 4) incorrect processing of fluxes (i.e. incorrect application of the Webb, Pearman and Leuning correction or the high frequency loss correction). Businger (1986) compared 6 eddy covariance systems and found systematic errors up to 30% between the various systems. Random errors, on the other hand, are inherent in the fact that we are measuring turbulence at one point in space and time, the site is not always homogeneous, weather is not constant (non-stationarity), and the size of the flux footprint varies (Moncrieff et al., 1996). Random errors will decrease with increasing sample size, however, systematic errors are cumulative and are often the hardest to detect. The natural variability of turbulence is between 10 and 20% (Wesely and Hart 1985).

The rest of this section describes some of the steps taken to ensure the best quality data, and in the last section an estimate of the total uncertainty of the flux measurements is presented.

2.7.1. Raw Data Analysis

Obviously the first place for quality control of the data is with the raw instantaneous data. Statistical tests performed on the raw data can help to identify instrument and data acquisition errors before data analysis. Spikes in the data caused by random electronic noise or sonic transducer blockage (i.e. during precipitation) are usually the first analysis done to the raw data. Spikes can be detected using absolute limits for each variable (previously described as hard spikes) and algorithms can be developed to detect and remove other spikes, previously referred to as soft spikes

(discussed in §2.5.). Instead of replacing data that has been removed, the flagged data is simply replaced with "not a number" and is consequently ignored in all future analyses. If over 50% of the raw data for one 30-minute period is missing, then the flux for that 30-minute period is not computed due to insufficient data. The number of spikes removed from the raw data can vary tremendously from one day to the next, but for a typical day <2% of the 10 Hz data is removed during the hard and soft spike filters. By minimizing problems with the raw data the objective is to compute fluxes with less random noise.

2.7.2. Energy Balance Closure

Theoretically based on the first law of thermodynamics, the energy input to a forested system should equal the energy associated with all the processes such as evaporation, sensible heat, photosynthesis, and canopy storage. Therefore, if independent measurements of the above processes are made, then the energy balance can be computed for periods of a day or across an entire season, and the balance of the energy budget should indicate the validity of the measurements. However, almost all researchers employing eddy covariance trace gas flux measurements report an underestimate of the sum of the various processes compared to the available energy. In general it appears that the incoming energy is typically 10-30% greater than the sum of the canopy processes (Massman and Lee 2002; Wilson et al., 2002). Thus, corrections for this apparent underestimate are necessary, however, as of now, no one has been able to determine which of the terms are incorrect. Several have proposed that a possible loss of the low frequency portion of the flux is primarily responsible for the lack of energy balance closure (Sakai et al., 2001; Finnigan et al., 2003). Nonetheless, performing an energy balance is one way to assess the uncertainty associated with flux measurements for a

system. Even though the energy balance closure does not involve isoprene fluxes or CO_2 fluxes, atmospheric transport processes are similar between all the various scalars, all scalars are determined using eddy covariance (Wilson et al., 2002), and there is close biophysical coupling between carbon, energy, water and isoprene fluxes. The general equation for the energy balance is:

$$LE + H = R_n - G - S - Q \quad (10)$$

where LE is latent heat flux, H is sensible heat flux, R_n is net radiation, G is the soil heat flux, S is the rate of change of heat storage (air and biomass) between the ground level and the measurement height, and Q is the sum of all additional energy sources and sinks, (i.e. photosynthesis). Q is typically neglected as a small term, but S can potentially be important in tall, forested canopies (Wilson et al., 2002). Linear regression coefficients (slope and y-intercept) were determined based on the ordinary least squares (OLS) relationship between 30-minute averaged LE + H versus R_n. Soil heat flux (G) and the rate of change of heat storage (S) were not available for analysis. Results for the four years are shown in Figure 2.8, using the entire dataset (i.e. including nighttime fluxes). Table 2.3 summarizes the regression coefficients for the OLS relationship between all fluxes, and just daytime fluxes (10:00 am – 4:00 pm local time) when generally flux measurements are more reliable.

The slopes and intercepts reported in this study compare very well with those reported by Wilson et al., (2002) in his review of energy balance closure across all the FLUXNET sites. Considering that G and S are not included in our analysis, the slopes

still compare well to the mean slope of 0.79 ± 0.01 derived from 50 site-years worth of data. Of the 50 site-years presented, 26 site-years reported canopy heat storage (S). Including S in the regression for forested sites increased the slope on average by 7%. In contrast, soil heat flux (G) had less of an impact in the forested sites. Including G in the OLS regression only increased the slope on average by 3%. By including a very crude estimate for G and S in our OLS regression (estimated to be 10% of H + LE), the slopes increased by 7% for 1999, 2000, and 2001, and 5% for 2002. Similarly, Su et al., (2004) report energy balance closure results for the same site (measurements made at the 46 m level). Using hourly measurements during the day within the growing season but outside of the transition periods when S is large, and forcing the linear regression through the origin, they report slopes of 0.97 (1999), 0.94 (2000), and 0.96 (2001). In comparison to Su et al., (2004), our lower slopes for the energy balance closure may be indicative of a systematic error, possibly related to the difference in measurement height, or the difference in LE measurements (open-path IRGA vs. closed-path IRGA). However, without measurements of G and S, we can only speculate on these potential errors. Overall the reported energy balance results compare quite well with other eddy covariance flux sites, and even though energy balance closure isn't a true error analysis, the degree of closure can indicate the general soundness of a system and the associated methods of analysis (Schmid et al., 2003).

2.7.3. Comparison with UMBS~Tower Fluxes

Independent measurements of CO_2, H, LE, and momentum fluxes were measured at two different heights (46 m and 34 m) by the UMBS~Flux group. Details regarding

their flux system setup and measurements are summarized in Schmid et al., (2003), Su et al., (2004), and Curtis et al., (2002). Obviously a comparison between 3 independent systems should provide some quantitative measure of how the systems compare. The primary differences between the 3 systems include different measurement heights (thus slightly different footprints), a different type of analyzer for CO_2/H_2O fluxes, different processing procedures, and different averaging time periods. More specifically, the UMBS~Flux tower employs a closed-path IRGA. Therefore, air is transported through a sample line to the base of the tower (tube attenuation occurs) where it is measured in a temperature-controlled environment. The WSU system employs an open-path IRGA which is located near the sonic so no transport and attenuation occurs, but measurements must be corrected for density fluctuations using the Webb, Pearman and Leuning correction (Webb et al., 1980). In addition, the UMBS~Flux system computes hourly averaged fluxes using a 15-minute blocked average vs. the WSU 30-minute averaged fluxes based on a 3-minute running mean detrending routine.

However, if we remove as many differences as possible, and then compare the measured fluxes, how well do the fluxes compare? A comparison between just the UMBS~Flux measurements at 34 m and 46 m was briefly presented by Schmid et al., (2003). For this comparison, the system and the processing steps are identical and the only difference is the sample height. They report marked differences in the cumulative net ecosystem exchange (NEE) between the two heights, with the differences stemming from small but persistent biases that affect the CO_2 fluxes more than the sensible heat fluxes. There are no magnitudes reported for the differences between the two fluxes, only that the 46 m CO_2 flux values are larger in magnitude (for both positive and

negative) than the 34 m values, and that the bias is reduced in the sensible heat fluxes (Schmid et al., 2003).

A more quantitative comparison between the WSU (31 m) fluxes and the UMBS~Flux (46 m) fluxes was done by determining linear regression statistics between hourly averaged fluxes. The UMBS~Flux 34 m level fluxes should be more comparable to the WSU 31 m fluxes, however, only the 46 m level fluxes were available. As shown in Figure 2.9, the 2000 UMBS~Flux hourly measurements are plotted against the WSU hourly averaged fluxes for CO_2, H, LE, and friction velocity. The best-fit line is shown as a solid line, while the dashed line represents the one-to-one line. In 2000, the slope of the LE fluxes is 1.35 indicating that the WSU LE fluxes are less than the UMBS~Fluxes. The opposite is true for CO_2 fluxes. With a slope of 0.68 for CO_2, the WSU fluxes are greater in magnitude than the UMBS~Fluxes. The linear regression statistics for all three years are reported in Table 2.4. The "Offset" is the expected UMBS~Flux value when the WSU flux value is zero and "relative offset" is the offset divided by the standard deviation of the UMBS~flux value. For all years, friction velocity compares the best between the two systems with the slope ranging from 1.0 to 1.2. Sensible heat flux also compares well between the systems with relative offsets <3%, while LE and CO_2 have relative offsets ranging from 1 to 16%. Table 2.4 also contains linear regression statistics between the UMBS~Flux system at 46 m and at 34 m (for H and CO_2 only) (Schmid et al., 2003).

2.7.4. Estimate of Uncertainty

To estimate the overall uncertainty in flux measurements, we can identify the uncertainties associated with each measurement (i.e. isoprene concentration, temperature,

wind speed, etc.), however, combining the errors from the measurements along with the errors associated with the theoretical assumptions inherent in the eddy covariance technique makes it more difficult. Table 2.5 identifies the various contributions to the total error involved with flux measurements. Many of these have been explained in previous sections. Based on the errors listed in Table 2.5 and discussed in the previous sections, we estimate that the uncertainty associated with H is ~20%, and for CO_2 and LE the uncertainty is ~30%. As previously mentioned, this is for daytime fluxes, and it is expected that uncertainties are probably greater for nighttime fluxes of H, LE, and CO_2. The uncertainty related to isoprene fluxes is on the order of 40%. Errors may not be this large at all times, but to be conservative we must anticipate the possibility. Currently, the uncertainty in biogenic emission estimates is 50% or more (Guenther et al., 2000; Geron et al., 1997).

2.8. References

Auble, D. L. and Meyers, T. P. 1992. An open path, fast response infrared absorption gas analyzer for H2O and CO2. *Boundary-Layer Meteorology* 59, 243-256.

Baldocchi, D., Falge, E., Gu, L., Olson, R., Hollinger, D., Running, S., Anthoni, P., Bernhofer, C., Davis, K., Evans, R., Fuentes, J., Goldstein, A., Katul, G., Law, B., Lee, X., Malhi, Y., Meyers, T., Munger, W., Oechel, W., Paw U., K. T., Pilegaard, K., Schmid, H. P., Valentini, R., Verma, S., Vesala, T., Wilson, K., Wofsy, S. 2001. FLUXNET: a new tool to study the temporal and spatial variability of ecosystem-scale carbon dioxide, water vapor and energy flux densities. *Bulletin of the American Meteorological Society* 82, 2415-2434.

Baldocchi, D. D., Hicks, B. B., Meyers, T. P. 1988. Measuring biosphere-atmosphere exchanges of biologically related gases with micrometeorological methods. *Ecology* 69, 1331-1340.

Businger, J. A. 1986. Evaluation of the accuracy with which dry deposition can be measured with current micrometeorological techniques. *Journal of Climate and*

Applied Meteorology 25, 1100-1124.

Carroll, M. A., Bertman, S. B., Shepson, P. B. 2001. Overview of the program for research on Oxidants: PHotochemistry, Emissions, and Transport (PROPHET) summer 1998 measurements intensive. *Journal of Geophysical Research* 106, 24275-24288.

Curtis, P. S., Hanson, P. J., Bolstad, P., Barford, C., Randolph, J. C., Schmid, H. P., Wilson, K. B. 2002. Biometric and eddy-covariance based estimates of annual carbon storage in five eastern North American deciduous forests. *Agricultural and Forest Meteorology* 113, 3-19.

Dabberdt, W. F., Lenschow, D. H., Horst, T. W., Zimmerman, P. R., Onlcey, S. P., Delany, A. C. 1993. Atmosphere-Surface Exchange Measurements. *Science* 260, 1472-1481.

Finnigan, J. J., Clement, R., Malhi, Y., Leuning, R., Cleugh, H. A. 2003. A Re-Evaluation of Long-Term Flux Measurement Techniques - Part I: Averaging and Coordinate Rotation. *Boundary-Layer Meteorology* 107, 1-48.

Geron, C. D., Nie, D., Arnts, R. R., Sharkey, T. D., Singsaas, E. L., Vanderveer, P. J., Guenther, A., Sickles, J. E., Kleindienst, T. E. 1997. Biogenic isoprene emission: model evaluation in a southeastern United States bottomland deciduous forest. *J. Geophys. Res.* 102, 18889-18901.

Guenther, A. B. and Hills, A. J. 1998. Eddy covariance measurement of isoprene fluxes. *Journal of Geophysical Research* 103, 13145-13152.

Guenther, A., Geron, C., Pierce, T., Lamb, B., Harley, P., Fall, R. 2000. Natural emissions of non-methane volatile organic compounds; carbon monoxide, and oxides of nitrogen from North America. *Atmos. Environ.* 34, 2205-2230.

Hills, A. J. and Zimmerman, P. R. 1990. Isoprene measurement by ozone-induced chemiluminescence. *Anal. Chem.* 62, 1055-1060.

Horst, T. W. 1997. A simple formula for attenuation of eddy fluxes measured with first-order-response scalar sensors. *Boundary-Layer Meteorology* 82, 219-233.

Jarvis, P. G., Massheder, J. M., Hale, S. E., Moncrieff, J. B., Rayment, M., Scott, S. L. 1997. Seasonal variation of carbon dioxide, water vapor, and energy exchanges of a boreal black spruce forest. *Journal of Geophysical Research* 102, 28953-28966.

Kaimal, J. C. and Finnigan, J. J. 1994. *Atmospheric Boundary Layer Flows: Their Structure and Measurement.*, New York: Oxford University Press.

Kristensen, L., Mann, J., Oncley, S. P., Wyngaard, J. C. 1997. How close is close enough when measuring scalar fluxes with displaced sensors? *Journal of Atmospheric and Oceanic Technology* 14, 814-821.

Lenschow, D. H. and Raupach, M. R. 1991. The attenuation of fluctuations in scalar concentrations through sampling tubes. *Journal of Geophysical Research* 96, 15259-15268.

Leuning, R. and Moncrieff, J. 1990. Eddy-covariance CO2 flux measurements using open- and closed-path CO2 analysers: corrections for analyser water vapour sensitivity and damping of fluctuations in air sampling tubes. *Boundary-Layer Meteorology* 53, 63-76.

Leuning, R. and Judd, M. J. 1996. The relative merits of open- and closed-path analysers for measurement of eddy fluxes. *Global Change Biology* 2, 241-253.

Massman, W. J. 2000. A simple method for estimating frequency response corrections for eddy covariance systems. *Agricultural and Forest Meteorology* 104, 185-198.

Massman, W. J. and Lee, X. 2002. Eddy covariance flux corrections and uncertainties in long-term studies of carbon and energy exchanges. *Agricultural and Forest Meteorology* 113, 121-144 .

Massman, W. J. 1991. The attenuation of concentration fluctuations in turbulent flow through a tube. *Journal of Geophysical Research* 96, 15269-15273.

Moncrieff, J. B., Malhi, Y., Leuning, R. 1996. The propagation of errors in long-term measurements of land-atmosphere fluxes of carbon and water. *Global Change Biology* 2, 231-240.

Munger, J. W., Wofsy, S. C., Bakwin, P. S., Fan, S.-M., Goulden, M. L., Daube, B. C., Goldstein, A. H. 1996. Atmospheric deposition of reactive nitrogen oxides and ozone in a temperate deciduous forest and a subarctic woodland. I. Measurements and mechanisms. *Journal of Geophysical Research* 101D, 57-63.

Pearsall, D. R. 1995. Landscape ecosystems of the University of Michigan Biological Station, northern lower Michigan: Ecosystem diversity and biological diversity. Thesis. University of Michigan.

Sakai, R. K., Fitzjarrald, D. R., Moore, K. E. 2001. Importance of Low-Frequency Contributions to Eddy Fluxes Observed over Rough Surfaces. *Journal of Applied Meteorology* 40, 2178-2192.

Schmid, H. P., Su, H.-B., Vogel, C. S., Curtis, P. S. 2003. Ecosystem-atmosphere exchange of carbon dioxide over a mixed hardwood forest in northern lower Michigan. *Journal of Geophysical Research* 108, art. no.-4417.

Schmid, H. P., Grimmond, C. S. B., Cropley, F., Offerle, B., Su, H.-B. 2000. Measurements of CO2 and energy fluxes over a mixed hardwood forest in the mid-western United States. *Agricultural and Forest Meteorology* 103, 357-374.

Stull, R. B. 1989. *An Introduction to Boundary Layer Meterology*, Norwell, MA: Kluwer Academic Publishers.

Su, H. B., Schmid, H. P., Grimmond, C. S. B., Vogel, C. S., Oliphant, A. J. 2004. Spectral Characteristics and Correction of Long-Term Eddy-Covariance Measurements Over Two Mixed Hardwood Forests in Non-Flat Terrain. *Boundary-Layer Meteorology* 110, 213-253.

Swinbank, W. C. 1951. The measurement of vertical transfer of heat and water vapour by eddies in the lower atmosphere. *Journal of Meteorology* 8, 135-145.

Webb, E. K., Pearman, G. J., Leuning, R. 1980. Correction of flux measurements for density effects due to heat and water vapor transfer. *Quarterly J. R. Meteorological Society* 106, 85-100.

Wesely M.L, Hart R.L. 1985. Variability of short term eddy-correlation estimates of mass exchange. In *The Forest-Atmosphere Interaction*, ed. Hutchison, B. A., Hicks, B. B., pp. 591-661

Westberg, H., Lamb, B., Hafer, R., Hills, A., Shepson, P., Vogel, C. 2001. Measurement of isoprene fluxes at the PROPHET site. *Journal of Geophysical Research* 106, 24347-24358.

Wilson, K., Goldstein, A., Falge, E., Aubinet, M., Baldocchi, D., Berbigier, P., Bernhofer, C., Ceulemans, R., Dolman, H., Field, C., Grelle, A., Ibrom, A., Law, B. E., Kowalski, A., Meyers, T., Moncrieff, J., Monson, R., Oechel, W., Tenhunen, J., Valentini, R., Verma, S. 2002. Energy balance closure at FLUXNET sites. *Agricultural and Forest Meteorology* 113, 223-243.

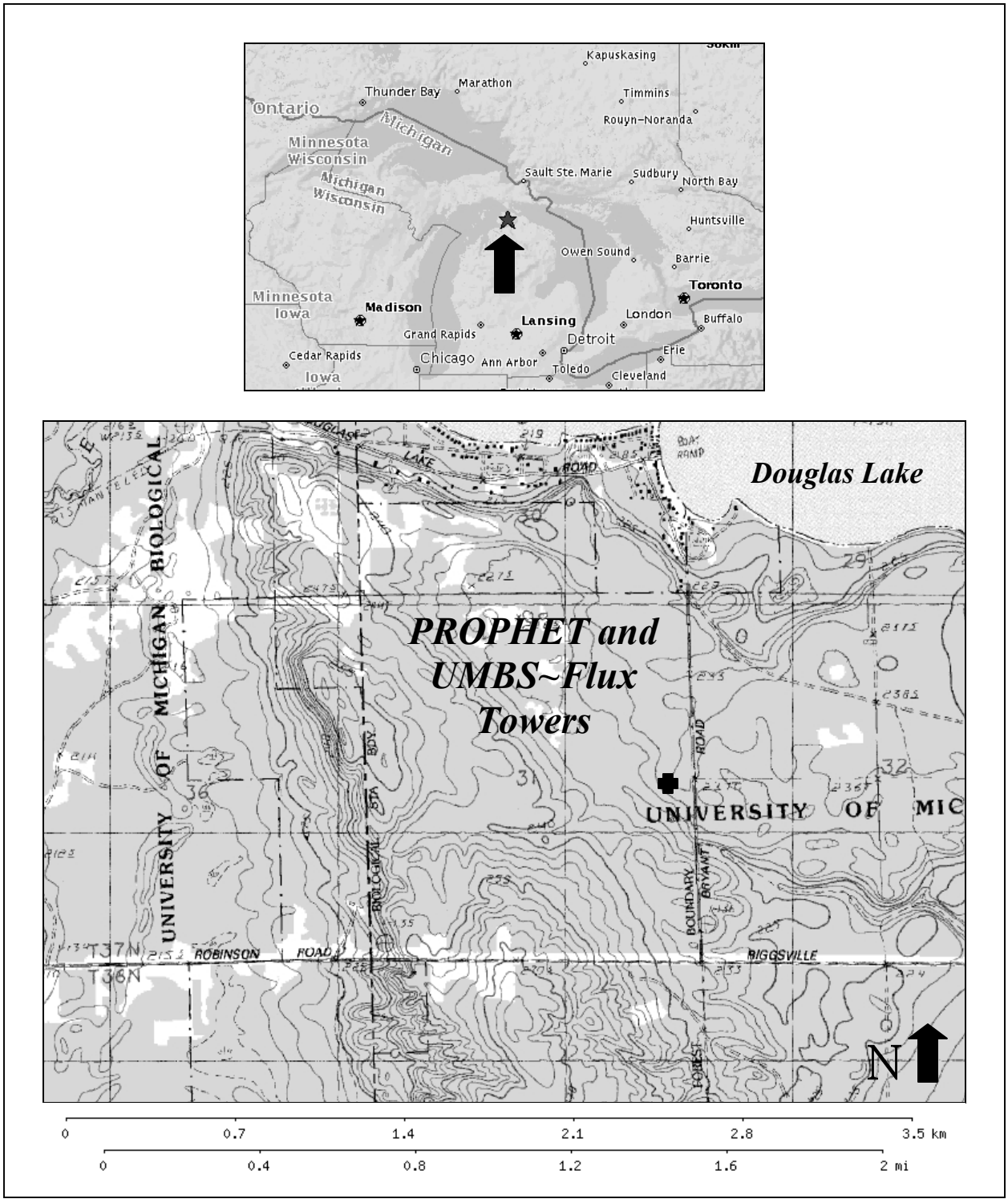

Figure 2.1: Location of the UMBS~Flux and PROPHET towers in the northern part of Michigan's lower peninsula. The closest town is Pellston, located approximately 7 km to the west. Top map provided by Mapquest and bottom map provided by USGS.

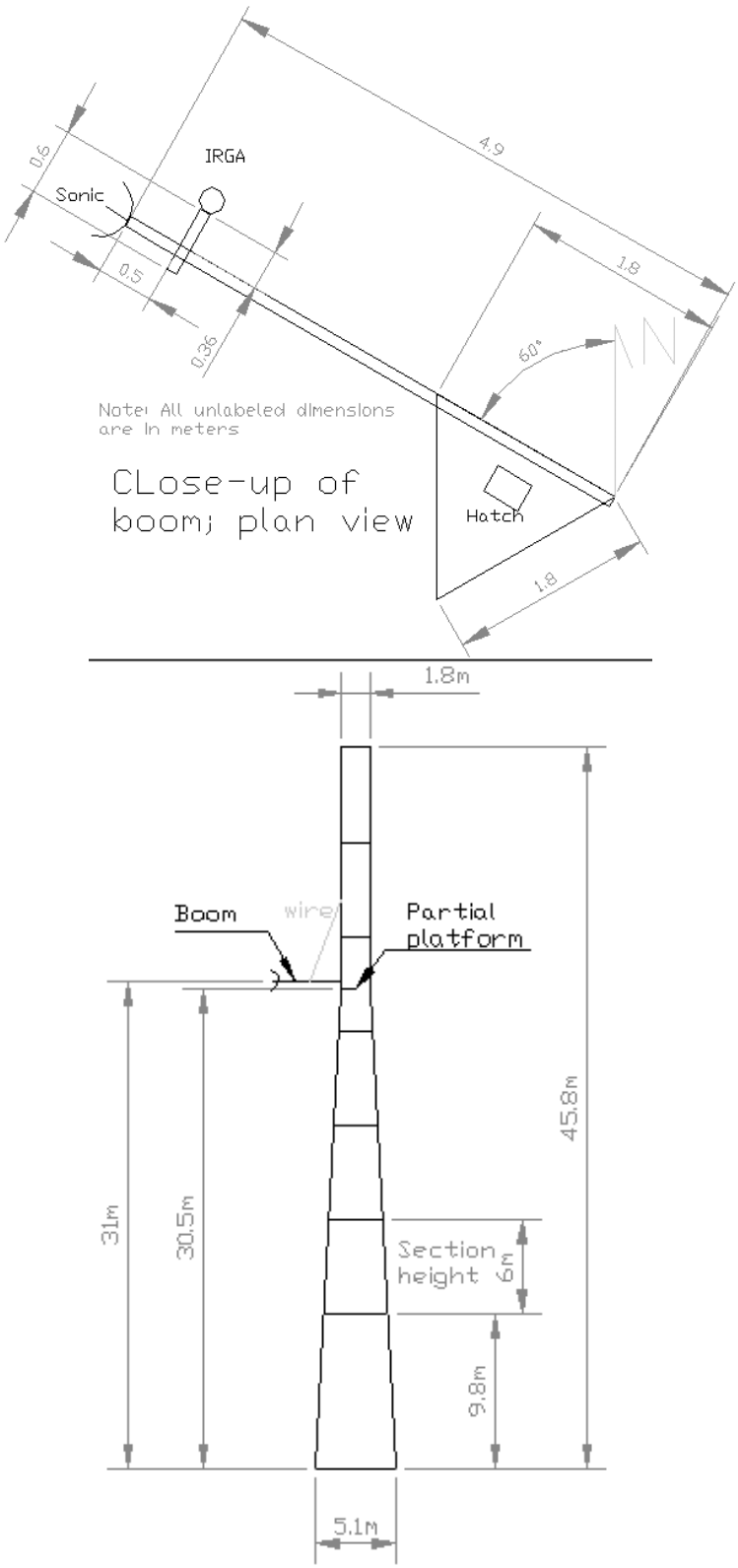

Figure 2.2: Schematic of the WSU flux system on the AmeriFlux tower for years 1998-2001.

Figure 2.3: Isoprene flux instrumentation mounted on the UMBS~Flux tower.

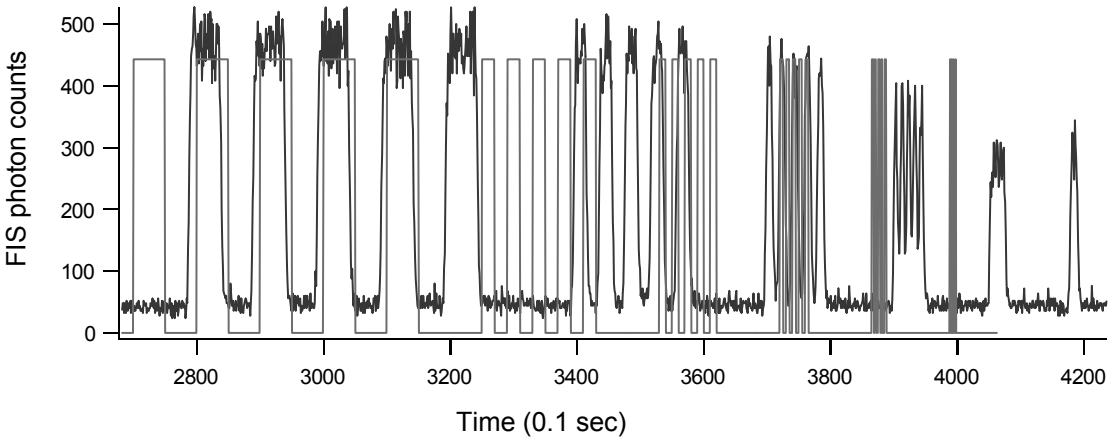

Figure 2.4: Frequency response test results performed in the laboratory in the spring of 2000. Square plots (gray trace) indicate the solenoid valve position, which controlled the isoprene standard, and the dark trace is the FIS response (photon counts).

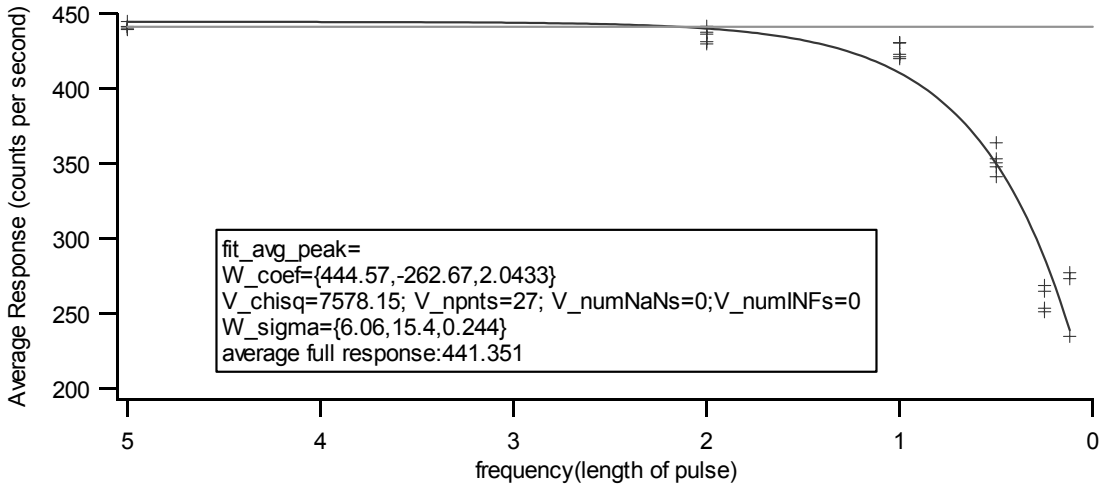

Figure 2.5: System response (sample line and FIS) vs. frequency of test.

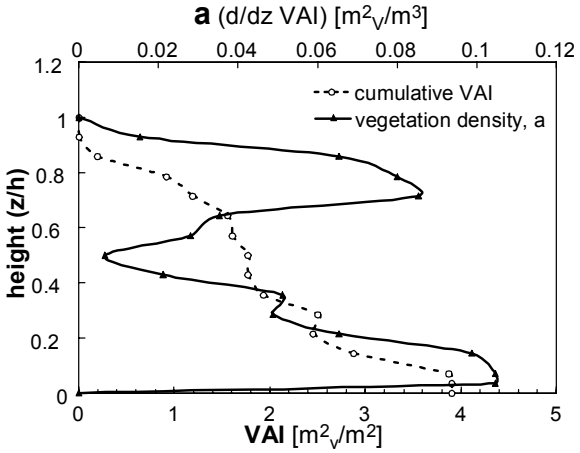

Figure 2.6: Vegetation area index (VAI) profile measured at UMBS~Flux tower in 1999. Cumulative VAI measured with leaf area index 2000 (LAI-2000, Li-Cor) sensor nine times at same height. Vegetation density derived from the average cumulative VAI. Figure provided by UMBS~Flux group.

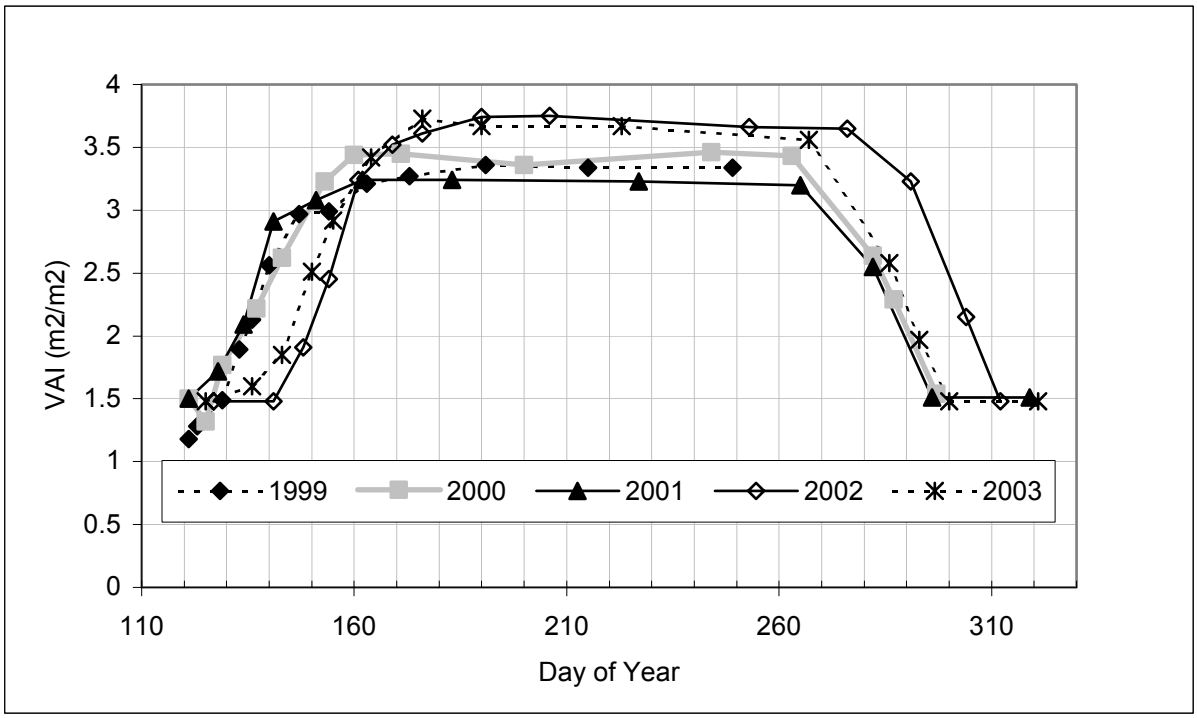

Figure 2.7: Seasonal VAI for 1999-2003 in the 60 m main plot measured with the LAI 2000 plant canopy analyzer. Each point represents the mean of multiple measurements along different transects emanating from the tower.

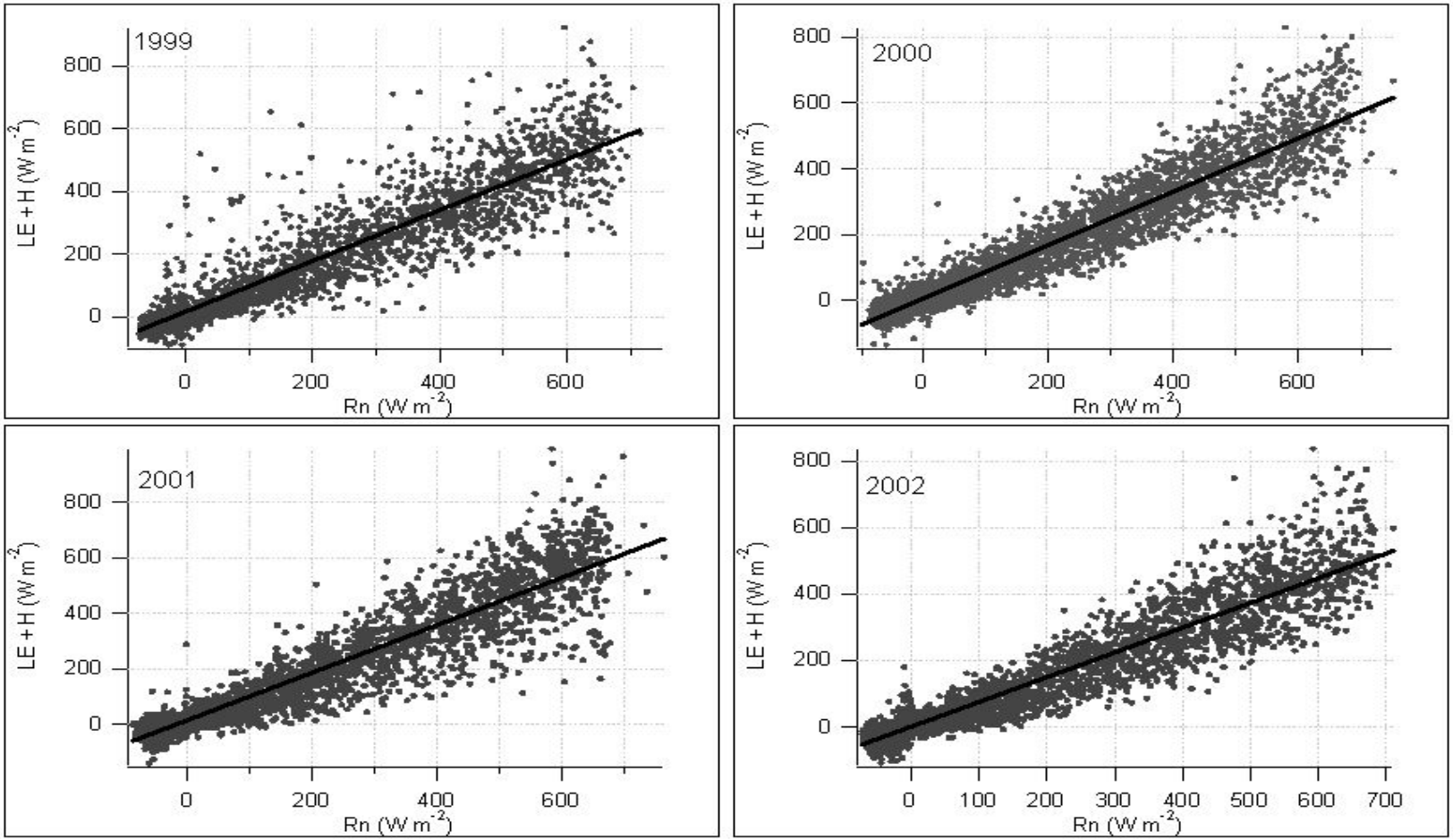

Figure 2.8: Energy Balance graphs for each growing season (including leaf out and leaf senescence periods). Each point represents a 30-minute averaged sum of the energy fluxes vs. net radiation. Day and night values are shown. Regression coefficients are presented in Table 2.3.

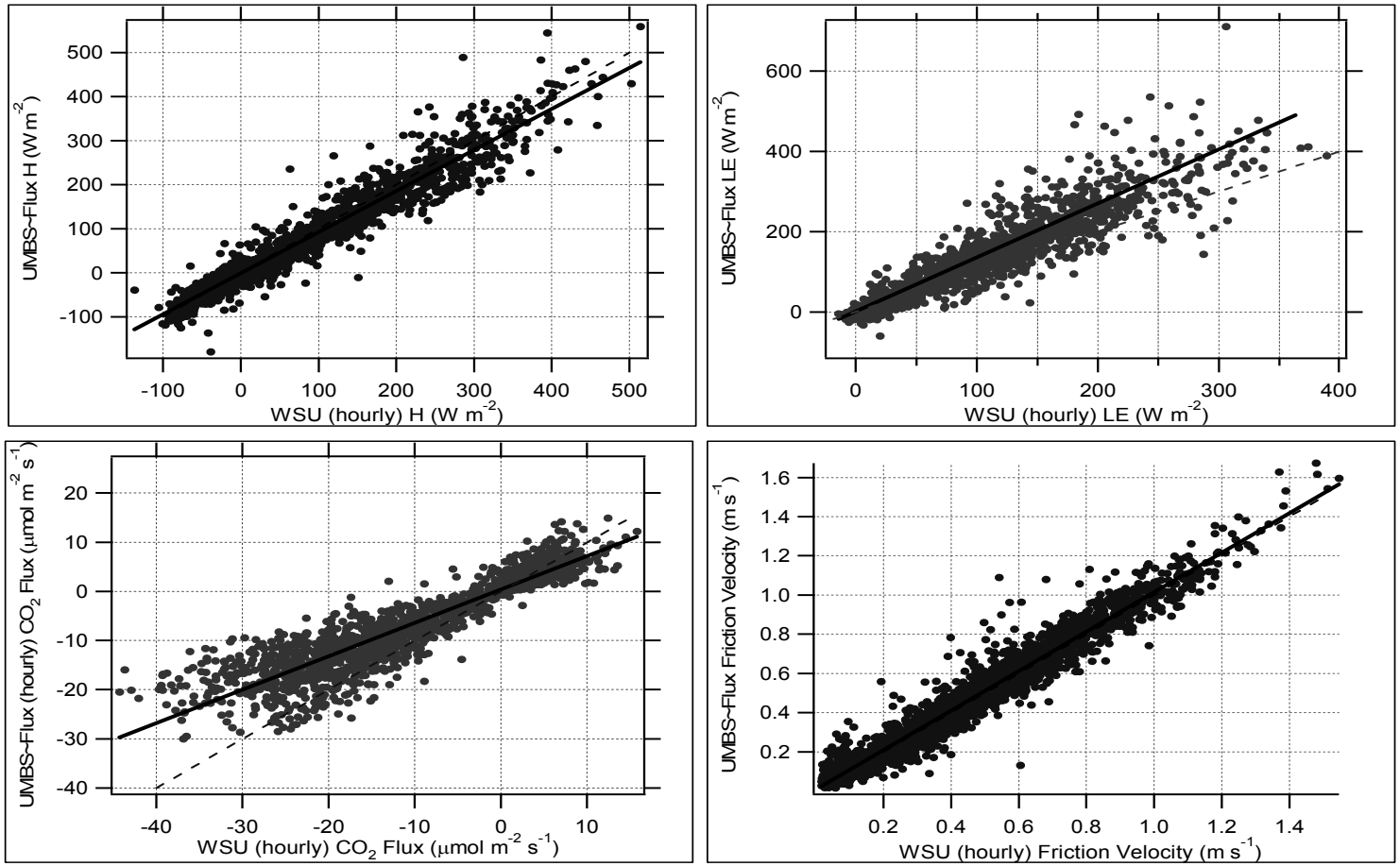

Figure 2.9: Linear regressions of the UMBS~Flux tower data (46 m) against the WSU 31 m level measurement data for 2000. All data shown are hourly fluxes for the entire dataset. Solid line is the linear regression; dashed line is the 1:1 line. Linear regression coefficients are summarized for 2000, 2001, and 2002 in Table 2.4.

Table 2.1: Summary of WSU flux operating conditions from 1997 through 2002 at the UMBS PROPHET/AmeriFlux site.

Item	1997	1998	1999	2000	2001	2002
Tower	PROPHET	UMBS~Flux	UMBS~Flux	UMBS~Flux	UMBS~Flux	PROPHET
Sonic Height (m)	30	31	31	31	31	32
Sonic Anemometer	ATI (K probe)	ATI (K probe)	ATI (K probe)	ATI (K probe)	ATI (K probe)	ATI (K probe)
CO_2/H_2O	No	Open path IRGA[a]	Open path IRGA[a] at 31m	Open path IRGA[a] at 31m	Open path IRGA[a] at 31m	Open path IRGA[a] at 32m
Boom Orient. (deg)		300°	300°	300°	300°	340°
Start Day	8 days total	August 2	May 20	May 28	June 7	May 14
End Day		August 17	October 20	October 5	September 23	September 28
Inlet	WSU REA system	¼ in.Teflon (25 ft.)	¼ in. Teflon (25 ft.)	5/8 in. Teflon + ¼ in. Teflon	5/8 in. Teflon + ¼ in. Teflon	5/8 in. Teflon + ¼ in. Teflon
Data collection software	QB REAflux.bas	QB Isoflux.bas (realtime flux calculations)	QB sonic.bas (raw data collection)	QB sonic.bas (raw data collection)	QB sonic.bas (raw data collection)	QB sonic.bas (raw data collection)
Data Scan Rate	10 Hz	10 Hz	2 Hz	10 Hz	10 Hz	10 Hz
Fast Isoprene Sensor (FIS)	None	SD FIS-99	NCAR FIS-00	WSU FIS-00	WSU FIS-00	WSU FIS-00 upgraded
FIS Calibration	NA	Manual 2 to 3 times daily	Manual 2 to 3 times daily	Manual 2 to 3 times daily	Manual 2 to 3 times daily	Automatic 3 times daily
Peripheral Data					T, RH Vaisala	T, RH Vaisala
Ameriflux data	None	Limited	34 m & 46 m	34 m & 46 m	34 m & 46 m	34 m & 46 m
Last day of season where 21m T < 0.5°C	NA	NA	108 (-0.79°C)	110 (-0.82°C)	108 (-1.64°C)	139 (-1.4°C)

Notes: ATI = Applied Technologies, Inc., a = Auble and Meyers open path Infrared gas analyzer (IRGA) (Auble and Meyers 1992)

REA = relaxed eddy accumulation, QB = Quick Basic program, SD = South Dakota (Pat Zimmerman)

Table 2.2: Total above-ground woody biomass C (kg C·ha^{-1}) and foliar biomass C (kg C·ha^{-1}) for 1999, 2000, and 2001 across the UMBS~Flux footprint. Total woody and leaf biomass estimated from measurements made after leaf fall in November 1999, 2000, and 2001. N = 61 for all variables except for leaves in year 2000 and 2001 where N = 60. Mean ± (SE) includes 60m plot. Data provided by C. Vogel, UMBS~Flux.

Species	**Leaf Biomass C**					
Year	**1999**	**2000**	**2001**	**1999**	**2000**	**2001**
A. rubrum	8484	8702	8923	308.3	361.2	356.0
(red maple)	(1053)	(1081)	(1109)	(24.6)	(30.2)	(30.6)
A. saccharum	896	918	942	19.5	19.7	20.9
(sugar maple)	(429)	(440)	(453)	(8.6)	(9.4)	(9.8)
B. papyrifera	6658	6829	6990	129.4	139.3	125.7
(paper birch)	(1081)	(1108)	(1134)	(21.0)	(20.7)	(18.8)
F. grandifolia	2625	2679	2741	64.7	72.1	71.4
(American beech)	(913)	(933)	(955)	(20.4)	(23.7)	(23.6)
Pinus strobus	1285	1335	1389	25.6	26.7	23.2
(eastern white pine)	(450)	(466)	(484)	(7.7)	(8.3)	(7.1)
P. grandidentata	24562	25218	25878	345.8	405.1	362.0
(bigtooth aspen)	(3082)	(3163)	(3245)	(35.5)	(41.7)	(35.7)
P. tremuloides	12111	12488	12861	189.8	224.0	152.6
(quaking aspen)	(2836)	(2914)	(2987)	(41.7)	(49.1)	(36.9)
Q. rubra	7499	7734	7905	163.5	195.6	224.2
(red oak)	(1535)	(1583)	(1618)	(22.8)	(30.6)	(38.1)
Other	239	242	246	16.2	50.8	13.2
	(51)	(53)	(53)	(4.0)	(6.0)	(3.2)
Total	64357	66146	67876	1262.9	1494.6	1349.1
	(2825)	(2887)	(2948)	(32.1)	(38.7)	(49.0)

Table 2.3: Ordinary least squares (OLS) regression coefficients for energy balance closure for each year with all flux data available and with just daytime fluxes (10:00 – 4:00 local time). *n* is the number of 30-minute periods.

	n	y-intercept	Slope	r^2
All fluxes				
1999	3786	16.2	0.81	0.94
2000	4863	7.2	0.81	0.96
2001	3772	15.2	0.85	0.94
2002	4065	0.42	0.75	0.95
Daytime Fluxes				
1999	924	42.8	0.77	0.80
2000	1221	-11.4	0.86	0.88
2001	956	-18.6	0.92	0.79
2002	993	-22.4	0.79	0.84

Table 2.4: Linear regression statistics of hourly averaged values of sensible heat flux, latent heat flux, CO_2 flux and friction velocity from the UMBS~Flux tower (46 m) against the WSU 31 m measurement level for 2000 and 2001. Values in ( ) for 2000 are the UMBS~Flux tower (46 m) against the UMBS~Flux tower (34 m) level. For 2002 it is the UMBS~Flux tower (46 m) against the WSU-PROPHET 34 m tower. The offset is the expected UMBS~Flux tower value when the WSU value is zero, relative offset is the offset divided by the standard deviation of the UMBS~Flux value, a slope greater than unity indicates that the UMBS~Flux values are larger than the WSU values, r^2 is the coefficient of determination and *n* is the number of values in the regression.

	Sensible Heat flux ($W\ m^{-2}$)	Latent Heat flux ($W\ m^{-2}$)	CO_2 flux ($\mu mol\ m^{-2}\ s^{-1}$)	Friction velocity ($m\ s^{-1}$)
2000				
Offset	-1.31 (-1.2)	1.35	0.40 (0.17)	0.010
Relative Offset	1.3% (0.9%)	1.2%	4.4% (1.9%)	3.4%
Slope	0.93 (0.98)	1.35	0.68 (1.03)	1.01
r^2	0.97 (0.98)	0.92	0.93 (0.96)	0.97
n	2434 (1824)	1678	2100 (1824)	2485
2001				
Offset	-2.75	19.60	-0.36	0.009
Relative Offset	2.7%	16.1%	4.0%	3.2%
Slope	0.91	0.97	0.37	1.02
r^2	0.97	0.89	0.87	0.97
n	1888	1432	1442	1990
2002				
Offset	1.00	12.38	0.42	-0.012
Relative Offset	0.97%	9.3%	4.4%	4.4%
Slope	0.95	1.33	0.72	1.00
r^2	0.95	0.90	0.92	0.94
n	2631	1530	1633	2631

Table 2.5: Known errors and uncertainties associated with eddy covariance flux measurements.

Description	Uncertainty
Sonic wind speed	5%
Sonic temperature	5%
CO_2 and H_2O fluxes	10%
Isoprene concentrations (10 Hz)	20%
Sensor separation	2%
Random errors	10-20%
Systematic errors	Up to 30%

CHAPTER 3

LONG TERM ISOPRENE FLUX MEASUREMENTS ABOVE A NORTHERN HARDWOOD FOREST

3.1. Abstract

We report continuous whole canopy isoprene emission fluxes from a northern hardwood forest in Michigan for the 1999-2002 growing seasons. The eddy covariance fluxes of isoprene, CO_2, latent heat, and sensible heat are presented along with an analysis of the seasonal and year-to-year variations. Measurements were made in collaboration with the AmeriFlux site located at the University of Michigan Biological Station (UMBS) and the Program for Research on Oxidants: PHotochemistry, Emissions, and Transport (PROPHET). In general, isoprene emissions increased throughout the day with increasing temperature and light levels, peaked at mid-afternoon, and declined to zero by night. There were significant variations from one 30-minute period to the next, and from one day to the next. Average midday isoprene fluxes were 2.8, 3.2, and 2.9 mg C m^{-2} h^{-1} for 2000 through 2002 respectively. Insufficient data was available to include 1999. Last frost and full leaf out were significantly later in 2002 compared to the other years, however, total accumulated isoprene emissions for each year varied by less than 10%. Fully developed isoprene emissions occurred between 400 and 500 heating degree days, roughly half those required at other sites. Using long-term net ecosystem exchange measurements from the UMBS~Flux group, isoprene emissions represents between 1.7 to 3.1% of the net carbon uptake at this site. Observations for 2000-2002 were compared with the BEIS3 emission model. Estimates agree well with observations during the mid-

summer period, but BEIS3 overestimates observations during the spring onset of emissions and the fall decline in emissions. This work provides a unique long-term dataset useful for verifying canopy scale models and to help us better understand the dynamics of biosphere atmosphere exchange of isoprene.

3.2. Introduction

Isoprene (2-methyl-1,3-butadiene) is one of the most reactive naturally emitted hydrocarbons, and it is one of the most abundant biogenic hydrocarbon species found over forested environments. Isoprene, along with other biogenic hydrocarbons, plays an important role in tropospheric chemistry at regional and global scales, and improved quantification of the biospheric source strength is crucial for photochemical modeling applications. The primary removal mechanism for isoprene from the troposphere is oxidation by hydroxyl radicals (HO), ozone and nitrate radicals. Isoprene oxidation products (alkyl peroxy radicals RO_2) will preferentially react with anthropogenic nitric oxides ($NOx = NO + NO_2$) leading to increased levels of ozone (O_3) and other reactive species involved in the production of photochemical smog (Fehsenfeld et al., 1992; Andreae & Crutzen 1997; Atkinson 2000). Various photochemical model studies have shown that biogenic emissions have the potential to markedly influence atmospheric photochemistry by contributing to the production of carbon monoxide (CO) and O_3 concentrations, in addition to altering the tropospheric lifetime of methane (CH_4) (Jiang et al., 2003; Poisson et al., 2000; Wang & Shallcross 2000).

Isoprene is produced via the novel glyceraldehyde phosphate/pyruvate pathway (Lichtenthaler et al., 1997), and its biosynthesis is associated with the carboxylation process in the leaf chloroplast (Sharkey & Yeh 2001). The final step of isoprene synthesis involves a membrane bound, light activated enzyme isoprene synthase (Silver & Fall 1991; Wildermuth & Fall 1996). Changes in isoprene emission have been shown to correlate with changes in the activity of isoprene synthase (Monson et al., 1992; Kuzma & Fall 1993), thus linking isoprene emissions to availability of light and hence photosynthetic activity (Sharkey et al., 1991). However, isoprene synthesis and emission will continue (through the stomata) even when stomata are closed due to increased vapor pressures within the leaf (Fall & Monson 1992). Two environmental variables that affect isoprene emission are temperature and photosynthetic photon flux density (PPFD). Other factors also affect the rate at which a particular leaf will emit isoprene. These include the leaf environment (sun vs. shade) (Harley et al., 1996), leaf phenology (Harley et al., 1994), water stress (Sharkey & Loreto 1993), and historical temperatures (Geron et al., 2000), among others. Theories currently used to explain the reason for production and emission of isoprene include thermal tolerance or protection from short periods of high temperatures (Singsaas et al., 1997), anti-oxidant role to protect intercellular areas from harmful oxidants such as O_3 (Loreto & Velikova 2001), and a pathway for removing excess carbon (Logan et al., 2000). Needless to say, our understanding of the function of isoprene is incomplete, but the role isoprene plays in atmospheric chemistry is well understood.

Isoprene emissions from vegetation have been measured from various environments using techniques ranging from leaf and branch enclosures (Zimmerman

1979; Lamb et al., 1985; Monson et al., 1994) to whole canopy measurements using micrometeorological techniques (Baldocchi et al., 1995; Guenther et al., 1996a; Guenther et al., 1996b; Goldstein et al., 1998). Isoprene emission rates are known to depend on temperature and light and to go to zero at night, they change as a function of height within the canopy (Harley et al., 1996), and there is a seasonal switch which controls emissions that appears to be a function of the number of growing days after the last frost (Monson et al., 1994; Geron et al., 2000).

In this paper, we describe results of growing season isoprene emission studies at the Program for Research on Oxidants: PHotochemistry, Emissions and Transport (PROPHET) site (Carroll et al., 2001). This study is a continuation of measurements made at this site beginning in 1997 (Westberg et al., 2001) and continuing through 2002. These data provide one of the longest records of isoprene emissions from any ecosystem, and they provide an invaluable record for studying long-term controls over isoprene emissions. Concurrent work during the summers of 2000 and 2001 include the PROPHET 6-week intensive measurement campaigns, the continuous operation of an AmeriFlux tower focusing on CO_2 flux measurements (Schmid et al., 2003), and the operation of a smaller instrumented tower focusing on transport and turbulence within and above the canopy (Villani et al., 2003).

The primary objective of this work is to present the long-term isoprene flux measurements along with the biosphere-atmosphere exchange of energy (momentum, sensible heat, and latent heat flux) and CO_2. Discussions regarding the eddy covariance technique and the inherent uncertainties are presented, along with a brief description of the daily and annual isoprene flux observations. The response of isoprene to temperature,

light, and phenology is presented, and the performance of the current U.S. Environmental Protection Agency (USEPA) biogenic emission model (BEIS3) is evaluated for isoprene emissions at this site. Because observations of isoprene differ from the models, and there is variability in isoprene fluxes that cannot be explained with current biogenic emission models, long-term observations may help us to better understand the dynamics of these differences.

3.3. Site Description

Measurements were made from the University of Michigan Biological Station (UMBS) ~Flux tower (part of the AmeriFlux program) (Baldocchi et al., 2001) located near Pellston, Michigan (45°30'N, 84º42'W). The secondary successional hardwood forest contains a mix of bigtooth aspen (*Populus grandidentata* Michx.), quaking aspen (*P. tremuloides* Michx.), beech (*Fagus grandifolia* Ehrh.), paper birch (*Betula papyrifera* Marsh.), maple (*Acer rubrum* L.*, A. saccharum* Marsh.) and red oak (*Quercus rubra* L.), with an under story component of young eastern white pine (*Pinus strobus* L.) and bracken fern (*Pteridium aquilium*) (Schmid et al., 2003). Douglas Lake is located 1 km to the north and Burt Lake 3.5 km to the southeast. The fetch is relatively flat with a maximum change in elevation of 20 m over 1 km distance in any direction from the tower. Approximately 130 m to the south east of the UMBS~Flux tower is the PROPHET tower, used for studying regional atmospheric chemistry. A more detailed description of the PROPHET program and the site is provided by Carroll et al., (2001). The average canopy height (h_c) is 22 m, and measurements were made at the 31 m height

of the UMBS~Flux tower ($1.4h_c$). In 2002, the flux system was moved to the PROPHET tower and measurements were made at the 32 m height ($1.5h_c$). Footprint analysis for each year, using a model developed by Hsieh et al,. (2000), indicates that the typical daytime fetch (unstable conditions) that encompasses 90 to 95% of the measured flux extends approximately 100-200 m from the tower. The model was run using a zero plane displacement height, $d = 0.75\ h_c = 16.5$ m, and a roughness height of $z_0 = 0.4$ m. Aspen and red oak are the primary isoprene emitters and account for approximately 69% of the total biomass within a 1 km radius of the UMBS~Flux tower. Measurements were conducted each year (1999 – 2002) from roughly mid-May through the end of September at which time leaf senescence occurred, and isoprene emissions became effectively zero.

Both towers are accessed via an unimproved driveway and gravel foot-path off of Bryant Road (east of the site). The UMBS~Flux tower has a triangular cross section with a large base at the bottom (5.1 m sides) that tapers to 1.8 m sides at 30.5 m in height, and steel grid work platforms every 6 m. An interior ladder provides access to the top of the tower, and a shelter at the base of the tower houses data acquisition equipment and other instruments (Schmid et al., 2003). The PROPHET tower is a 31 m high walk-up scaffolding tower, rectangular in shape with 1.5 by 1.8 m platforms and a small laboratory at the base of the tower that houses the sampling equipment (Carroll et al., 2001).

3.4. Measurements and Calculations

Eddy covariance flux measurements of isoprene, sensible heat, latent heat, CO_2 and momentum were made within the surface boundary layer. Environmental parameters such as air temperature, relative humidity (RH), net radiation (R_n) Photosynthetically active photon flux density (PPFD), short wave radiation, rain, and atmospheric pressure were also monitored by the UMBS~Flux group. The data acquisition system for the eddy covariance data was a fast response (10 Hz) system, which stored 30-minute data files for processing off-line. The environmental parameters were stored via a series of Campbell data loggers (Campbell Scientific, Inc., Logan UT) at various temporal resolutions (ranging from 1 s to 10 min averages) (Schmid et al., 2003).

3.4.1. Eddy Covariance Measurements

Wind speed and temperature were measured using an ATI sonic anemometer (K-configuration) aligned toward the northwest. An open-path infrared gas analyzer (Auble & Meyers 1992) (IRGA) 0.5 m from the sonic measured CO_2 and H_2O mixing ratios. The IRGA was calibrated for CO_2 mixing ratios approximately every 2 weeks (Scott-Marrin, Riverside, CA, 290 and 402 ppm CO_2 in N_2). The H_2O channel was calibrated using pressure, temperature and RH measured simultaneously with nearby sensors. A 1.27 cm (I.D.) Teflon sampling line mounted 0.2 m from the sonic array drew air to the ground for analysis via a fast isoprene sensor (FIS, Hills Scientific, Inc.). The FIS is a total alkene analyzer using a chemiluminescent technique with a fast response time (0.4 s) (Hills & Zimmerman 1990). Due to low concentrations of other alkenes at the site and a low relative response of the FIS to these alkenes, the interference for isoprene measurements is negligible (see Westberg et al., 2001 for more details). The detection limit when operating the instrument at 10 Hz is 0.5 ppbv isoprene with 20% uncertainty.

Calibrations were performed using a dynamic dilution of isoprene (Scott-Marrin, 6.09 ppm ±2% isoprene in N_2) at a minimum of once per day to determine the zero and the slope, or sensitivity (photon counts per ppbv isoprene per time). In 2002, the FIS was upgraded with automated calibration capabilities, so calibrations were performed approximately every 7 hours or about 3 times per day. The FIS sensitivity varied slightly, with standard deviations of 27%, 25%, 28% and 19% for years 1999-2002, respectively. There was no discernable trend or drift with the FIS zero for any year. Guenther and Hills (1998) reported that instrument noise is primarily high frequency, random noise that is relatively independent of mixing ratio.

The processing of the 10 Hz data was done for each 30-minute period using the following approach: (1) calibration coefficients were applied and the raw (10 Hz) data was converted from the digital signal into scientific units; (2) correlations of the vertical wind component (w) and the isoprene mixing ratio were calculated for a range of times (τ) (mid-day periods only) and the τ corresponding to the maximum correlation for each 30-minute period were averaged to determine the daily lag time between the sonic signal and the fast isoprene sensor located on the ground (lag times ranged between 9-14 seconds); (3) hard spikes were removed from the raw data including errors from instrumentation and interference with weather such as rain; (4) coordinate rotation was performed on the 3 wind components to orient *u* in the mean wind direction (Kaimal and Finnigan 1994); (5) Reynolds decomposition, based on a recursive filter technique with a running mean of 3-minutes was used to compute averages and standard deviations for each variable; (6) soft-spikes were removed from the w component (vertical) of wind based on the magnitude of the standard deviation and the length of the spike as explained

by Schmid et al. (2000); (7) the means were removed from each variable creating the prime quantities; (8) instantaneous fluxes were calculated (taking into account appropriate lag times previously determined) as $w'c'$ where c is the scalar (or u' in the case of momentum); (9) 30-minute average fluxes were determined for momentum, sensible heat, latent heat, CO_2, and isoprene; (10) the isoprene, CO_2, and latent heat fluxes were corrected for the effects of density fluctuations as described by Webb et al. (1980); and lastly, (11) isoprene flux was corrected for the high-frequency loss due to transport through the sampling line using a ratio of the unfiltered heat flux to the low-pass-filtered heat flux (Kaimal and Finnigan 1994; Massman 2000; Massman & Lee 2002).

3.4.2. Flux Uncertainties

Systematic errors are consistent over- or under- readings of fluxes, and some examples of those associated with the eddy covariance method include: 1) sensor separation between the sonic and scalar measurements, 2) under predicted nighttime fluxes due to drainage flow, 3) inadequate sensor response or flow distortion, 4) damping of high frequency fluctuations due to travel through a sample line, and 5) incorrect processing of fluxes.

Filtering effects due to the path length of the sonic and the IRGA were assumed negligible and there were no spectral corrections applied to these signals. This assumption is based on the fact that the filtering effect due to path length is much smaller than the filtering effect due to a recursive filter provided that the height of the sensor above the surface level is much greater than the path length (Massman & Lee 2002). Co-spectra of $w'T'$ (sensible heat flux), $w'H_2O'$ (latent heat flux), and $w'c'$ (CO_2 flux) were

compared and their shapes were all similar with the expected slope of –7/3 (Kaimal and Finnigan 1994) (Data not shown but similar to Figure 2 in Westberg et al., 2001). It was also assumed that the separation distance between sonic and IRGA contributed minimal flux loss (possible phase shifts) to the CO_2 and latent heat fluxes. Phase differences are small for relatively low frequencies, but they can be important for larger frequencies. For all years considered in this report, the horizontal separation distance between the IRGA and the sonic was 0.5 m. Based on work done by Kristensen et al., (1997), for a ratio of displacement (D) to measurement height (z), where D/z = 0.5/31 = 0.02, the measured flux is 98% of the "true" flux. Thus, there were no frequency loss corrections applied to other fluxes except isoprene. The power density cospectra for *w'I'* (isoprene flux) exhibited a similar shape as that presented in Westberg et al., (2001) with a cutoff frequency of ~0.7 Hz. By integrating the area under the curve for a typical 30-minute mid-day period and an idealized co-spectrum, uncorrected 30-minute averaged isoprene fluxes are approximately 17% low due to high frequency losses. A similar analysis done on the corrected isoprene flux (using the ratio of unfiltered heat flux to the low-pass-filtered heat flux) shows the correction increases the measured flux by 19%. Thus, we feel this technique does an adequate job of correcting for high frequency losses due to tube attenuation and instrument response.

Flux measurements made during periods of atmospheric stability, and flux measurements collected during periods when the mean wind passes through the tower have a higher level of uncertainty and in some cases may not be reliable. One tool used to filter reasonable flux measurements from those with higher uncertainties is the value of the friction velocity (u*, m s^{-1}). When the atmosphere is stable (typically during night

time periods), u_* values can be quite low (i.e. < 0.3 m s^{-1}) which indicates generally calm or low winds, and low turbulence. Between 33 and 39% of the recorded flux data each year had u* values < 0.3 m s^{-1}. Almost all of these periods were at night. Measurements of eddy covariance fluxes during these periods can be very uncertain, and for H, LE, and CO_2 fluxes, this should be considered. However, the emission rate of isoprene is effectively zero at night. The first graph in Figure 3.1 shows a polar plot of the fraction of winds sorted by 20° sectors over all four years, and the second plot presents only the data with u* > 0.3 m s^{-1}. The same figure presents the average isoprene flux contributed from each 20° sector. Winds were predominantly from the west, and most of the time the source footprint for isoprene fluxes was to the west of the tower, with some contribution from the NE.

It is also important to orient the sonic anemometer (and other sensors) to minimize interference from the tower structure. In 1999-2001 the sonic was oriented northwest at 300°, in 2002 the orientation was 340°. On average, about 24% of the time winds blew through the tower (between 75° and 165° for 1999-2001 and between 115° and 205° in 2002). Data corresponding to low u* values and to winds from behind the tower were left in the dataset so as to not introduce a bias, since these data points typically are low value isoprene fluxes.

To estimate the overall uncertainty in flux measurements, we can identify the uncertainties associated with each measurement (i.e. isoprene concentration, temperature, wind speed, etc.), and combine those with the errors associated with the theoretical assumptions inherent in the eddy covariance technique. Uncertainty associated with the sonic wind speed and temperature is 5%, for the CO_2 and H_2O fluxes the instrument

uncertainty is 10%, and for isoprene concentrations the uncertainty is 20% (for 10 Hz operation). Combining these errors with estimates of the errors associated with the eddy covariance technique, we estimate that the uncertainty associated with H is ~20%, and for CO_2 and LE the uncertainty is ~30%. These are for daytime fluxes, and it is expected that uncertainties are probably greater for nighttime fluxes of H, LE, and CO_2. The maximum estimated uncertainty related to isoprene fluxes is on the order of 40%. Currently, the uncertainty in biogenic emission estimates is 50% or more (Guenther et al., 2000; Geron et al., 1997).

3.4.3. Environmental measurements

At the UMBS~Flux site, total vegetative area index (VAI) was measured periodically at over 30 locations on 6 transects using a LiCor LAI-2000 (Li-Cor Inc., Lincoln, NE) sensor, with full sky reference measured at the top of the tower. Figure 3.2 presents the evolution of VAI for each year between 1999 and 2002. Surveys were conducted to determine timing of bud break and fraction of foliation expansion for each species on-site. The vertical lines in Figure 3.2 represent full leaf out (>90%) for the two dominant isoprene emitting species (red oak and bigtooth aspen). As seen in the figure, leaf out during years 1999-2001 was fairly consistent (between May 22 (DOY 142) and June 1 (DOY 152)), however, leaf out in 2002 was delayed until June 18 (DOY 169). Total VAI for 2002 was also greater than the other three years with a peak at 3.7 m^2 m^{-2} compared to 3.2 – 3.5 m^2 m^{-2}.

Meteorological parameters were monitored continuously by the UMBS~Flux group, and all measurements were from the 46 m level of the UMBS~Flux tower. Above canopy R_n was recorded using an REBS Q*7.1 (REBS, Inc., Seattle, WA) net radiometer,

PPFD (0.4 – 0.7 μm) was measured using a Li-Cor LI-190SZ quantum sensor, and short wave radiation (0.4 – 1.1 μm) was measured using a Li-Cor LI-200SA pyranometer. Rainfall was recorded using a Texas Electronics (model TR-525-M) tipping bucket, and a Rotronic probe (Rotronic Instrument Corp., Huntington, NY, model HPO-43) measured RH and temperature. Details regarding the UMBS~Flux system setup can be found in Schmid et al., (2001) and Curtis et al., (2002).

3.4.4. Biogenic Emission Inventory System (BEIS3) model

Photochemical models used to predict tropospheric O_3 concentrations, particulate matter (PM), and other atmospheric pollutants require accurate estimates of biogenic emissions. The Biogenic Emission Inventory System 3 (BEIS3) is the current USEPA model for simulating all biogenic emissions, including isoprene (Pierce et al., 2002). Using the Biogenic Emission Land Dataset (BELD3) (Kinnee et al., 1997), and isoprene emission rates at standard temperature and PPFD levels, BEIS3 estimates normalized biogenic emissions at the desired spatial and temporal (typically hourly) resolution. With above canopy meteorological inputs, the normalized emissions are adjusted for ambient temperature and light levels using the Guenther algorithm (Guenther et al., 1993). BEIS3 has also been implemented into the Sparse Matrix Operator Kernel Emissions (SMOKE) model (Pierce et al., 2002) and the Community Multiscale Air quality Modeling System (CMAQ) (Pierce et al., 2002). This makes biogenic emission inventory development more integrated with the latest photochemical models.

3.5. Results

Measurements were made continuously each year from roughly mid-May through mid-October. Minor interruptions were caused by instrument calibrations, data transfer, weather events (i.e. rain), and routine sensor maintenance. There were some larger data gaps due to instrument failures. In 1999, a light-leak in the FIS developed slowly over the course of the summer, which ultimately resulted in unreliable isoprene emissions for most of the summer. Data acquisition problems delayed the start date in 2001 until after the onset of isoprene emissions, and the flux system was turned off earlier than expected in the fall (mid-September) due to computer problems. In 2002, the IRGA was not operational for approximately 4 weeks from early July to early August, at which point a replacement IRGA was installed. Combining all four years, there was on average 133 days of measurements resulting in an average of 4130 half-hour periods of data each year. Approximately 12% of the data each year was discarded due to sensor malfunction during extreme weather conditions (i.e. rain or power outages). Sensor calibration and sensor repair/maintenance (not including the FIS light leak) accounted for 3 – 9% of unusable 30-minute periods. If data gaps due to sensor calibration or maintenance exceeded 15 minutes, then the entire 30-minute period was considered a missing observation. Overall, approximately 21% of the data used to determine the energy and CO_2 fluxes was discarded. Of the data required to generate isoprene fluxes, approximately 31% was discarded due to operational problems (again, not including the 1999 light leak).

3.5.1. Seasonal Course of Energy and Isoprene Fluxes

Eight typical days of measurements are shown in Figure 3.3. The figure presents PPFD (μmol m^{-2} s^{-1}), ambient temperature (°C), H and LE (W m^{-2}), isoprene flux (mg C m^{-2} h^{-1}), and CO_2 flux (mg m^{-2} s^{-1}) beginning on July 7, 2000 (DOY 189). The diamonds indicate FIS calibration events, and rain periods are shaded lightly. All the fluxes show a diurnal profile, with isoprene fluxes and the energy fluxes (H + LE) highly correlated with PPFD and temperature. For example, day 190 was cloudy with relatively low temperatures (18-22°C mid-day), consequently neither sensible heat flux nor latent heat flux reached 200 W m^{-2}, and isoprene flux was less than 5 mg C m^{-2} h^{-1} all day. On the next day (191), temperatures increased by 10°C, sensible and latent heat fluxes doubled (~400 W m^{-2}), and isoprene fluxes quintupled (25.5 mg C m^{-2} h^{-1}). The peak isoprene emission for the year in 2000 occurred on this day, but it still illustrates the large variation in isoprene fluxes that can occur from one day to the next. These examples show how closely linked isoprene is with environmental parameters (temperature and PPFD) and consequently the energy fluxes (H and LE). Another example can be seen by studying days 192 – 195. The diel temperature profiles for days 192, 193 and 194 were practically identical, and as expected isoprene fluxes for those 3 days were fairly consistent. Temperatures increased by almost 5°C on day 195 and isoprene fluxes followed suit by doubling in magnitude. Variations from one 30-minute period to the next were also quite high for all of the flux measurements, as seen in the "sawtooth" shapes. Similar patterns and shapes can be seen in the day-to-day fluxes each year.

The measurements (PPFD, temperature, LE, H, and isoprene flux) during each year are summarized in Table 3.1 and presented in Figure 3.4. This figure presents the

daily average of each measurement (the dark line) along with the daily maximum and minimum (shaded bars) for all sampling days in 1999-2002. Due to incomplete measurements in 1999, the following discussion focuses on years 2000-2002 only. Daily average isoprene fluxes for 2000-2002 ranged from 1.1 to 1.4 mg C m^{-2} h^{-1}, and average mid-day (10:00 am to 4:00 pm) isoprene fluxes were 2.8, 3.2 and 2.9 mg C m^{-2} h^{-1} for 2000 - 2002 respectively (Table 3.2). Peak emissions occurred on July 9, 2000 (25.5 mg C m^{-2} h^{-1} DOY 191), August 9, 2001 (18.3 mg C m^{-2} h^{-1} DOY 221) and July 1, 2002 (13.3 mg C m^{-2} h^{-1} DOY 182). Year 2001 was the warmest and the driest of the three years, with approximately half of the rainfall compared to 2000. This is probably the reason that the highest average isoprene flux occurred in 2001 (1.4 mg C m^{-2} h^{-1}).

For years 2000 and 2002 in particular, there is a gradual increase of isoprene emissions, then during the middle of the summer, variations in isoprene are linked to variations in temperature and light, and in the late summer/early fall there is a gradual decline in emissions. There is insufficient data in 1999 and 2001 to see the complete seasonal pattern. The onset of isoprene emissions and fully developed emission rates are discussed in the next section. Regardless of when isoprene emissions begin, however, the cumulative isoprene emissions for each year appear to remain fairly consistent. Cumulative isoprene emissions are shown in Figure 3.5. The annual cumulative total isoprene emissions are presented in Table 3.2. The average cumulative isoprene emission for days 158-265 during years 2000-2002 is 2547 ± 133 mg C m^{-2}. The variation between each year is less than 10%. The cumulative isoprene emissions may be slightly underestimated due to 1) not including the period during which isoprene emissions are gradually increasing (pre day 158), and 2) missing observational data. For 2000 and

2002 (the years which we have observations during the spring/early summer), including all available observations only increased the cumulative emissions by 1%. If we assume these are annual isoprene emissions, and based on the long-term measurements of net ecosystem exchange (NEE) reported by Schmid et al., (2003), isoprene emissions account for 1.7% in 2000 and 3.1% in 2001 of the net carbon uptake (net ecosystem production (NEP) for 2000 = 160, and NEP for 2001 = 80 g C m^{-2}). The fraction of carbon emitted as isoprene is typically between 0.1 and 3% for most sites, and it has been reported at 2% in 1995 for the Harvard forest (annual isoprene emission = 4.2 g C m^{-2}, NEP = 220 g C m^{-2}) (Goldstein et al., 1998).

3.5.2. Onset of Isoprene emissions

Isoprene emission rates are typically delayed from bud break for up to 2 - 4 weeks in some cases, and most plants do not reach their fully developed emission rates (basal emission rate) until full leaf development and expansion (Monson et al., 1994; Fuentes et al., 1999). Several methods for estimating the onset of isoprene emissions as a function of phenology for modeling purposes have been proposed including growing days (Monson et al., 1994), effective temperature sum (Hakola et al., 1998; Hakola et al., 2000), and heating degree-days (H°D) (Geron et al., 2000). Heating degree-days are measured using the cumulative average daily temperature (°C) since the last spring frost. Table 3.1 summarizes the dates of the phenological stages, and Table 3.2 summarizes the associated heating degree-days. The last spring frost occurred between days 108 and 110 for years 1999-2001, with bigtooth aspen budbreak following approximately 20 days later when 230-244°D was reached. Red oak budbreak was much more variable from year-to-year. Full leaf out (>90%) for both species, and the onset of isoprene emissions, occurred

approximately 40 days after the last frost when heating-degree days reached between 437-507°D. These three years (1999-2001) appear to be the average, while 2002 was quite different. The last spring frost in 2002 was one month later than the previous years, yet full leaf out and fully developed isoprene emissions occurred 26-31 days after last frost at approximately 406°D. In comparison, 1000°D was required to reach fully developed isoprene emissions from white oak (*Q. alba* L.) at the Duke Forest in North Carolina (Geron et al., 2000), and 1050°D was needed at Harvard Forest (Goldstein et al., 1998).

3.5.3. Energy Budget

One simple tool that may indicate systematic errors in a flux measurement system is to balance the surface energy budget by comparing total energy input into the system with the sum of energy output from the system: $R_n - S - G - Q = LE + H$. Where R_n is net radiation, S is the rate of change of heat storage (air and biomass) between the ground level and the measurement height, G is the soil heat flux, Q is the sum of all additional energy sources and sinks, (i.e. photosynthesis), and LE and H are latent and sensible heat flux, respectively. Soil heat flux was not available for analysis, Q is typically neglected as a small term, and over long time periods S is approximately zero. The average diel course of net radiation typically exceeds the sum of H and LE by 50-100 W m^{-2} during the middle of the day, while at night the outgoing radiation is greater (in magnitude) than the sum of H and LE by about 20 W m^{-2} (Figure 3.6). For each year, the ordinary least squares (OLS) regression between 30-minute average H+LE versus R_n was performed using all of the available data. For all four years, results indicated that the energy fluxes were less than the available energy by 10-30% (Massman & Lee 2002; Wilson et al.,

2002). The slopes of the OLS regressions for each year were 0.81, 0.81, 0.85, and 0.75 for years 1999-2002 respectively. Soil heat flux and canopy storage were not included in this analysis, and based on Wilson et al., (2002), including canopy storage can increase the slope on average by 7%, and including soil heat flux can increase the slope on average by 3%. Overall, the energy balance results for 1999-2002 compare quite well with results from other eddy covariance flux sites (Su et al., 2004; Wilson et al., 2002) which can indicate the general soundness of a system and the associated methods of analysis (Schmid et al., 2003).

3.5.4. Comparison with BEIS3

Isoprene emissions were estimated using the BEIS3 model for years 2000-2002. BEIS3 biogenic emissions from the 1 km grid from the BELD3 database that encompassed the site were compared to the observational data. For all model runs, hourly observational meteorological data including above canopy temperature (K), atmospheric pressure (Pa), and short-wave radiation (W m^{-2}) were used to drive the BEIS3 model. Originally, the default emission factors and BELD3 1 km resolution land classifications were employed, however, isoprene observations were 2-3 times larger than those predicted. Based on these results, the land use data was modified to better reflect the species present at UMBS. Land use categories were set to zero for all species except the two dominant isoprene emitters, Populus and Northern Red Oak. Based on biomass density data from the UMBS~Flux group, 76% and 24% were assumed for the proportion of Populus and Northern Red Oak, respectively. The BEIS3 emission factor table was also modified with a biomass density of 183 g m^{-2} (compared to the default value of 375

g m^{-2}), and an LAI of 4 instead of 5 m^2 m^{-2}. All three years were simulated using these same land use and biomass data.

With these site-specific biomass data, BEIS3 does a good job of estimating isoprene emissions over all three years. Model results for 20 days in 2001 and 2002 are shown in Figure 3.7, compared to the measured isoprene fluxes. As shown, the model slightly tends to overestimate emissions for most days (i.e. DOY 197 through 201, 2001), with the exception of days where observed isoprene fluxes are quite large and the predicted emissions are typically less than those observed (i.e. DOY 195 and 196, 2002). Model statistics were determined for all three years and they are summarized in Table 3.3. The gradual increase of emissions early during the measurement period and the decline of emissions during leaf senescence are not captured correctly by BEIS3. Therefore, the model statistics reported in Table 3.3 are for mid-summer days only when the basal emission rate is assumed to be fairly constant. Results for mean bias indicate that on average BEIS3 slightly overestimates observations for 2001 and 2002, yet BEIS3 slightly underestimates measured isoprene fluxes in 2000. Mean errors range from 1.08 to 1.69 mg C m^{-2} h^{-1}, with BEIS3 predictions for 2002 having the lowest mean error. Fractional bias and fractional errors are also reported, with the lowest fractional error reported for 2002 (31%) and the highest fractional error during 2000 (65%).

For the mid-summer period (days 158-265), when observational isoprene flux data are available, the BEIS3 cumulative isoprene emissions are 2087, 2771, and 3854 mg C m^{-2} for 2000 – 2002 respectively. This corresponds to a difference of –23%, +11%, and +57% between the observations (Table 3.2) and BEIS3 predictions for 2000-2002, respectively. The large over-predictions in 2001 and 2002 could be due to the BEIS3

inability to model the decline in observational emissions late in the season when temperatures are still somewhat elevated, however, this doesn't explain the BEIS3 under prediction for 2000. The variation among the three years using the BEIS3 predictions is also much greater than the variations in observations. The average BEIS3 isoprene accumulation (for all periods) is 3550 ± 982 mg C m^{-2}, with the difference between 2000 and 2002 almost 60%. We have no explanation for this phenomenon. The fraction of net carbon uptake emitted as isoprene for 2001 increases with the BEIS3 estimate to 4.2%, which is probably an overestimate.

Predicted vs. observed comparisons from other sites show similar results to those presented here. Overall model performance is reported in several papers in terms of normalized mean square error (NMSE) (equation presented in Table 3.3). Good model performance is indicated by NMSE < 0.4 and poor model performance is indicated by NMSE > 4 (Lamb et al., 1996). NMSE results for this northern Michigan site, including all available observational data, were 1.5, 0.62, and 0.95 for 2000-2002 respectively. Lamb et al., (1996) reports a range of NMSE of 0.4 to 1.3 for different versions of a canopy model compared to measurements made in a mixed deciduous forest near Oak Ridge, TN. Geron et al., (1997) reports NMSE values ranging from 0.44 to 1.06 for various modifications to the BEIS2 model compared to measured above canopy relaxed eddy accumulation fluxes at the Duke University Research Forest in NC. Lastly, gradient measurements of above canopy isoprene fluxes were compared to BEIS2 predictions at the Harvard Forest, with midday measurements typically exceeding model estimates by 40% (Goldstein et al., 1998). In summary, model predictions are still within 40-50% of

observed fluxes, with the average fractional error for all three years at this site equal to 46%.

3.6. Conclusions

Canopy scale emissions of isoprene from a northern hardwood forest in Michigan were measured using the eddy covariance technique during the summer growing periods from 1999 through 2002. With the exception of 1999, fluxes of isoprene, CO_2, H and LE were measured almost continuously from mid-May through the end of September and provide an unprecedented long-term isoprene flux dataset. Day-to-day variations in isoprene flux can be quite significant (factor of 5), yet the average daily isoprene flux for each year is quite consistent, with an overall variation of 30% (1.2, 1.4, and 1.1 mg C m^{-2} h^{-1}). The warmest and driest year, 2001, had the highest average midday isoprene flux (3.2 mg C m^{-2} h^{-1}), but the largest 30-minute isoprene flux occurred in 2000 (25.5 mg C m^{-2} h^{-1}) when the 30-minute averaged temperature was 28.8 °C and PPFD was 1810 W m^{-2}. Total cumulative isoprene emissions between years 2000-2002 were within 10% of each other, regardless of the differing phenological cycles each year. Last frost was delayed by roughly one month, and full leaf out was delayed by roughly 2.5 weeks in 2002, compared to the other 3 years. Isoprene emissions were fully developed in 1999 roughly 18 days after full leaf out, but in 2000 and 2002 isoprene emissions were fully developed shortly after leaf out (5 days in 2000) or before full leaf out (2002). Thus, for this site, isoprene emissions are fully developed between 400 – 500 °D, which is less than half the heating degree-days required at either the Duke Forest or the Harvard Forest.

Based on our analysis of the long-term flux data, we find that there is variation from day-to-day that current biogenic emission models cannot completely simulate, and the seasonal onset and decline of isoprene emissions is also an important aspect that current models do not predict correctly. The use of heating degree days to estimate the onset of emissions may improve model estimates, however, as previously pointed out, the emissions appear to "turn on" at different times, possibly as a function of ecosystem development. Although daily variations in isoprene emissions can be quite large, it appears that annual variations are surprisingly small. Model results again show the strong dependence of isoprene on the environmental drivers (temperature and light), but there are obviously additional environmental parameters that affect isoprene emissions. Continued work in this area will improve our understanding of what drives isoprene emissions. Meanwhile, this long-term isoprene flux dataset will be instrumental for further evaluation of canopy scale models that are used to generate emission inventories for regional photochemical models.

3.7. Acknowledgements

This research is part of the PROPHET and UMBS~Flux programs at the University of Michigan Biological Station. The authors wish to thank the National Science Foundation (NSF) and EPA for funding the research, and both the PROPHET and UMBS~Flux teams for their expertise and the use of their tower and laboratory facilities. The NSF Integrated Graduate Education Research Training (IGERT) program administered by Western Michigan University and entitled Biosphere Atmosphere

Research Training (BART); and the NSF Research Experience for Undergraduates (REU) Program provided support for this research. Support was also provided through a Boeing endowment to Washington State University.

The UMBS~Flux research was supported by the Office of Science (BER) Program, U.S. Department of Energy (DOE), and through its Midwest Regional Center of the National Institute for Global Environmental Change (NIGEC) under Cooperative Agreement No. DE-FC03-90ER61010. Any opinions, findings, and conclusions or recommendations expressed in this publication are those of the authors and do not necessarily reflect the views of the DOE.

3.8. References

Andreae, M. O. and Crutzen, P. J. 1997. Atmospheric aerosols: Biogeochemical sources and role in atmospheric chemistry. *Science* 276, 1052-1058.

Atkinson, R. 2000. Atmospheric chemistry of VOCs and NOx. *Atmospheric Environment* 34, 2063-2101.

Auble, D. L. and Meyers, T. P. 1992. An open path, fast response infrared absorption gas analyzer for H2O and CO2. *Boundary-Layer Meteorology* 59, 243-256.

Baldocchi, D., Falge, E., Gu, L., Olson, R., Hollinger, D., Running, S., Anthoni, P., Bernhofer, C., Davis, K., Evans, R., Fuentes, J., Goldstein, A., Katul, G., Law, B., Lee, X., Malhi, Y., Meyers, T., Munger, W., Oechel, W., Paw U., K. T., Pilegaard, K., Schmid, H. P., Valentini, R., Verma, S., Vesala, T., Wilson, K., Wofsy, S. 2001. FLUXNET: a new tool to study the temporal and spatial variability of ecosystem-scale carbon dioxide, water vapor and energy flux densities. *Bulletin of the American Meteorological Society* 82, 2415-2434.

Baldocchi, D., Guenther, A., Harley, P., Klinger, L., Zimmerman, P., Lamb, B., Westberg, H. 1995. The Fluxes and Air Chemistry of Isoprene Above a Deciduous Hardwood Forest. *Philosophical Transactions of the Royal Society of London Series a-Mathematical Physical and Engineering Sciences* 351, 279-296.

Carroll, M. A., Bertman, S. B., Shepson, P. B. 2001. Overview of the program for research on Oxidants: PHotochemistry, Emissions, and Transport (PROPHET) summer 1998 measurements intensive. *Journal of Geophysical Research* 106, 24275-24288.

Curtis, P. S., Hanson, P. J., Bolstad, P., Barford, C., Randolph, J. C., Schmid, H. P., Wilson, K. B. 2002. Biometric and eddy-covariance based estimates of annual carbon storage in five eastern North American deciduous forests. *Agricultural and Forest Meteorology* 113, 3-19.

Fall, R. and Monson, R. 1992. Isoprene emission rate and intercellular isoprene concentration as influenced by stomatal distribution and conductance. *Plant Physiol.* 100, 987-992.

Fehsenfeld, F., Calvert, J., Fall, R., Goldan, P., Guenther, A., Hewitt, C. N. 1992. Emissions of volatile organic compounds from vegetation and the implications for atmospheric chemistry. *Global Biogeochemical Cycles* 6, 389-430.

Fuentes, J. D., Wang, D., Gu, L. 1999. Seasonal variations in isoprene emissions from a Boreal Aspen forest. *Journal of Applied Meteorology* 38, 855-869.

Geron, C., Guenther, A., Sharkey, T., Arnts, R. R. 2000. Temporal variability in basal isoprene emission factor. *Tree Physiology* 20, 799-805.

Geron, C. D., Nie, D., Arnts, R. R., Sharkey, T. D., Singsaas, E. L., Vanderveer, P. J., Guenther, A., Sickles, J. E., Kleindienst, T. E. 1997. Biogenic isoprene emission: model evaluation in a southeastern United States bottomland deciduous forest. *Journal of Geophysical Research* 102, 18889-18901.

Goldstein, A. H., Goulden, M. L., Munger, J. W., Wofsy, S. C., Geron, C. D. 1998. Seasonal course of isoprene emissions from a midlatitude deciduous forest. *Journal of Geophysical Research* 103, 31045-31056.

Guenther, A., Baugh, W., Davis, K., Hampton, G., Harley, P., Klinger, L., Vierling, L., Zimmerman, P., Allwine, E., Dilts, S., Lamb, B., Westberg, H., Baldocchi, D., Geron, C., Pierce, T. 1996a. Isoprene Fluxes Measured by Enclosure, Relaxed Eddy Accumulation, Surface Layer Gradient, Mixed Layer Gradient, and Mixed Layer Mass Balance Techniques. *Journal of Geophysical Research* 101, 18555-

18567.

Guenther, A., Greenberg, J., Harley, P., Helmig, D., Klinger, L., Vierling, L., Zimmerman, P., Geron, C. 1996b. Leaf, Branch, Stand and Landscape Scale Measurements of Volatile Organic Compound Fluxes From Us Woodlands. *Tree Physiology* 16, 17-24.

Guenther, A., Geron, C., Pierce, T., Lamb, B., Harley, P., Fall, R. 2000. Natural emissions of non-methane volatile organic compounds; carbon monoxide, and oxides of nitrogen from North America. *Atmospheric Environment* 34, 2205-2230.

Guenther, A. B., Zimmerman, P. R., Harley, P. C., Monson, R. K., Fall, R. 1993. Isoprene and monoterpene emission rate variability - model evaluations and sensitivity analyses. *Journal of Geophysical Research* 98, 12609-12617.

Guenther, A. B. and Hills, A. J. 1998. Eddy covariance measurement of isoprene fluxes. *Journal of Geophysical Research* 103, 13145-13152.

Hakola, H., Laurila, T., Rinne, J., Puhto, K. 2000. The ambient concentrations of biogenic hydrocarbons at a northern European boreal site. *Atmospheric Environment* 34, 4971-4982.

Hakola, H., Rinne, J., Laurila, T. 1998. The hydrocarbon emission rates of tea-leafed willow (Salix phylicifolia), silver birth (Betula pendula) and European aspen (Populus tremula). *Atmospheric Environment* 32, 1825-1833.

Harley, P., Guenther, A., Zimmerman, P. 1996. Effects of light, temperature and canopy position on net photosynthesis and isoprene emission from Sweetgum (Liquidambar Styraciflua) leaves. *Tree Physiology* 16, 25-32.

Harley, P. C., Litvak, M. E., Sharkey, T. D., Monson, R. K. 1994. Isoprene emission from Velvet Bean-leaves - interactions among nitrogen availability, growth photon flux-density, and leaf development. *Plant Physiol.* 105, 279-285.

Hills, A. J. and Zimmerman, P. R. 1990. Isoprene measurement by ozone-induced chemiluminescence. *Anal. Chem.* 62, 1055-1060.

Hsieh, C.-I., Katul, G., Chi, T. 2000. An approximate analytical model for footprint estimation of scalar fluxes in thermally stratified atmospheric flows. *Advances in Water Resources* 23, 765-772.

Jiang, G., Lamb, B., Westberg, H. 2003. Using back trajectories and process analysis to investigate photochemical ozone production in the Puget Sound region. *Atmospheric Environment* 37, 1489-1502.

Kaimal, J. C. and Finnigan, J. J. 1994. *Atmospheric Boundary Layer Flows: Their Structure and Measurement.*, New York: Oxford University Press.

Kinnee, E., Geron, C., Pierce, T. 1997. United States land use inventory for estimating biogenic ozone precursor emissions. *Ecological Applications* 7, 46-58.

Kristensen, L., Mann, J., Oncley, S. P., Wyngaard, J. C. 1997. How close is close enough when measuring scalar fluxes with displaced sensors? *Journal of Atmospheric and Oceanic Technology* 14, 814-821.

Kuzma, J. and Fall, R. 1993. Leaf isoprene emissions rate is dependent on leaf development and the level of isoprene synthase. *Plant Physiol.* 101, 435-440.

Lamb, B., Pierce, T., Baldocchi, D., Allwine, E., Dilts, S., Westberg, H., Geron, C., Guenther, A., Klinger, L., Harley, P., Zimmerman, P. 1996. Evaluation of forest canopy models for estimating isoprene emissions. *Journal of Geophysical Research* 101, 22787-22797.

Lamb, B., Westberg, H., Allwine, E., Quarles, T. 1985. Biogenic Hydrocarbon Emissions from Deciduous and Coniferous Trees in the United States. *Journal of Geophysical Research* 90, 2380-2390.

Lichtenthaler, H. K., Schwender, J., Disch, A., Rohmer, M. 1997. Biosynthesis of isoprenoids in higher plant chloroplasts proceeds via a mevalonate-independent pathway. *FEBS Lett.* 400, 271-274.

Logan, B. A., Monson, R. K., Potosnak, M. J. 2000. Biochemistry and physiology of foliar isoprene production. *Trends in Plant Science* 5, 477-481.

Loreto, F. and Velikova, V. 2001. Isoprene produced by leaves protects the photosynthetic apparatus against ozone damage, quenches ozone products, and

reduces lipid peroxidation of cellular membranes. *Plant Physiol.* 127, 1781-1787.

Massman, W. J. 2000. A simple method for estimating frequency response corrections for eddy covariance systems. *Agricultural and Forest Meteorology* 104, 185-198.

Massman, W. J. and Lee, X. 2002. Eddy covariance flux corrections and uncertainties in long-term studies of carbon and energy exchanges. *Agricultural and Forest Meteorology* 113, 121-144 .

Monson, R., Jaeger, C., Adams, W., Driggers, E., Silver, G., Fall, R. 1992. Relationships among isoprene emission rate, photosynthesis, and isoprene synthesis, as influenced by temperature. *Plant Physiol.* 92, 1175-1180.

Monson, R. K., Harley, P. C., Litvak, M. E., Wildermuth, M., Guenther, A. B., Zimmerman, P. R., Fall, R. 1994. Environmental and developmental controls over the seasonal pattern of isoprene emission from aspen leaves. *Oecologia* 99, 260-270.

Pierce, T., Geron, C., Pouliot, G., Kinnee, E., and Vukovich, J. 2002. Integration of the Biogenic Emissions Inventory System (BEIS3) into the Community Multiscale Air Quality modeling system. The 25th Agricultural and Forest Meteorology/12th Air Pollution/4th Urban Environment Meeting. Norfolk, VA

Poisson, N., Kanakidou, M., Crutzen, P. J. 2000. Impact of non-methane hydrocarbons on tropospheric chemistry and the oxidizing power of the global troposphere: 3-dimensional modelling results. *Journal of Atmospheric Chemistry* 36, 157-230.

Schmid, H. P., Su, H.-B., Vogel, C. S., Curtis, P. S. 2003. Ecosystem-atmosphere exchange of carbon dioxide over a mixed hardwood forest in northern lower Michigan. *Journal of Geophysical Research* 108, art. no.-4417.

Schmid, H. P., Grimmond, C. S. B., Cropley, F., Offerle, B., Su, H.-B. 2000. Measurements of CO2 and energy fluxes over a mixed hardwood forest in the mid-western United States. *Agricultural and Forest Meteorology* 103, 357-374.

Sharkey, T. D. and Loreto, F. 1993. Water-stress, temperature, and light effects on the capacity for isoprene emission and photosynthesis of kudzu leaves. *Oecologia* 95, 328-333.

Sharkey, T. D., Loreto, F., Delwiche, C. F., Treichel, I. W. 1991. Fractionation of Carbon Isotopes During Biogenesis of Atmospheric Isoprene. *Plant Physiol.* 97, 463-466.

Sharkey, T. D. and Yeh, S. S. 2001. Isoprene emission from plants. *Annual Review of Plant Physiology and Plant Molecular Biology* 52, 407-436.

Silver, G. M. and Fall, R. 1991. Enzymatic synthesis of isoprene from dimethylallyl diphosphate in aspen leaf extracts. *Plant Physiol.* 97, 1588-1591.

Singsaas, E. L., Lerdau, M., Winter, K., Sharkey, T. D. 1997. Isoprene increases thermotolerance of isoprene-emitting species. *Plant Physiol.* 115, 1413-1420.

Su, H. B., Schmid, H. P., Grimmond, C. S. B., Vogel, C. S., Oliphant, A. J. 2004. Spectral Characteristics and Correction of Long-Term Eddy-Covariance Measurements Over Two Mixed Hardwood Forests in Non-Flat Terrain. *Boundary-Layer Meteorology* 110, 213-253.

Villani, M. G., Schmid, H. P., Su, H. B., Hutton, J. L., Vogel, C. S. 2003. Turbulence Statistics Measurements in a Northern Hardwood Forest. *Boundary-Layer Meteorology* 108, 343-364.

Wang, K. Y. and Shallcross, D. E. 2000. Modeling terrestrial biogenic isoprene fluxes and their potential impact on global chemical species using a coupled LSM-CTM model. *Atmospheric Environment* 34, 2909-2925.

Webb, E. K., Pearman, G. J., Leuning, R. 1980. Correction of flux measurements for density effects due to heat and water vapor transfer. *Quarterly J. R. Meteorological Society* 106, 85-100.

Westberg, H., Lamb, B., Hafer, R., Hills, A., Shepson, P., Vogel, C. 2001. Measurement of isoprene fluxes at the PROPHET site. *Journal of Geophysical Research* 106, 24347-24358.

Wildermuth, M. C. and Fall, R. 1996. Light-dependent isoprene emission-characterization of a thylakoid-bound isoprene synthase in Salix discolor chloroplasts. *Plant Physiol.* 112, 171-182.

Wilson, K., Goldstein, A., Falge, E., Aubinet, M., Baldocchi, D., Berbigier, P., Bernhofer, C., Ceulemans, R., Dolman, H., Field, C., Grelle, A., Ibrom, A., Law, B. E., Kowalski, A., Meyers, T., Moncrieff, J., Monson, R., Oechel, W., Tenhunen, J., Valentini, R., Verma, S. 2002. Energy balance closure at FLUXNET sites. *Agricultural and Forest Meteorology* 113, 223-243.

Zimmerman, P. 1979. *Determination of emission rates of hydrocarbons from indigenous species of vegetation in the Tampa/St. Petersburg Fla. Area*. *Rep. EPA-904/9-77-028*, U.S. Environmental Protection Agency, Research Triangle Park, N.C.

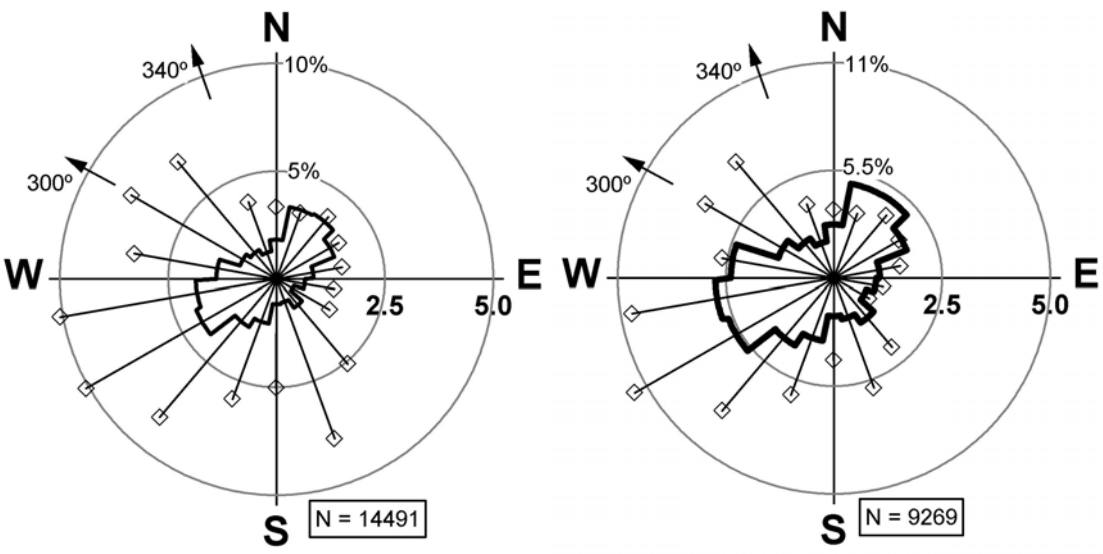

Figure 3.1: Polar plots of 30-minute averaged isoprene fluxes (shown by black line, mg C m^{-2} h^{-1}) and the fraction of total wind (indicated by diamond points) sorted into 20° sectors for all years (1999-2002). Polar plot on the left is all data, polar plot on the right is only data with u* > 0.3 m s^{-1}. Sonic anemometer mounted at 300° in 1999-2001 and at 340° in 2002.

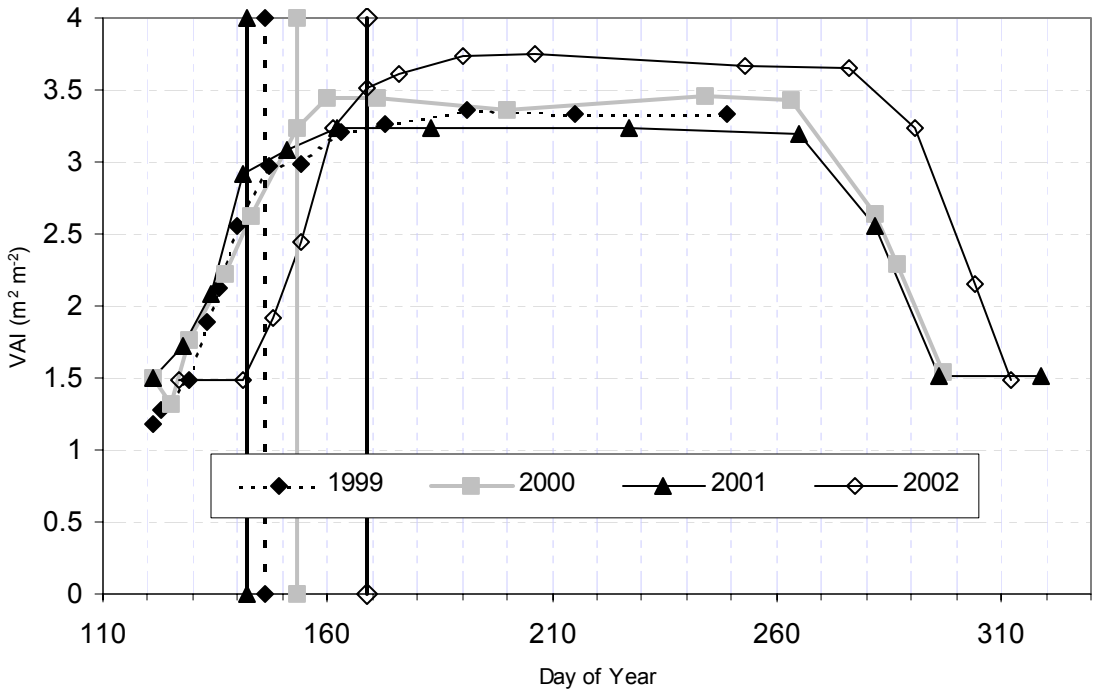

Figure 3.2: Evolution of total vegetative area index (VAI) (m^2 m^{-2}) over the growing seasons of 1999 to 2002. Vertical lines indicate the date of full leaf out (> 90%) for red oak and bigtooth aspen combined. Note the delayed leaf out in 2002.

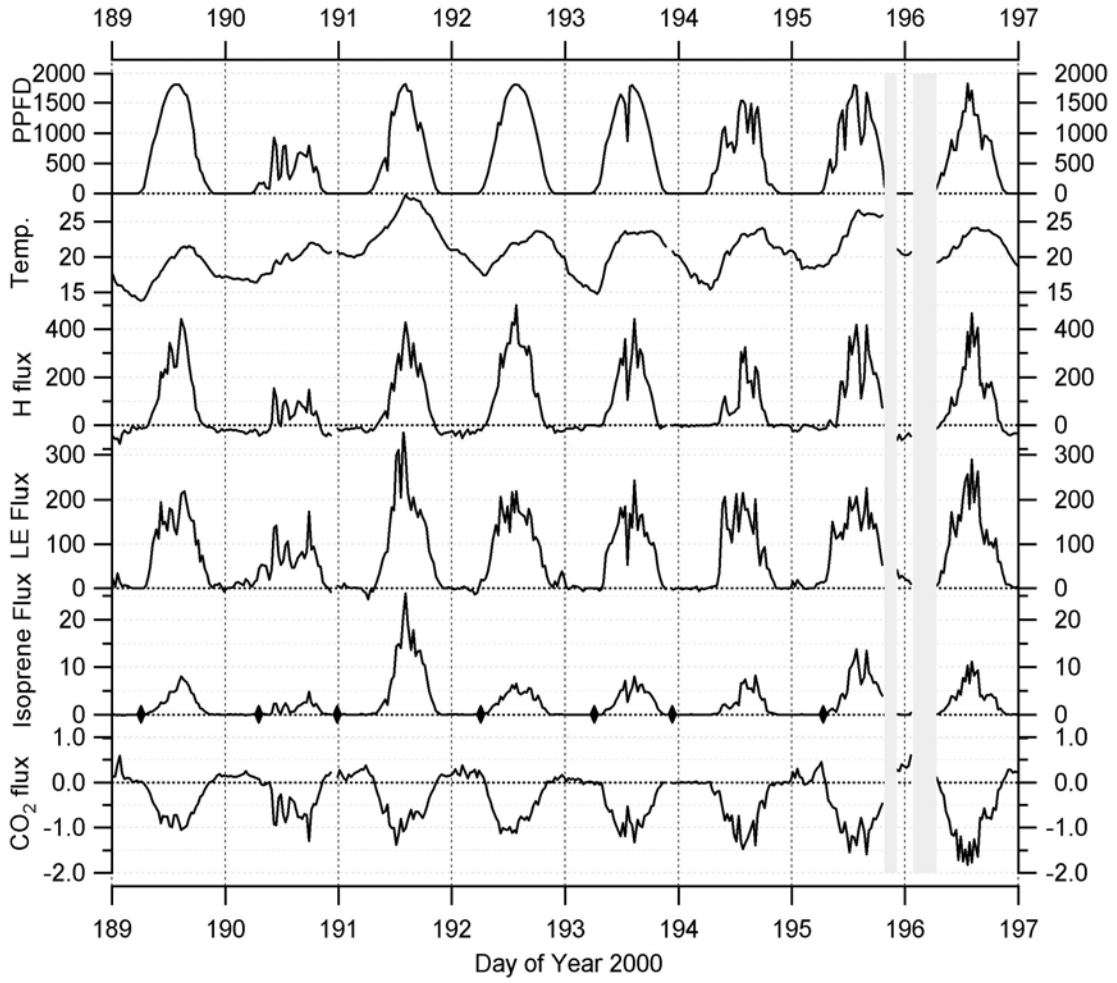

Figure 3.3: An example of typical 30-minute averaged fluxes beginning July 7, 2000 (DOY 189) through July 14, 2000 (DOY 196). From the top, traces represent PPFD (μmol m^{-2} s^{-1}), ambient temperature (°C), sensible heat flux (H: W m^{-2}), latent heat flux (LE: W m^{-2}), isoprene flux (mg C m^{-2} h^{-1}) and CO_2 flux (mg m^{-2} s^{-1}). Diamond markers indicate FIS calibrations and shaded area indicates missing data due to rain.

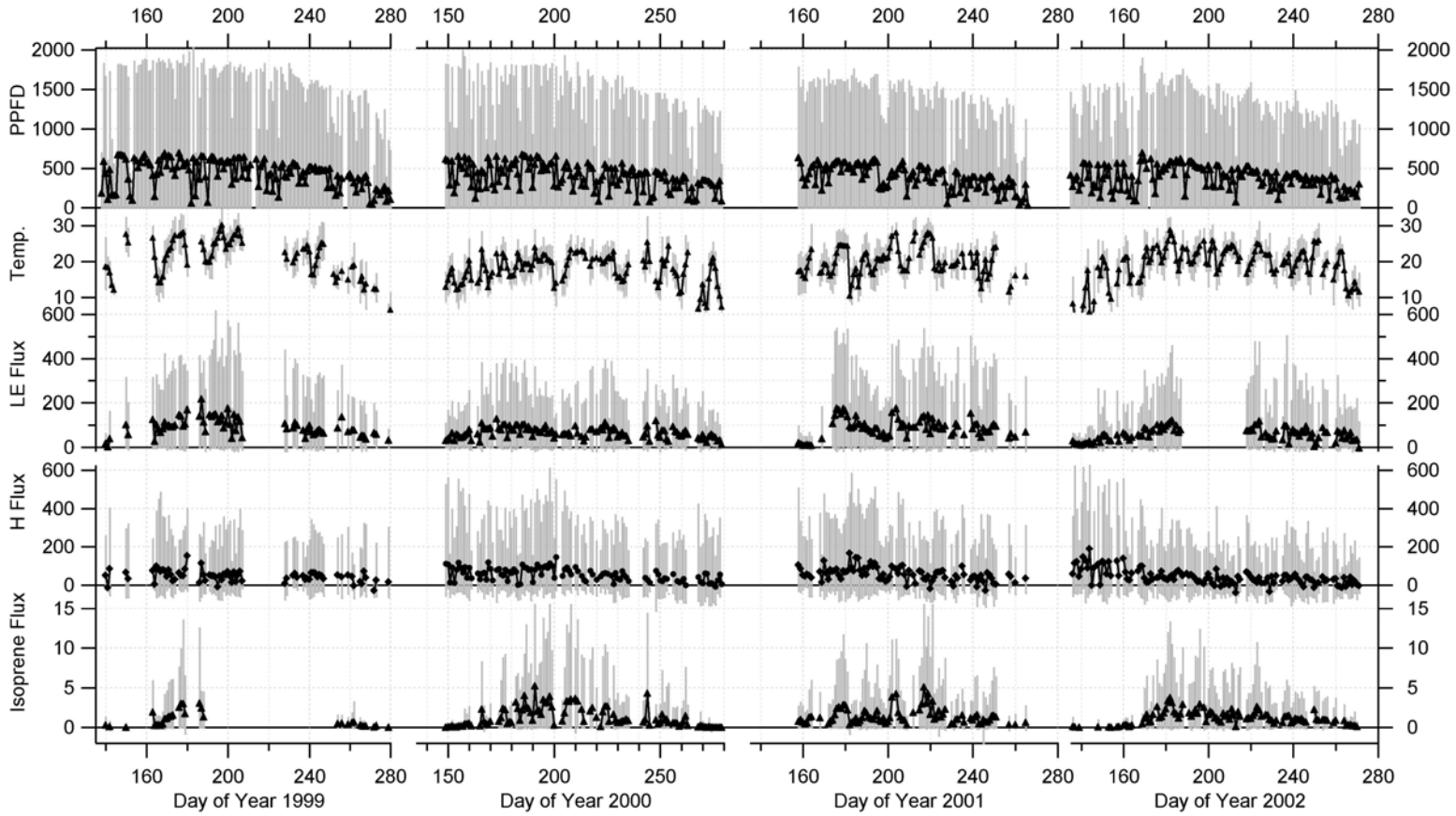

Figure 3.4: Daily average PPFD (μmol m^{-2} s^{-1}), ambient temperature (°C), latent heat flux (LE: W m^{-2}), sensible heat flux (H: W m^{-2}), and isoprene flux (mg C m^{-2} h^{-1}) indicated by dark traces. Range (maximum and minimum) of daily values indicated gray colored bars.

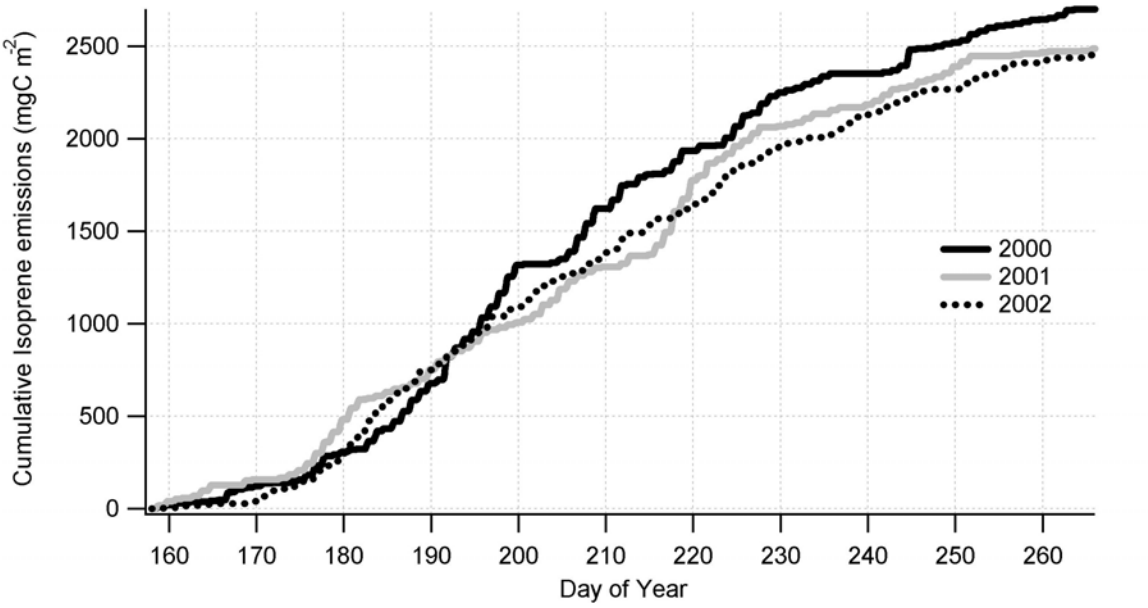

Figure 3.5: Cumulative isoprene emissions for years 2000-2002 in mgC m^{-2} beginning on day 158 (June 6 or 7) through day 265 (Sept 21 or 22). Solid black line (2000, *n*=3601), light gray solid line (2001, *n*=3637), and dashed line (2002, *n*=3780).

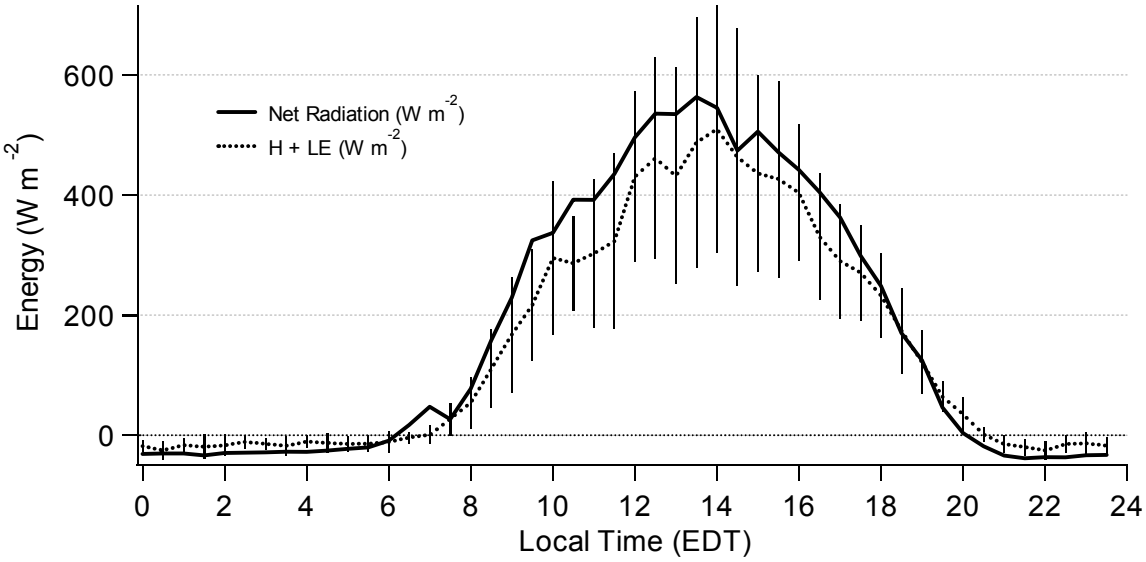

Figure 3.6: Energy balance for days shown in Figure 3.2, July 7 – July 14, 2000 (DOY 189-196). Solid black line is net radiation in W m^{-2} and dashed line is the sum of eddy covariance measurements of latent (LE) plus sensible heat (H) flux (W m^{-2}). Variations of H and LE between each day are shown by the vertical bars, which represent ± one standard deviation.

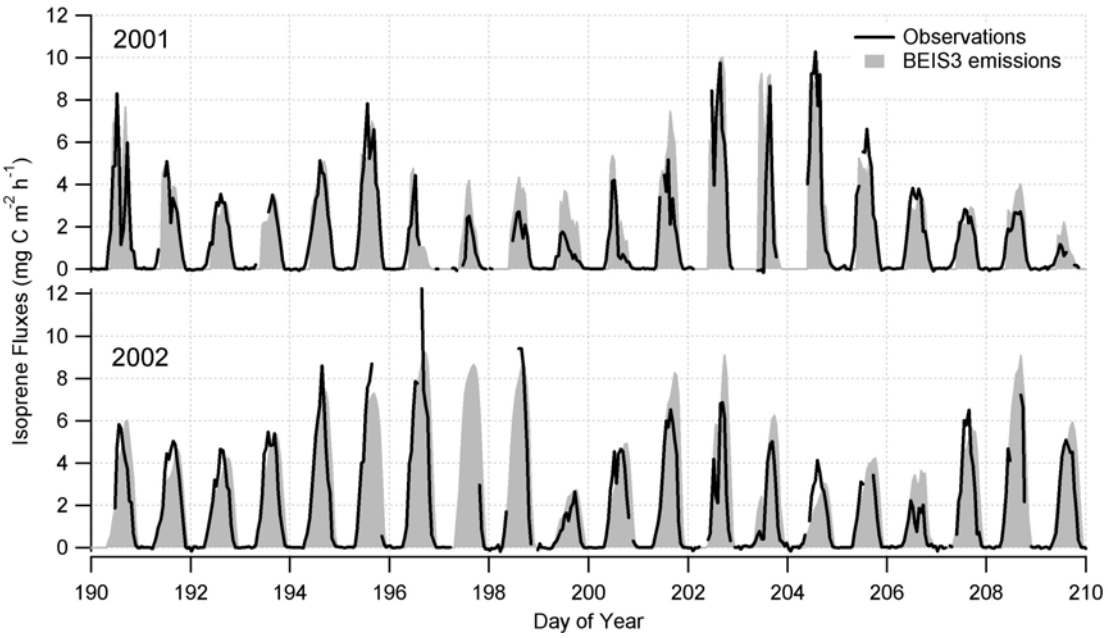

Figure 3.7: Measured isoprene fluxes (solid black line) vs. BEIS3 predicted isoprene emissions (shaded areas) for days July 9 (DOY 190) through July 28 (DOY 209) for 2001 (top graph) and 2002 (bottom graph). 30-minute observational data was averaged to create hourly data for comparison with BEIS3.

Table 3.1: Climate and phenology comparison for years 1999-2002.

	1999	2000	2001	2002
Avg. air temp[a] (°C)	18.0	16.3	17.7	17.0
Avg. soil temp[a] (2cm,°C)	16.1	14.7	15.7	14.0
Avg. PPFD[a] (W m^{-2})	113	108	100	97
Cum. Rain[a] (mm)	300	466	239	318
Last frost[b]	Apr. 18 (108)	Apr. 19 (110)	Apr. 18 (108)	May 18 (138)
Budbreak – aspen	May 8 (128)	May 8 (129)	May 8 (128)	June 5 (156)
Budbreak - red oak	May 5 (125)	May 8 (129)	May 3 (123)	May 22 (142)
Full Leaf out (>90%)	May 26 (146)	June 1 (153)	May 22 (142)	June 18 (169)

[a] The average air temperature, soil temperature, PPFD, and cumulative rainfall were determined only for 123 days from May 1 through August 31 (DOY 121 – 243).

[b] The last frost is the last day in spring when the 21 m air temperature < 0.5°C

Table 3.2: Isoprene emission annual characteristics and heating degree-day (°D) benchmarks.

	1999	2000	2001	2002
Budbreak bigtooth aspen	230 °D	240 °D	244 °D	193 °D
Budbreak red oak	188 °D	240 °D	181 °D	26 °D
Full Leaf out (>90%)	438 °D	507 °D	437 °D	406 °D
Earliest isoprene detection	Jun 10 (161)	May 31 (152)	NA	Jun 9 (160)
Fully developed emissions	Jun 13 (164)	June 6 (158)		Jun 13 (164)
Max. F_{iso} (mgC m^{-2} h^{-1})	14.7	25.5	18.3	13.3
Avg. F_{iso} (mgC m^{-2} h^{-1})	NA	1.2	1.4	1.1
Avg. Midday F_{iso} (mgC m^{-2} h^{-1})	NA	2.8	3.2	2.9
Cum. Isoprene[a] (mgC m^{-2}) (*n*)	NA	2699 (3601)	2487(3637)	2454 (3780)

[a] Cumulative isoprene fluxes for June 6 (DOY 158) through Sept. 21 (DOY 265) only in kg C m^{-2}, and (*n*) number of 30 minute periods included in sum.

Table 3.3: Model evaluation statistics for BEIS3 vs. observations for the days indicated in the table during years 2000-2002.

	2000	**2001**	**2002**
Days included	165-265	160-250	170-255
Mean bias (mg C m^{-2} h^{-1})	-0.68	0.46	0.24
Mean error (mg C m^{-2} h^{-1})	1.69	1.25	1.08
Fractional bias (%)	12	13	9
Fractional error (%)	65	43	31
Normalized mean square error (all days)	1.5	0.62	0.95

Note: $MeanBias = \frac{1}{N}\sum_{i=1}^{N}(Cm - Co)$, $MeanError = \frac{1}{N}\sum_{i=1}^{N}\left|Cm - Co\right|$,

$FractionalBias = \frac{1}{N}\sum_{i=1}^{N}\frac{(Cm - Co)}{\left(\frac{Co + Cm}{2}\right)}$, $FractionalError = \frac{1}{N}\sum_{i=1}^{N}\frac{\left|Cm - Co\right|}{\left(\frac{Co + Cm}{2}\right)}$, and

$NormalizedMeanSquareError = \frac{\overline{(Co_i - Cm_i)^2}}{\overline{Co}\,\overline{Cm}}$, where *Co* is magnitude of the observation and *Cm* is the modeled or predicted magnitude.

CHAPTER FOUR

RELATIONSHIPS AMONG CANOPY SCALE ENERGY FLUXES AND ISOPRENE FLUX DERIVED FROM LONG-TERM, SEASONAL EDDY COVARIANCE MEASUREMENTS OVER A HARDWOOD FOREST

4.1. Abstract

The flux of isoprene, one of the more reactive biogenic volatile organic compounds, was measured using eddy covariance techniques on a continuous basis during the 2000 to 2002 growing seasons at a mixed hardwood forest in northern lower MI. Daytime fluxes of isoprene and both sensible (H) and latent heat flux (LE) were linearly correlated with a positive slope on a daily basis, but the slopes of these relationships varied from one day to the next. Under drought conditions and longer time periods, LE fluxes were suppressed yet isoprene emissions were enhanced, thus the slope of the isoprene to LE relationship was increased. For example, seasonally averaged LE fluxes were reduced in 2000 as a result of reduced rainfall, and average isoprene fluxes were 1.5 times greater in 2000 compared to years 2001 and 2002. The strong daily correlation between isoprene fluxes and associated energy fluxes is an important relationship that should be accurately reflected in canopy models used for estimating biogenic emissions. In addition, in cases where land surface model output includes latent heat fluxes, the latent heat fluxes may be used as a surrogate for above canopy light and temperature to provide a simple estimate of isoprene emissions. Observed isoprene fluxes are compared to the BEIS3 biogenic emission model and to a canopy scale biogenic emission model (WSU-BEIS) that includes a leaf energy budget and accounts

for vertical changes in light and temperature through the canopy. Comparison of the emission models with observations showed that the fractional gross errors in isoprene flux estimates were approximately 37% for both models in 2001 and 2002, but increased to approximately 62% in 2000 when less rain occurred and LE fluxes were reduced. The BEIS3 model does not treat sensible or latent heat flux, but the simple scaling and leaf energy budget used in WSU-BEIS yields estimates of LE within approximately 50% of observations. Estimates of sensible heat flux with WSU-BEIS were larger than observed and indicate that the simple scaling approach may not be capable of treating all of the dynamics of canopy energy transfer accurately. Nonetheless, the strong relationships observed between isoprene flux and the energy flux terms provide a basis for testing these and other canopy models used for estimates of biogenic emissions.

4.2. Introduction

Isoprene is one of the most abundant and reactive naturally emitted volatile organic compounds (VOCs). Currently it is estimated that isoprene emissions for North America account for 35% of the total non-methane VOC emissions (approximately 29 Tg/yr) (Guenther et al., 2000). In combination with anthropogenic NOx ($NO + NO_2$), isoprene can contribute to increased regional ozone levels. Since it reacts rapidly with the hydroxyl radical, it modifies the oxidative capacity of the atmosphere effectively increasing the lifetime of greenhouse gases such as methane (Fehsenfeld et al., 1992; Monson and Holland 2001; Atkinson 2000). Results based on a global atmospheric chemistry model indicate that oxidation products from non-methane hydrocarbons (including isoprene) lead to 20-80% higher O_3 concentrations in NOx-rich regions

(Poisson et al., 2000). Thus, understanding the magnitude and seasonal patterns of isoprene emissions is necessary in order to accurately model regional and global atmospheric chemistry.

During the past decade there have been many studies aimed at quantifying isoprene emissions from forest vegetation (Bowling et al., 1998; Fuentes et al., 1999; Goldstein et al., 1998; Isebrands et al., 1999; Kuhn et al., 2002). The early studies involved leaf or branch level measurements (enclosure methods), which provided emissions estimates for specific isoprene emitters, but were difficult to extrapolate to larger scales. The scaling problem was addressed by measuring isoprene fluxes on a tower above a forest canopy. Isoprene flux determinations have evolved from use of a gradient approach (Fuentes et al., 1999; Lamb et al., 1985) to relaxed eddy accumulation methods (Lamb et al., 1996) and currently eddy covariance techniques. Each step in this evolution has produced better flux estimates. It is now possible to obtain continuous isoprene flux measurements during the growing season, and since isoprene is only emitted during the day when the atmosphere is typically well mixed, eddy covariance techniques are especially suitable for flux quantification. These long-term data sets will help to reduce the uncertainty in emissions estimates.

While much has been learned about the biological processes that regulate leaf-level isoprene emissions, there is a need to better understand the physical canopy exchange mechanisms. Energy exchange between the biosphere and the atmosphere is the fundamental driving force for atmospheric and physiological processes that also control biophysical fluxes of trace gases, such as isoprene. Latent heat (LE) and sensible heat (H) fluxes have diurnal patterns that vary based on the net radiation, atmospheric boundary layer, temperature, vapor pressure deficit, and the availability of water (from

vegetation) (Wilson et al., 2003). Plants respond to atmospheric conditions in various ways. By changing stomatal conductance, they control the availability of water for evaporation, which affects LE. The change in transpiration rates can cause the leaf temperature to increase, which can affect H. In turn, an increase in leaf temperature will increase volatile emissions of isoprene. The diurnal pattern of H and LE is almost identical to the diurnal pattern of isoprene flux (Westberg et al., 2001). Is there a link between the physiological processes, or do they simply respond to the same environmental parameters?

In this manuscript, a long-term record of eddy covariance isoprene, sensible heat and latent heat fluxes, along with associated environmental parameters, is used to explore relationships between isoprene flux and the surface energy fluxes. Given the similarities of the biosphere drivers for both isoprene and energy fluxes, we hypothesize that correlations between these fluxes could be a useful tool both for testing existing canopy emission models and to guide the development of improved isoprene emission models. We present quantitative relationships between the fluxes of isoprene, sensible heat and latent heat measured over multiple growing seasons at a forested site in northern lower Michigan. These data are then used to evaluate the accuracy of two current isoprene emission models.

4.3. Materials and Methods

Beginning in 1999, continuous eddy covariance measurements of CO_2, isoprene, sensible and latent heat fluxes have been made above a northern hardwood forest during the growing season. Flux measurements were also made in 1997 and 1998 (Westberg et

al., 2001), however, measurement periods were limited to a few weeks each summer. Measurements were made from the University of Michigan Biological Station Flux (UMBS~Flux) tower (part of the AmeriFlux network) (Curtis et al., 2002; Schmid et al., 2003) during the summers of 1999 through 2001. Beginning in 2002, flux instrumentation was shifted from the UMBS~Flux tower to an adjacent tower, part of the Program for Research: Oxidation, PHotochemistry, Emissions and Transport (PROPHET) (Carroll et al., 2001). The distance between the two towers is about 130 m, and there is no reason to suspect significant differences in the flux footprints of the two towers. However, this is an area of uncertainty. The distribution of species was determined within a 60 m radius plot and 16 m radius subplots (n = 60) along transects extending 1 km into the primary fetch immediately surrounding the UMBS~Flux tower. Bigtooth aspen (*Populus grandidentata* Michx.), quaking aspen (*P. tremuloides* Michx.) and red oak (*Quercus rubra* L.) are the primary isoprene emitters and account for approximately 69% of the total biomass within a 1 km radius of the UMBS~Flux tower. Portions of this survey include the PROPHET tower and some of its fetch; however, a species distribution map was not compiled for the area immediately surrounding the PROPHET tower. Footprint analysis, using a model developed by Hsieh et al., (2000), indicates that the typical daytime fetch (unstable conditions) that encompasses 90 to 95% of the measured flux extends approximately 100-200 m from either tower. More specifics on the tower and site can be found in various papers (Westberg et al., 2001; Carroll et al., 2001). Measurement techniques have been described in detail in Pressley et al., (submitted), including a discussion on the data processing techniques. For completeness though, a brief description of the measurement techniques is provided here.

Eddy covariance fluxes of CO_2 and water vapor were determined using an open-path infrared gas analyzer (IRGA) (Auble and Meyers 1992) located at the same height (31 m) as the ATI sonic anemometer (ATI, Inc., Denver, CO). Canopy height is roughly 22 m. A fast isoprene sensor (FIS, Hills Scientific, Inc., Boulder, CO) (Guenther and Hills 1998; Hills and Zimmerman 1990) was located at the base of the tower. Air from the 31 m level was delivered to the tower base at a high rate of turbulent flow (Re = 18,839) through a 1.59 cm-I.D. Teflon sample line. The lag time between the inlet at 31 m and the FIS sensor at the base of the tower averaged 10 s. All measurements were collected at 10 Hz and processed offline to generate 30-minute average fluxes. Density corrections were applied according to Webb et al., (1980) and high frequency attenuations in the isoprene flux were accounted for by applying a low-pass filter to the sensible heat flux to determine a correction based on the ratio of the unfiltered to filtered sensible heat flux (Westberg et al., 2001; Guenther and Hills 1998; Massman 2000).

The estimate of uncertainty associated with H is approximately 20%, and for CO_2 and LE the uncertainty is approximately 30%. The error estimates are for daytime fluxes, and it is expected that uncertainties are probably greater for nighttime fluxes of H, LE, and CO_2. The maximum estimated uncertainty related to isoprene fluxes is on the order of 40%.

Additional data collected from and within 60 m of the UMBS~Flux tower include wind speed and direction, vertical profiles of temperature and relative humidity, photosynthetic photon flux density (PPFD) and net radiation (ht = 46 m), atmospheric pressure, above canopy rainfall, mean soil temperature (depth = 2 cm, n = 3), mean soil moisture (time domain reflectometry, n = 4), biomass density, and vertical distribution of leaf area index (LAI).

4.4. Results

4.4.1. Daily Correlation between Energy and Isoprene Fluxes

The eddy covariance flux data from 2000 through 2002 were selected for in-depth analysis of correlations between half-hourly averaged isoprene, sensible and latent heat fluxes. Figure 4.1 shows fluxes typical of those observed each year. During this three-week period in July 2001, strong diurnal patterns in the isoprene and energy fluxes can be seen. Isoprene, sensible heat and latent heat fluxes all show values of zero or less during the nighttime period, and then rise during the day with increasing temperatures and incoming radiation.

Linear regression coefficients (slope and intercept) were derived from the ordinary least squares relationship between the half-hour eddy covariance isoprene fluxes versus the corresponding half-hour eddy covariance H or LE fluxes (Figure 4.2). We have chosen to compare only mid-day fluxes (10:00 am to 4:00 pm EDT) when determining the daily slope and intercept for two reasons. First isoprene is only emitted during the day, and second, isoprene fluxes measured during the transition periods (morning and late afternoon) are typically small and highly variable, depending on atmospheric stability more than temperature and light. Linear regression coefficients were not reported if more than 3 of the possible 6 hours of data were missing, or if eddy

covariance measurements were suspect, such as when winds blew through the tower. Figure 4.3 and Table 4.1 present the slopes and the correlation coefficients (R^2) between isoprene and the two energy fluxes for most of the summer growing period in 2001. As seen in Figure 4.3, there is day-to-day variation in the slope, however, the correlation between isoprene flux and either H or LE is strong with average correlation coefficients for all days of 0.85 (H) and 0.81 (LE).

Yearly average linear regression coefficients determined for days from late June through early September in 2000, 2001 and 2002 are summarized in Table 4.2. The average isoprene – sensible heat correlation coefficient for each of the three years was 0.80 or greater. The isoprene – latent heat correlation coefficient was slightly lower (0.71-0.81) but still very good. Many of the individual daily correlations between isoprene and the heat fluxes had R^2 values above 0.90 (Figure 4.3). Each of these daily comparisons included as many as twelve 30-min flux determinations.

4.4.2. Annual Correlation between Energy and Isoprene Fluxes

Comparisons between one year and the next can often illuminate seasonal patterns or trends that may indicate an environmental parameter that is influencing isoprene emissions. Since climatic conditions vary from one year to the next, comparisons must be made during consistent stages of the phenological cycle of the forest. Table 4.3 summarizes some of the climatic and biological characteristics observed during the three years studied. The years 2000 and 2001 are strikingly similar, but in 2002, canopy average bud break and leaf development were delayed by almost one month. This delay in 2002 can be seen in the growing season LAI profile shown in Figure 4.4. Mid-summer LAI and biomass density varied by less than 14% among all three years, and the length of the growing season was between 100 and 103 days for each year. The wettest year was

in 2001, with cumulative rainfall exceeding rainfall in 2002 by 20% and rainfall in 2000 by more than 30%.

The flux data for each year were compared using diurnal averaged profiles of H, LE and isoprene flux. The time period used in this analysis started 82 days after the last frost and ended 44 days later. This guaranteed that isoprene emissions were fully developed, LAI was fairly constant, and we could avoid a period in 2002 when LE data were missing due to instrument problems. To calculate the diurnal profiles, the 30-minute eddy covariance fluxes were averaged for each time period during the 44-days. Figure 4.5 shows the diurnal average isoprene fluxes for all three years, as well as the diurnal average partitioning of energy fluxes.

Diurnal averaged sensible heat peaked at about 260 W m^{-2} in 2000 and decreased in each succeeding year. Latent heat values were very similar in 2000 and 2002 (180-200 W m^{-2}) and somewhat higher in 2001 (240 W m^{-2}). During 2000, which had the least amount of rain of the three years, sensible heat fluxes exceeded the LE fluxes. During 2001 and 2002, the average LE flux was always larger than H. The enhanced sensible heat fluxes during the midday period in 2000 were probably a result of the greater PPFD during 2000. Midday averages of PPFD in 2000 exceeded those for 2001 by 5% and for 2002 by 18%.

The diurnal averaged isoprene fluxes shown in Figure 4.5 track the changes in sensible heat flux. The peak isoprene flux of about 6 mgC m^{-2} h^{-1} was observed in 2000. It decreased to about 5 mgC m^{-2} h^{-1} in year 2001 and less than 4 mgC m^{-2} h^{-1} in 2002. Linear regression coefficients (slope and correlation) are listed in Table 4.4 for the relationship between the diurnal average half-hour isoprene fluxes and the corresponding half-hour eddy covariance H and LE fluxes. The correlations between the energy fluxes

and isoprene flux are all greater than 0.92 for this data set. The isoprene-sensible heat slope varies from 0.019 to 0.023. The relationship is similar between the latent heat flux and isoprene flux if year 2000 is omitted.

The slope of the regression potentially provides a simple way of filling gaps in isoprene flux measurements due to instrument malfunction. If the slope between isoprene flux and latent heat flux was constant at this forested site, anytime latent heat data were available isoprene fluxes could be predicted. Thus, on an annual basis a simple linear regression model might be satisfactory, but large errors in predicted isoprene fluxes could occur on individual days. The slope of the isoprene-LE line is 0.032 for 2000, 0.020 for 2001, and 0.018 for 2002. Using these factors and the observed LE fluxes, isoprene emissions were estimated for each year and compared to the measured isoprene fluxes. Model statistics are summarized at the bottom of Table 4.5 and discussed in the modeling section.

4.5. Discussion

The strong correlations between isoprene flux and energy fluxes are quite significant for a complex biological system involving biosphere-atmosphere interactions. Leaf level isoprene emissions are driven by abiotic (temperature and light) and biotic controls (isoprene synthesis rates), while isoprene flux from the canopy depends on the leaf-level emission and the canopy ventilation rate. Many of the same factors control the H and LE fluxes, so it can be hypothesized that positive correlations should exist. It was shown that over the long term, slopes of the linear regression between isoprene and the

energy fluxes are nearly constant. However, the slope of the correlation varies on a daily basis. The reasons for this day-to-day variation are not completely understood at present.

There may be additional environmental mechanisms that provide feedback between the energy and isoprene fluxes. Many of the physiological responses of isoprene emissions have been determined with leaf level enclosure studies (Fall and Monson 1992; Monson and Fall 1989), and it is expected that these responses would be evident at the canopy scale. Isoprene emissions are known to increase when ambient temperatures rise, but isoprene emissions will also increase if the individual leaf temperatures increase. Sun flecks that strike the leaf for milliseconds at a time, or changes in the LE, both increase the leaf temperature. The primary mechanism for reducing leaf temperature is the evaporation of water in the form of latent heat flux. So as H increases and LE typically decreases (in order to reduce water loss), there is less cooling of the leaves, resulting in higher leaf temperatures and increased isoprene emissions. It is known that decreased stomatal conductance or stomatal closure does reduce LE, but it has been shown to have no direct effect on isoprene emissions (Fall and Monson 1992; Niinemets and Reichstein 2003). The data presented here (in particular Figure 4.5) indicate that isoprene emissions may be directly affected by LE fluxes. There is still a diurnal increase of LE fluxes, but overall the magnitudes of the LE fluxes are lower due to water stress. During 2000 when LE fluxes were suppressed, and H fluxes were at a maximum, diurnal averaged isoprene fluxes were approximately 1.5 times greater than average isoprene fluxes during 2001 or 2002.

Soil moisture is the primary source of water available to the canopy. Lack of soil moisture or water stress is an important parameter that affects stomatal behavior and ultimately LE fluxes. Previous studies have shown that water stress does not affect

isoprene emissions (Tingey et al., 1981; Guenther et al., 1999), and in general isoprene emissions are less sensitive to water stress conditions than photosynthesis (Fang et al., 1996). Without water, the canopy will conserve water through decreased stomatal conductance, thus decreasing LE and it's cooling capacity, possibly increasing leaf temperature and, in turn, isoprene fluxes. This idea was explored with the long-term record available. During periods with low soil moisture, LE fluxes were decreased, but there was still a positive daily correlation between isoprene fluxes and LE fluxes. A cross-correlation analysis showed that the maximum correlation between slope and soil moisture occurred with a lag of approximately one week. Figure 4.6 shows daily average soil moisture and the slope of isoprene flux vs. each energy flux for June 18 – Sept. 6, 2001 (DOY 170 – 250). During days 185 – 205, and days 215 – 220 soil moisture was very low (~6-8%) and the isoprene flux vs. LE slope peaked between 0.03 and 0.05. Other days (i.e. 232-235, and 242-246) do not show as strong a correlation, however, it is possible that use of the stored water within the xylem may have "protected" the trees from experiencing severe water stress. In 2000, the middle part of the summer was consistently under water stress, with soil moisture between 7-9% for days 187 through 223 (July 5 – Aug. 10, 2000) (Data not shown). Corresponding isoprene flux vs. energy flux slopes for this period were relatively high, but there was significant variation that cannot be explained by the relatively constant soil moisture. Almost the opposite occurred in 2002. Soil moisture was considerably higher in 2002, and it was less than 10% for only 15 days during the entire summer (data not shown). When it was reduced to less than 10%, the periods were relatively short (3-6 consecutive days), thus the water stress felt by the canopy was most likely minimal, and may not have affected isoprene emissions.

Understanding the physiological drivers for isoprene emissions is an important step in developing accurate models to predict emissions. However, to date, isoprene emission inventories have been developed solely on empirical and mechanistic algorithms. Most are "modeled" after biological mechanisms, such as the Guenther C_L term that was developed based on equations used to model the light dependency of photosynthesis (Guenther et al., 1993). The estimated uncertainty in biogenic emissions of isoprene is approximately 50% or higher (Geron et al., 1997; Guenther et al., 2000). It is therefore important to address the question: "Do the current canopy scale models simulate energy fluxes that are correlated with isoprene flux?" The observed correlations between isoprene flux and energy fluxes are significant, which should be reproduced in simulated canopy scale models. The following section compares the observational data with the Environmental Protection Agency (EPA) Biogenic Emission Inventory System (BEIS3) model and a more detailed model called WSU-BEIS, which employs a leaf energy budget and accounts for vertical changes in the canopy micro-climate to predict leaf temperature and thus isoprene and energy fluxes.

4.6. Modeling Application

4.6.1. Model Descriptions

BEIS3 is the current EPA model for simulating all biogenic emissions, including isoprene, monoterpenes, other VOCs, and NO (Pierce et al., 2002) (http://www.epa.gov/asmdnerl/biogen.html). The model starts with the Biogenic Emission Land Dataset (BELD3), which is a 1-km gridded land use data with 230

different land use types (Kinnee et al., 1997). Emission rates at standard temperature and, for the case of isoprene, at standard PPFD levels are provided for each land use type along with average LAI and biomass density estimates. BEIS3 estimates normalized biogenic emissions by multiplying the fraction of land use in each grid by the species specific emission factor and the corresponding biomass, and then the normalized emissions are adjusted for ambient temperature and light levels using above canopy meteorological parameters:

$$E = [\sum (f * E_s * b)] * (C_T * C_L) \quad (1)$$

where E is isoprene emissions (mgC per m^2 ground area per hour), f is the fraction of land use in a grid, E_s is the emission factor (μgC per g dry biomass per hour) for that land use class, b is the biomass density (g dry biomass per m^2 ground area), and C_T and C_L are the correction terms for ambient temperature and light respectively. Thus, biogenic emissions are estimated at appropriate spatial and temporal (typically hourly) resolution for inclusion into atmospheric photochemical models. A few of the assumptions BEIS3 uses include: 1) leaf temperature within the canopy is equal to ambient air temperature, 2) PPFD levels are attenuated through the canopy using a simple algorithm and the modified PPFD is incorporated into the light correction term, and 3) since specific leaf weight (SLW) varies as a function of height, there is an adjustment made to the foliar mass to account for the vertical change in SLW (Geron et al., 1994; Pierce et al., 2002).

Two models were used to simulate isoprene emissions for the site in northern MI. The first model used was a single grid version of BEIS3. More detailed species composition, biomass density, and LAI values were used based on the biological surveys

conducted at the site instead of the BELD3 database. BEIS3 was run using measured meteorological inputs on a 30-minute averaged basis. The second model used was WSU-BEIS. The initial version of WSU-BEIS is described in Lamb et al., (1993). The current version incorporates a 15-layer canopy model with light and temperature attenuation through the canopy and energy balance equations based on canopy light and leaf energy budgets given by Campbell and Norman (1998). The leaf energy budget requires iteration for each layer of the canopy based on air temperature, radiation, wind and vapor deficit, and leaf temperature is then used for calculating the C_T term. PPFD values are split into direct and diffuse components and attenuated through the canopy based on the vertical LAI profile. The C_L term is composed of a C_{Lshade} and a C_{Lsun} term. The same biomass data and meteorological inputs used for BEIS3 were used for WSU-BEIS, with the addition of humidity and wind speed for WSU-BEIS necessary to drive the leaf energy budget model. The additional energy balance equations allowed for the calculation of 30-minute averaged energy fluxes of H and LE. Lastly, the annual correlation coefficients for isoprene vs. LE (summarized in Table 4.4) were multiplied by the observed 30-minute averaged LE fluxes for each year to provide an estimate of isoprene emissions based on the correlation work presented in this paper. This is a very simple estimate of isoprene emissions using LE as a surrogate for ambient light and temperature conditions that could be used with land surface model output in place of running a full scale canopy biogenic emission model.

4.6.2. Model Performance

Equation 1 was employed with the standard BEIS3 emission factor of 70 μgC g^{-1} h^{-1} for aspen and an isoprene emitting biomass density of 183 g m^{-2} to calculate isoprene emissions for each year. Thus differences between the model results are a

function of the C_T and C_L terms, as the first part of equation 1 is constant. Figure 4.7 shows a time-series comparison between observations, BEIS3, and WSU-BEIS isoprene fluxes for all three years. Overall both models do a good job matching the observed isoprene fluxes. The timing is accurate, with peaks during midday, and in most cases the models capture the variability from one 30-minute period to the next. However, the magnitudes of the predicted fluxes are not always correct.

In order to assess the model performance, two performance metrics were selected. First, the mean bias (MB) and mean error (ME) are presented in order to show the difference between the model and the observations in absolute units (i.e. for H units of W m^{-2}). The second measurement chosen is fractional bias (FB) and fractional error (FE). Equations for the performance metrics are:

$$MB = \frac{1}{N}\sum_{i=1}^{N}(Cm - Co) \qquad ME = \frac{1}{N}\sum_{i=1}^{N}|Cm - Co| \tag{2}$$

$$FB = \frac{1}{N}\sum_{i=1}^{N}\frac{(Cm - Co)}{\left(\frac{Co + Cm}{2}\right)} \qquad FE = \frac{1}{N}\sum_{i=1}^{N}\frac{|Cm - Co|}{\left(\frac{Co + Cm}{2}\right)} \tag{3}$$

where Co is magnitude of the observation and Cm is the modeled or predicted magnitude. Table 4.5 summarizes the performance statistics for each year for LE, H, and isoprene fluxes. In general the isoprene estimates are fairly good for both models, with the FE for WSU-BEIS ranging between 38% and 57%, and the FE for BEIS3 ranging between 32% and 66%. The bottom of table 4.5 lists the performance statistics using the annual correlation factors for the isoprene vs. LE regression. As seen in the table, WSU-BEIS

and BEIS3 do a better job of predicting isoprene emissions than the simple LE surrogate, but for some years the estimate using the correlation factors are certainly within the current range of model uncertainty. Within a particular year, there are also day-to-day variations in model performance. For example, for the first 5 days shown in 2001, WSU-BEIS agrees well with observations, and BEIS3 under-predicts isoprene emissions. After the long rain event, BEIS3 matches observations better than WSU-BEIS. The timing or occurrence of rain events, as previously shown, affects the amount of water stress the canopy experiences, the LE fluxes, and the isoprene emissions.

The WSU-BEIS model was developed in order to estimate isoprene flux and the associated energy fluxes as a basis for improving the way biogenic emissions are modeled and to provide a basis for incorporation of biogenic emissions into meteorological land-surface models. Figures 4.8 and 4.9 show the comparison between measured and predicted H and LE fluxes for the same 12-day period shown in Figure 4.7. Considering this is still a simple-canopy model (in other words it does not include photosynthesis/transpiration feedbacks), the results were positive. As seen in Table 4.5, WSU-BEIS typically underestimates LE (FB averaged –31% over all three years) and over predicts H, in particular for 2002 with the FB for H over 100%. The overestimation of H helps to explain the overestimated isoprene fluxes, in particular in 2002. In the two previous years, days with good agreement between measured and modeled H typically have good agreement between measured and modeled (WSU-BEIS) isoprene fluxes.

4.6.3. Modeled Flux Correlations

Daily and seasonal correlations were quantified between the predicted isoprene fluxes and the predicted energy fluxes. For direct comparison with the measurement correlations (Table 4.2), only days 175-250 (end of June to early September) were

calculated for the daily correlations, and the same 44-day periods were selected for the seasonal correlations (Table 4.4). On the one hand the average daily slopes between the predicted isoprene fluxes and LE were very similar to the values calculated from the measurements for each year. The average daily slopes between the predicted isoprene fluxes and H, on the other hand, were significantly less than those from the measurements. This agrees with the results previously presented in which H was consistently overestimated by WSU-BEIS while the predicted fluxes of LE matched the observations better. Table 4.6 summarizes the average slopes determined from the daily linear regressions of estimated isoprene flux vs. estimated H or LE. Seasonal correlations were determined from the linear regression of the ensemble diurnal average of predicted isoprene flux vs. predicted H or LE. Results (data not shown) were similar to the daily correlations in that the predicted isoprene vs. LE slope was consistent with measurements, but the predicted isoprene vs. H slope was approximately 50% less than the slope calculated using observations.

4.7. Conclusions

A long-term record of eddy covariance isoprene flux measurements was obtained from a hardwood forest in northern lower Michigan. Strong linear correlations between isoprene fluxes and energy fluxes, in particular H and LE, were observed in the data. The biosphere-atmosphere exchange of energy is driven by environmental parameters that also drive isoprene emissions (e.g., temperature and radiation), and likewise canopy dynamics also affect both energy and isoprene fluxes (e.g., turbulence and the atmospheric boundary layer). The results from this study indicate that there is a strong

link between isoprene emissions and energy fluxes, in particular latent heat fluxes. On a day-to-day basis, as sensible and latent heat fluxes increase, isoprene fluxes increase and there is a positive, linear correlation between them. The magnitude of the slope of isoprene flux vs. energy flux varies from one day to the next. Some of the variation can be explained by comparing the magnitude of the slope with changes in soil moisture. More specifically, under drought conditions, low soil moisture suppresses latent heat flux and reduces the evaporative cooling capabilities of the leaf/canopy. In turn, this results in increased leaf temperatures and increased isoprene emissions. Thus, the magnitude of the daily slope between isoprene flux and latent heat flux is greater when soil moisture is reduced. We hypothesize that the reduced soil moisture and reduced LE fluxes in combination with increased isoprene fluxes explains some of the day-to-day variation in the daily slopes between isoprene fluxes and latent heat fluxes. Links between isoprene emissions and LE fluxes such as this indicate that LE in particular may be a valuable surrogate for modeling isoprene fluxes. The daily rise and fall of latent heat flux mimics the rise and fall of isoprene flux, and the magnitude of the maximum daily latent heat flux is an indicator of water availability and thus, latent heat fluxes also capture the effects of water stress on isoprene emission levels.

Correlations were quantified by performing a linear regression between midday isoprene fluxes and either H or LE. Average daily slopes between isoprene fluxes and the associated energy fluxes varied between 0.016 and 0.026 with correlation coefficients (R^2) that averaged 0.82 for isoprene flux vs. H and 0.77 for isoprene flux vs. LE. Isoprene fluxes appear to be linked more directly with LE fluxes, as is evident in the correlation coefficients for seasonally averaged fluxes. During 2000, there was significantly less rainfall than 2001 or 2002, and as a result of this LE fluxes for 2000

were suppressed during the midday periods, and isoprene fluxes were 1.5 times greater compared to the other years.

The last objective for this research was to determine if the observed daily correlations could be used to evaluate and improve current isoprene emission models. BEIS3, the current EPA biogenic emission model, was run using observational 30-minute meteorological data and detailed biomass data collected from the site. A second model, WSU-BEIS, was developed to directly compare estimated energy fluxes with observational fluxes, and evaluate how well our energy fluxes compare during different isoprene flux conditions. The fractional error for both models averaged 45% (for all three years) and the average fractional bias was 40% for WSU-BEIS and 14% for BEIS3. In addition to isoprene emissions, H and LE fluxes were compared between modeled (WSU-BEIS) and observed. With predicted H and LE fluxes, the overall performance of the canopy model can be evaluated in order to gauge if isoprene emissions are accurately estimated. For example, in years where H fluxes are over-estimated, the corresponding isoprene fluxes are also over-estimated. Overall if a canopy model predicts accurate H and LE fluxes, then isoprene fluxes in general match observations better. Applying the annual average correlation between isoprene emissions and LE fluxes to the observed LE fluxes yielded estimated isoprene emissions with fractional errors of 80%, 49% and 36% for 2000-2002 respectively. Fractional bias for the simple LE surrogate estimate of isoprene was 65%, 19%, and 14% for years 2000-2002 respectively. Combining all three years yields a fractional error (55%) slightly greater than the fractional error (45%) for both the WSU-BEIS and the BEIS3 models. Future work will determine if different ecosystems have similar slopes between isoprene flux and associated energy fluxes, and if so, then reasonable estimates of isoprene emissions may be possible given surface

energy fluxes. It is recommended that future biogenic emission models incorporate energy flux estimates in order to improve our understanding of the relationship between the biosphere-atmosphere exchange of energy and mass.

4.8. Acknowledgements

This research is part of the PROPHET and UMBS~Flux programs at the University of Michigan Biological Station. The authors wish to thank the National Science Foundation (NSF) for funding the research, and both the PROPHET and UMBS~Flux teams for their expertise and the use of their tower and laboratory facilities. The NSF Integrated Graduate Education Research Training (IGERT) program administered by Western Michigan University and entitled Biosphere Atmosphere Research Training (BART); and the NSF Research Experience for Undergraduates (REU) Program provided support for this research. Support was also provided through a Boeing endowment to Washington State University.

The UMBS~Flux research was supported by the Office of Science (BER) Program, U.S. Department of Energy (DOE), and through its Midwest Regional Center of the National Institute for Global Environmental Change (NIGEC) under Cooperative Agreement No. DE-FC03-90ER61010. Any opinions, findings, and conclusions or recommendations expressed in this publication are those of the authors and do not necessarily reflect the views of the DOE.

4.9. References

Atkinson, R. 2000. Atmospheric chemistry of VOCs and NOx. *Atmospheric Environment* 34, 2063-2101.

Auble, D. L. and Meyers, T. P. 1992. An open path, fast response infrared absorption gas analyzer for H2O and CO2. *Boundary-Layer Meteorology* 59, 243-256.

Bowling, D. R., Turnipseed, A. A., Delany, A. C., Baldocchi, D. D., Greenberg, J. P., Monson, R. K. 1998. The use of relaxed eddy accumulation to measure biosphere- atmosphere exchange of isoprene and other biological trace gases. *Oecologia* 116, 306-315.

Campbell G. S., and Norman J. M. 1998. *An Introduction to Environmental Biophysics*. New York: Springer.

Carroll, M. A., Bertman, S. B., Shepson, P. B. 2001. Overview of the program for research on Oxidants: PHotochemistry, Emissions, and Transport (PROPHET) summer 1998 measurements intensive. *Journal of Geophysical Research* 106, 24275-24288.

Curtis, P. S., Hanson, P. J., Bolstad, P., Barford, C., Randolph, J. C., Schmid, H. P., Wilson, K. B. 2002. Biometric and eddy-covariance based estimates of annual carbon storage in five eastern North American deciduous forests. *Agricultural and Forest Meteorology* 113, 3-19.

Fall, R. and Monson, R. 1992. Isoprene emission rate and intercellular isoprene concentration as influenced by stomatal distribution and conductance. *Plant Physiology* 100, 987-992.

Fang, C., Monson, R. K., Cowling, E. B. 1996. Isoprene emissions, photosynthesis, and growth in sweetgum (Liquidambar styraciflua) seedlings exposed to short- and long-term drying cycles. *Tree Physiology* 16, 441-446.

Fehsenfeld, F., Calvert, J., Fall, R., Goldan, P., Guenther, A., Hewitt, C. N. 1992. Emissions of volatile organic compounds from vegetation and the implications for atmospheric chemistry. *Global Biogeochemical Cycles* 6, 389-430.

Fuentes, J. D., Wang, D., Gu, L. 1999. Seasonal variations in isoprene emissions from a Boreal Aspen forest. *Journal of Applied Meteorology* 38, 855-869.

Geron, C. D., Guenther, A. B., Pierce, T. E. 1994. An Improved model for estimating emissions of volatile organic compounds from forests in the eastern United-States. *Journal of Geophysical Research* 99, 12773-12791.

Geron, C. D., Nie, D., Arnts, R. R., Sharkey, T. D., Singsaas, E. L., Vanderveer, P. J., Guenther, A., Sickles, J. E., Kleindienst, T. E. 1997. Biogenic isoprene emission: model evaluation in a southeastern United States bottomland deciduous forest. *Journal of Geophysical Research* 102, 18889-18901.

Goldstein, A. H., Goulden, M. L., Munger, J. W., Wofsy, S. C., Geron, C. D. 1998. Seasonal course of isoprene emissions from a midlatitude deciduous forest.

Journal of Geophysical Research 103, 31045-31056.

Guenther, A., Archer, S., Greenberg, J., Harley, P., Helmig, D., Klinger, L., Vierling, L., Wildermuth, M., Zimmerman, P., Zitzer, S. 1999. Biogenic Hydrocarbon Emissions and Landcover/Climate Change in a Subtropical Savanna. *Physics and Chemistry of the Earth Part B-Hydrology Oceans and Atmosphere* 24, 659-667.

Guenther, A., Geron, C., Pierce, T., Lamb, B., Harley, P., Fall, R. 2000. Natural emissions of non-methane volatile organic compounds; carbon monoxide, and oxides of nitrogen from North America. *Atmospheric Environment* 34, 2205-2230.

Guenther, A. B., Zimmerman, P. R., Harley, P. C., Monson, R. K., Fall, R. 1993. Isoprene and monoterpene emission rate variability - model evaluations and sensitivity analyses. *Journal of Geophysical Research* 98, 12609-12617.

Guenther, A. B. and Hills, A. J. 1998. Eddy covariance measurement of isoprene fluxes. *Journal of Geophysical Research* 103, 13145-13152.

Hills, A. J. and Zimmerman, P. R. 1990. Isoprene measurement by ozone-induced chemiluminescence. *Analytical Chemistry* 62, 1055-1060.

Hsieh, C.-I., Katul, G., Chi, T. 2000. An approximate analytical model for footprint estimation of scalar fluxes in thermally stratified atmospheric flows. *Advances in Water Resources* 23, 765-772.

Isebrands, J. G., Guenther, A. B., Harley, P., Helmig, D., Klinger, L., Vierling, L., Zimmerman, P., Geron, C. 1999. Volatile organic compound emission rates from mixed deciduous and coniferous forests in Northern Wisconsin, USA. *Atmospheric Environment* 33, 2527-2536.

Kinnee, E., Geron, C., Pierce, T. 1997. United States land use inventory for estimating biogenic ozone precursor emissions. *Ecological Applications* 7, 46-58.

Kuhn, U., Rottenberger, S., Biesenthal, T., Wolf, A., Schebeske, G., Ciccioli, P., Brancaleoni, E., Frattoni, M., Tavares, T. M., Kesselmeier, J. 2002. Isoprene and monoterpene emissions of Amazonian tree species during the wet season:direct and indirect investigations on controlling environmental functions. *Journal of Geophysical Research* 107, art. no.-8071.

Lamb, B., Gay, D., Westberg, H., Pierce, T. 1993. A Biogenic hydrocarbon emission inventory for the USA using a simple forest canopy model. *Atmospheric Environment* 27, 1673-1690.

Lamb, B., Pierce, T., Baldocchi, D., Allwine, E., Dilts, S., Westberg, H., Geron, C., Guenther, A., Klinger, L., Harley, P., Zimmerman, P. 1996. Evaluation of forest canopy models for estimating isoprene emissions. *Journal of Geophysical Research* 101, 22787-22797.

Lamb, B., Westberg, H., Allwine, E., Quarles, T. 1985. Biogenic Hydrocarbon

Emissions from Deciduous and Coniferous Trees in the United States. *Journal of Geophysical Research* 90, 2380-2390.

Massman, W. J. 2000. A simple method for estimating frequency response corrections for eddy covariance systems. *Agricultural and Forest Meteorology* 104, 185-198.

Monson, R. and Fall, R. 1989. Isoprene emission from Aspen leaves: Influence of environment and relation to photosynthesis and photorespiration. *Plant Physiology* 90, 267-274.

Monson, R. K. and Holland, E. A. 2001. Biospheric trace gas fluxes and their control over tropospheric chemistry. *Annual Review of Ecology and Systematics* 32, 547-576.

Niinemets, U. and Reichstein, M. 2003. Controls on the emission of plant volatiles through stomata: differential sensitivity of emission rates to stomatal closure explained. *Journal of Geophysical Research* 108, art. no.-4208.

Pierce, T., Geron, C., Pouliot, G., Kinnee, E., and Vukovich, J. 2002. Integration of the Biogenic Emissions Inventory System (BEIS3) into the Community Multiscale Air Quality modeling system.

Poisson, N., Kanakidou, M., Crutzen, P. J. 2000. Impact of non-methane hydrocarbons on tropospheric chemistry and the oxidizing power of the global troposphere: 3-dimensional modelling results. *Journal of Atmospheric Chemistry* 36, 157-230.

Pressley, S. N., Lamb, B. K., Westberg, H., Hatten, G., Flaherty, J., Vogel, C. S. Long term isoprene flux measurements above a northern hardwood forest, *submitted to Journal of Geophysical Research.*

Schmid, H. P., Su, H.-B., Vogel, C. S., Curtis, P. S. 2003. Ecosystem-atmosphere exchange of carbon dioxide over a mixed hardwood forest in northern lower Michigan. *Journal of Geophysical Research* 108, art. no.-4417.

Tingey, D. T., Evans, R., Gumpertz, M. 1981. Effects of environmental conditions on isoprene emission from live oak. *Planta* 152, 565-570.

Webb, E. K., Pearman, G. J., Leuning, R. 1980. Correction of flux measurements for density effects due to heat and water vapor transfer. *Quarterly J. R. Meteorological Society* 106, 85-100.

Westberg, H., Lamb, B., Hafer, R., Hills, A., Shepson, P., Vogel, C. 2001. Measurement of isoprene fluxes at the PROPHET site. *Journal of Geophysical Research* 106, 24347-24358.

Wilson, K. B., Baldocchi, D., Falge, E., Aubinet, M., Berbigier, P., Bernhofer, C., Dolman, H., Field, C., Goldstein, A., Granier, A., Hollinger, D., Katul, G., Law, B. E., Meyers, T., Moncrieff, J., Monson, R., Tenhunen, J., Valentini, R., Verma, S., Wofsy, S. 2003. Diurnal centroid of ecosystem energy and carbon fluxes at FLUXNET sites. *Journal of Geophysical Research* 108, 4664.

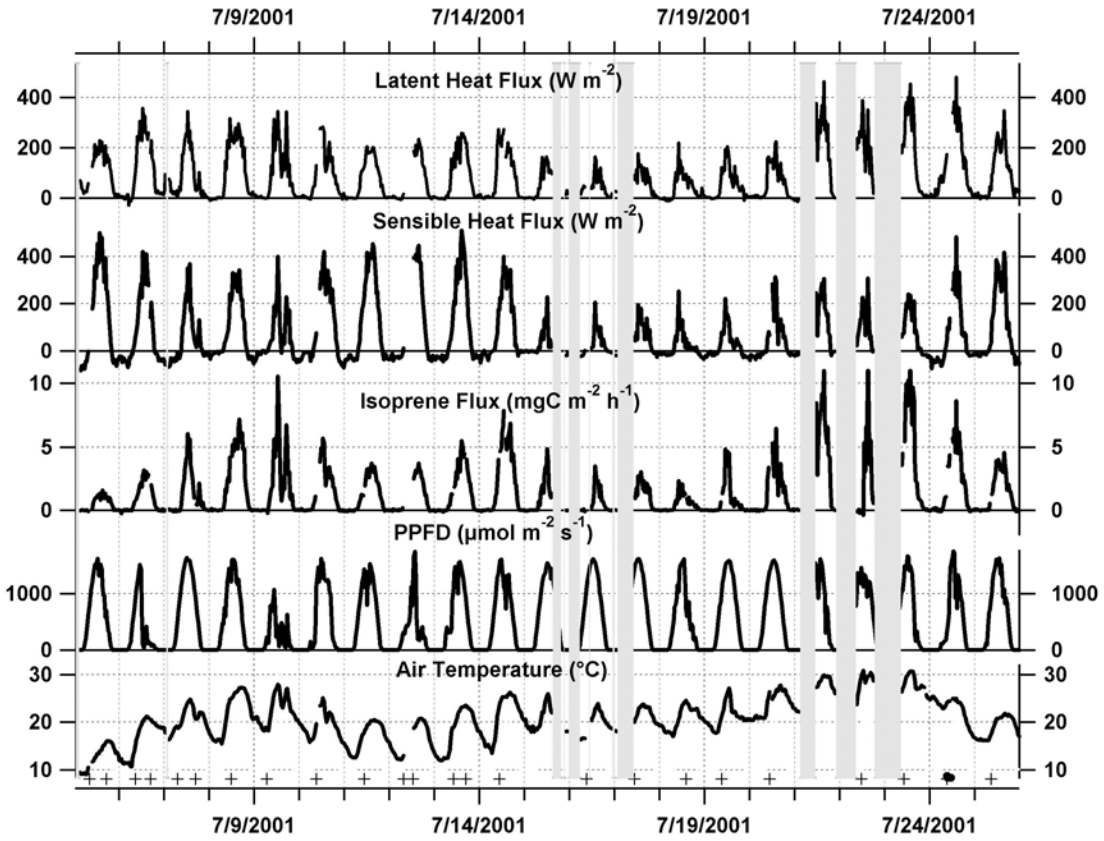

Figure 4.1: Continuous 30-minute averaged latent heat flux (W m^{-2}), sensible heat flux (W m^{-2}), isoprene flux (mgC m^{-2} h^{-1}), PPFD (µmol m^{-2} s^{-1}), and air temperature (ºC) for July 2001. Shaded vertical gray bars indicate rain events, plus symbols (+) indicate FIS calibrations, and dots (•) indicate instrumentation problems.

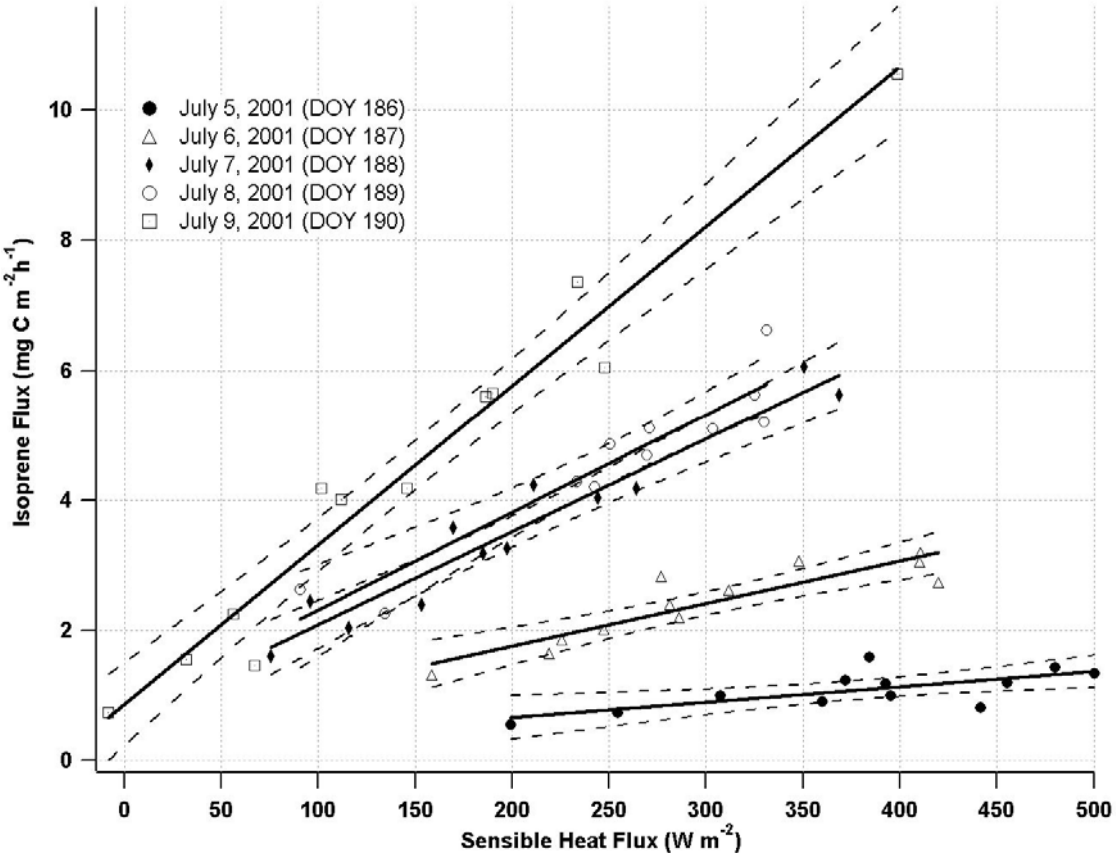

Figure 4.2: Isoprene flux (mg C m^{-2} h^{-1}) plotted against the corresponding 30-minute average sensible heat flux (W m^{-2}) for 5 typical days in early July 2001. Fluxes between 10:00 and 4:00 are shown by markers, the linear regression best fit line is indicated with a solid line, and the 95% confidence bounds are indicated by dashed lines. Days 188 and 189 have non-statistically different slopes, but all other days have significantly different slopes.

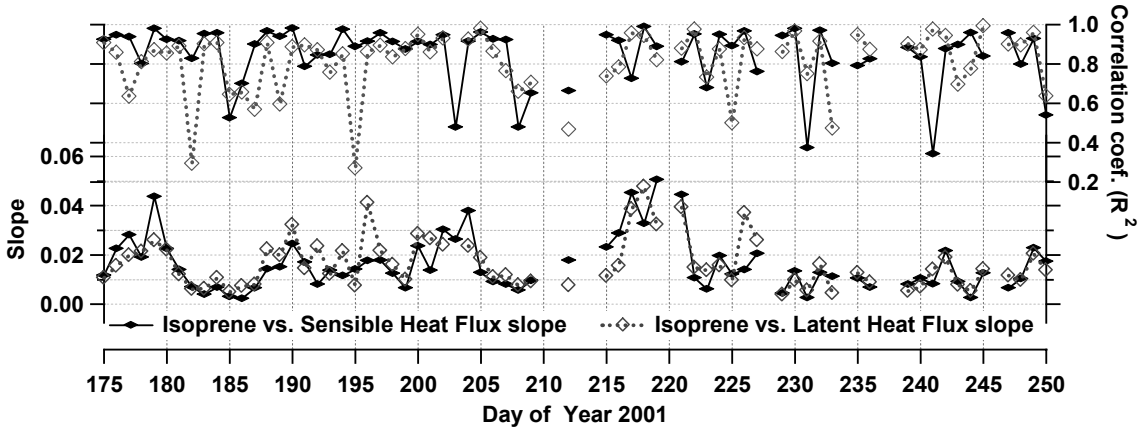

Figure 4.3: Linear regression coefficient (slope) and correlation coefficient (R^2) for eddy covariance isoprene flux vs. sensible hear flux (solid black line) and isoprene flux vs. latent heat flux (dashed gray line) for June 24 (day of year (DOY) 175) through Sept. 7 (DOY 250), 2001.

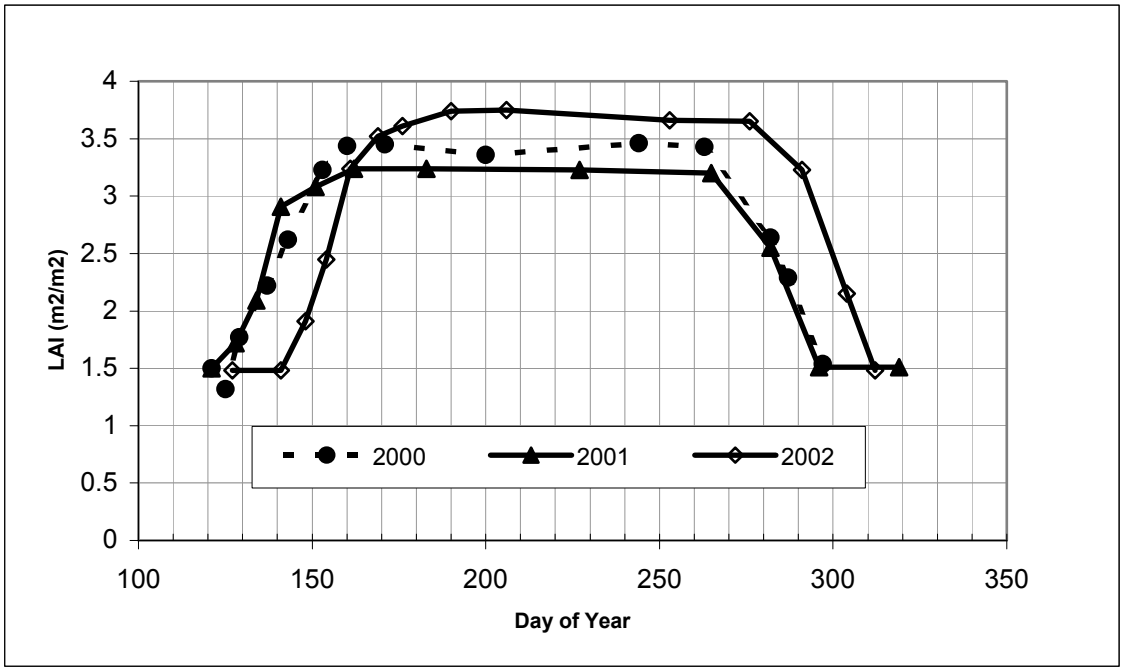

Figure 4.4: Seasonal Leaf Area Index (LAI) for the 60-m plot surrounding the UMBS~Flux tower for years 2000-2002.

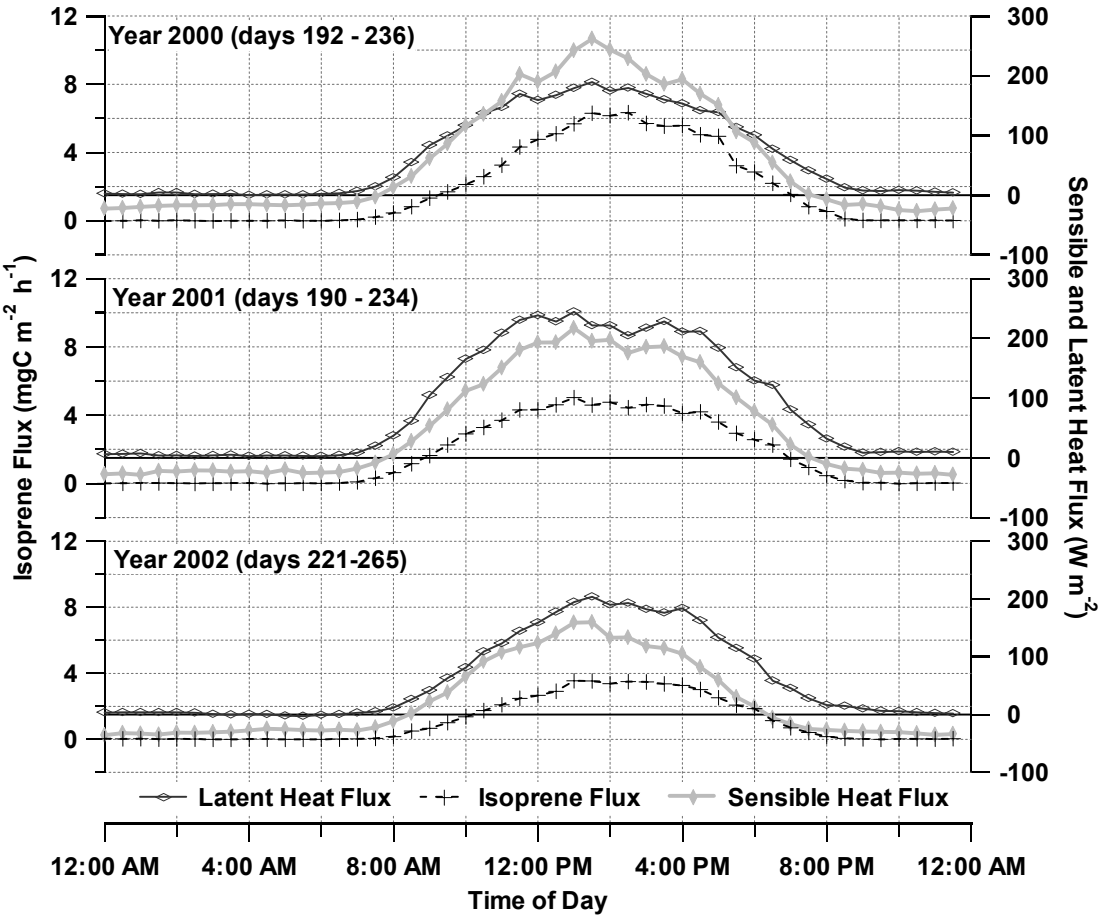

Figure 4.5: Diurnal average of sensible (filled vertical diamonds, gray), latent (open horizontal diamonds, black), and isoprene flux (cross marks, dashed line) for 2000-2002.

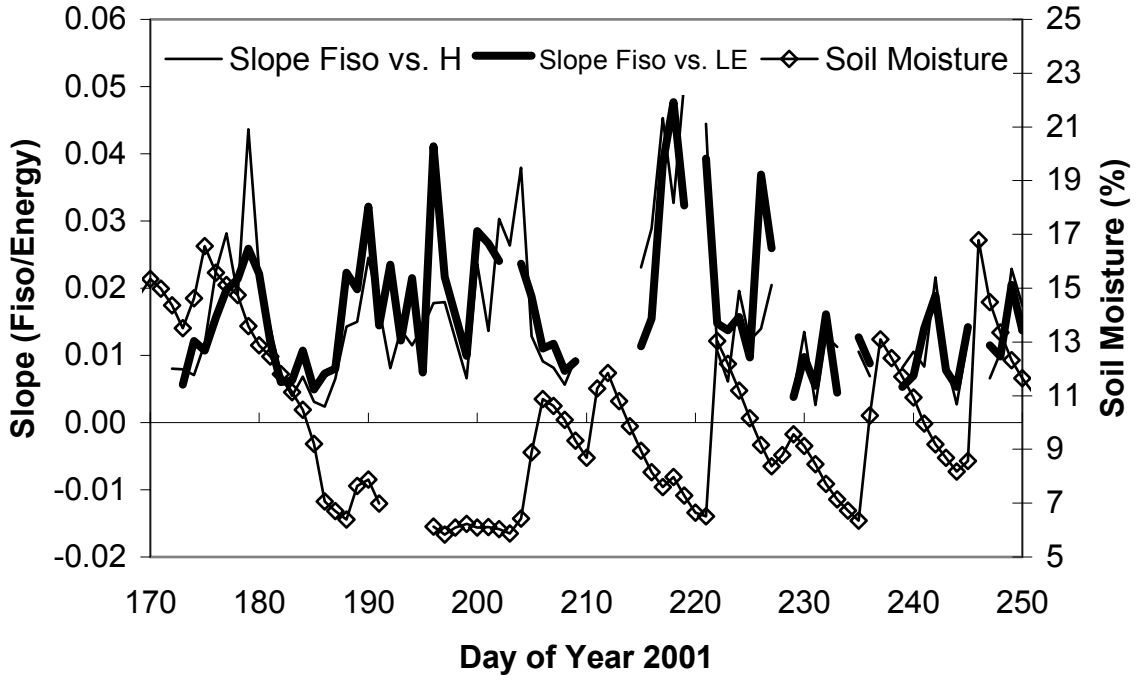

Figure 4.6: Daily average correlation between isoprene flux (Fiso) and H (solid line), and Fiso and LE (thick line) and daily average soil moisture (solid line with diamonds) plotted with a one-week lag time for DOY 170 (June 19) through 250 (Sept. 7), 2001. Decreased soil moisture results in decreased stomatal conductance thus increasing leaf temperature and resulting in a larger Fiso vs. LE slope (higher isoprene emissions with lower LE).

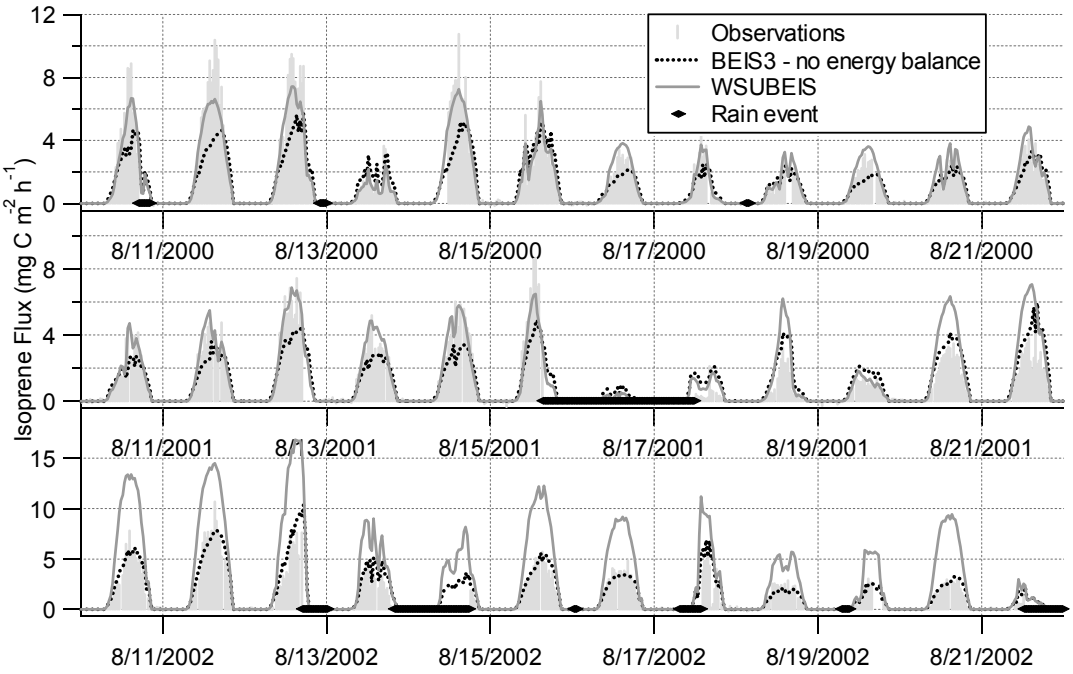

Figure 4.7: Model results using BEIS3 (dashed black line) and WSU-BEIS (solid gray line) and eddy covariance isoprene flux measurements (gray vertical sticks). Fluxes presented in mgC m^{-2} h^{-1} on a 30-minute averaged basis, rain events indicated by black dots on x-axis.

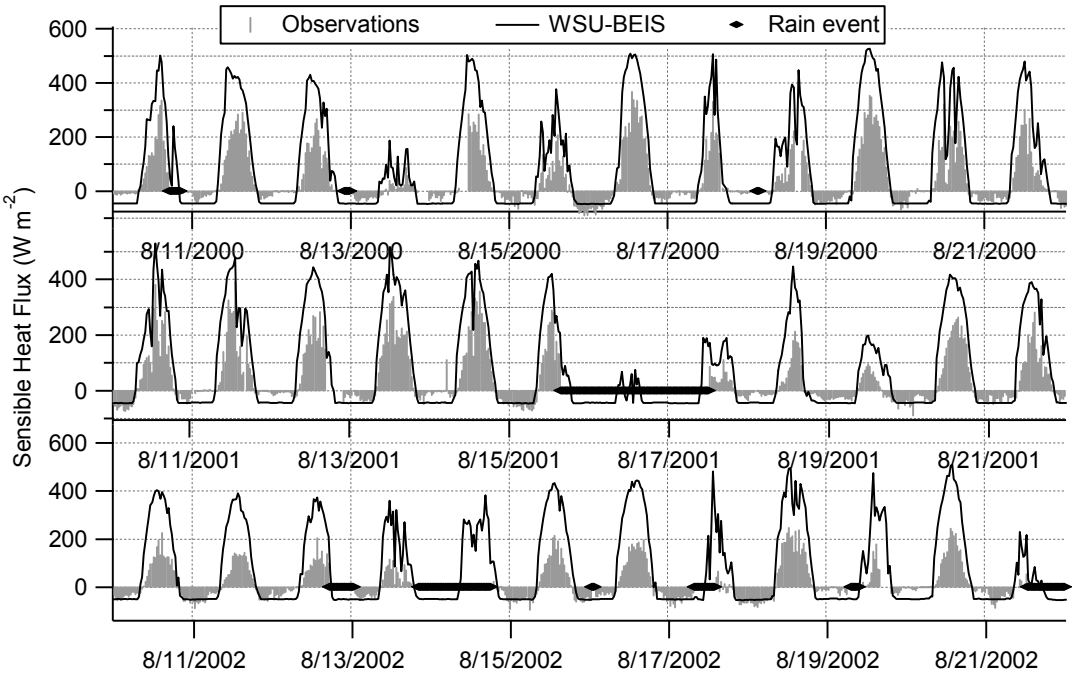

Figure 4.8: Model results (solid black line) from WSU-BEIS for H compared to observations (light gray shaded). Fluxes presented in W m^{-2} on a 30-minute averaged basis, rain events indicated by black dots on the x-axis.

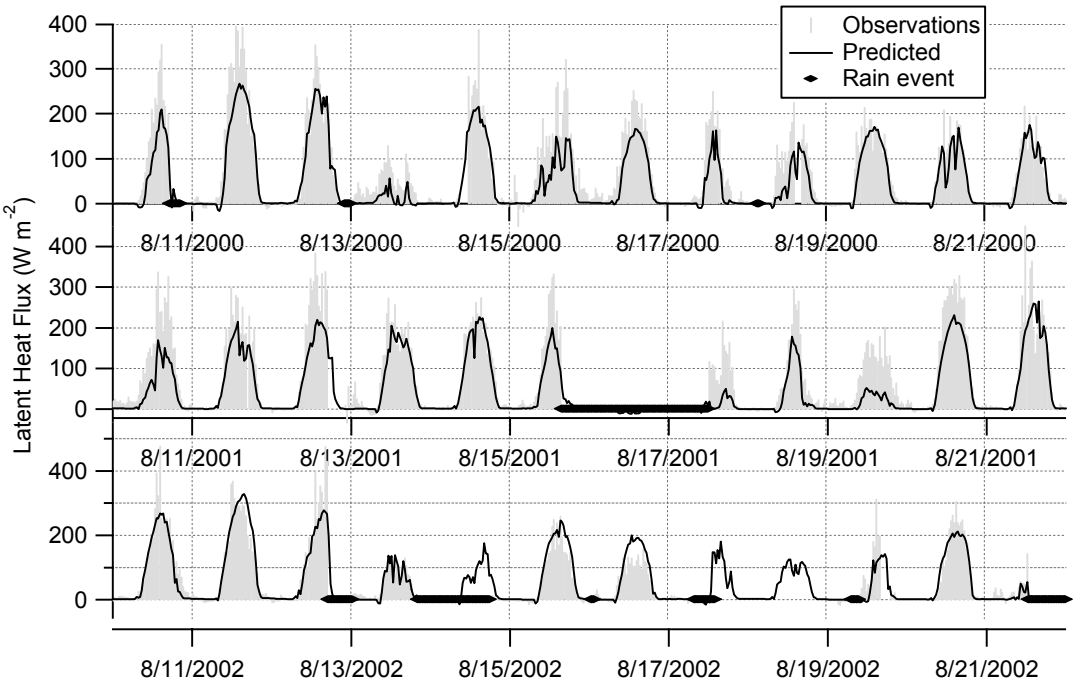

Figure 4.9: Model results (solid black line) from WSU-BEIS for LE compared to observations (light gray shaded). Fluxes presented in W m^{-2} on a 30-minute averaged basis, rain events indicated by black dots on the x-axis.

Table 4.1: Linear regression results for isoprene flux vs. sensible heat flux (H) and isoprene flux vs. latent heat flux (LE) for days in 2001. Slope ± 95% confidence interval, the correlation coefficient (r^2), and the number (n) of 30-minute averaged flux observations used for each day between 10:00 and 4:00.

	Isoprene vs. H		Isoprene vs. LE	
	Slope (± 95%)	R^2 (n)	Slope (± 95%)	R^2 (n)
July 5 (186)	0.002 (0.002)	0.70 (12)	0.007 (0.006)	0.66 (12)
July 6 (187)	0.007 (0.002)	0.90 (12)	0.008 (0.008)	0.57 (12)
July 7 (188)	0.014 (0.003)	0.97 (12)	0.022 (0.007)	0.91 (12)
July 8 (189)	0.015 (0.004)	0.94 (11)	0.020 (0.020)	0.59 (11)
July 9 (190)	0.024 (0.004)	0.98 (12)	0.032 (0.012)	0.89 (12)
July 10 (191)	0.017 (0.011)	0.79 (10)	0.014 (0.006)	0.90 (10)
July 11 (192)	0.008 (0.004)	0.84 (11)	0.023 (0.01)	0.87 (11)
July 12 (193)	0.014 (0.012)	0.85 (6)	0.012 (0.015)	0.76 (6)
July 13 (194)	0.012 (0.002)	0.98 (11)	0.021 (0.010)	0.85 (11)
July 14 (195)	0.014 (0.006)	0.89 (10)	0.007 (0.022)	0.27 (10)
July 15 (196)	0.018 (0.006)	0.91 (10)	0.041 (0.020)	0.86 (10)

Table 4.2: Average slope determined from the daily linear regressions of isoprene flux vs. H or LE over the period from day of year 175-250 (end of June to early September). Also listed are the standard deviation, the number of days when there was sufficient data, the range of the slope (minimum and maximum), and the average of the daily correlation coefficients (R^2).

	2000 F_{iso} vs H	2001 F_{iso} vs H	2002 F_{iso} vs H	2000 F_{iso} vs LE	2001 F_{iso} vs LE	2002 F_{iso} vs LE
Average R^2	0.82	0.84	0.80	0.71	0.81	0.79
Average slope	0.020	0.015	0.022	0.026	0.016	0.016
St. Deviation	0.013	0.010	0.015	0.022	0.010	0.009
Day count (n)	57	79	63	57	65	35
Minimum	0.001	0.002	0.002	0.002	0.004	0.007
Maximum	0.057	0.051	0.077	0.110	0.048	0.045

Table 4.3: Summary of climatic and biological variations between the three measurement years. Dates plus day of year (DOY) presented in parentheses, NA indicates data not available. With the exception of isoprene emission data, all data were provided by the UMBS~Flux group.

	2000	2001	2002
Last Frost (last day of season where 21m Temperature < 0.5°C)	April 19 (110) [-0.82°C]	April 18 (108) [-1.64°C]	May 18 (138) [-1.4°C]
red oak			
Bud Break	May 8 (129)	May 3 (123)	May 22 (142)
Full Leaf out (> 90%)	June 1 (153)	May 22 (142)	June 11 (162)
bigtooth aspen			
Bud Break	May 8 (129)	May 8 (128)	June 5 (156)
Full Leaf out (> 90%)	June 1 (153)	May 22 (142)	June 18 (169)
quaking aspen			
Bud Break	May 8 (129)	May 8 (128)	NA
Full Leaf out (> 90%)	May 16 (137)	May 15 (135)	
Onset of Isoprene Emissions			
Earliest detection	May 31 (152)	NA	June 9 (160)
Fully developed emissions	June 6 (158)		June 13 (164)
Isoprene delay after last frost (days)	42	NA	22
Biomass Density (total foliage) (g foliar biomass m^{-2})	331	299	304
LAI (mid-summer maximum) (m^2 m^{-2})	3.46	3.24	3.75
Mid-summer period with constant LAI and length of constant LAI growing season (number of days)	June 8 (160) – Sept. 19 (263) [103 days]	June 11 (162) – Sept. 22 (265) [103 days]	June 25 (176) –Oct. 3 (276) [100 days]
Ensemble average (midday) temperature for 44 days beginning 82 days after last frost (°C)	21.3	23.7	22.3
Ensemble average (midday) PPFD for 44 days beginning 82 days after last frost (μmol m^{-2} s^{-1})	1077	1019	879
Cumulative rain for days 160-280 (mm)	194	288	230

Table 4.4: Slope and correlation coefficient (R^2) determined from the linear regression of the ensemble diurnal average of isoprene flux vs. sensible heat flux or latent heat flux. A span of 44 days was selected starting 82 days after last frost for each year. Start date for each year was DOY 192, 190, and 221 for 2000, 2001, and 2002 respectively.

	Slope of isoprene flux vs. latent heat flux	Correl. coef R^2	Slope of isoprene flux vs. sensible heat flux	Correl. coef R^2
2000	0.032	0.94	0.023	0.96
2001	0.020	0.99	0.021	0.99
2002	0.018	0.99	0.019	0.92

Table 4.5: Performance Statistics for measured vs. modeled LE, H, isoprene (using WSU-BEIS model), isoprene (using BEIS3 model) and in the bottom row, isoprene estimated using the annual average correlation between isoprene and LE (listed in Table 4). Units for mean bias and mean error are W m^{-2} for LE and H, and mgC m^{-2} h^{-1} for WSU-BEIS and BEIS3. Model statistics were calculated using mid-day periods (10:00 am – 4:00 pm) and 44-day period beginning on DOY 192 (2000), 190 (2001) and 221 (2002).

	LE 2000	LE 2001	LE 2002
Mean bias	-32.1	-56.5	-32.8
Mean error	57.4	86.2	58.4
Fractional bias	-36.9%	-27.3%	-29.0%
Fractional error	53.0%	52.6%	47.8%

	H 2000	H 2001	H 2002
Mean bias	139.3	144.3	196.3
Mean error	141.7	145.7	196.3
Fractional bias	58.4%	62.3%	111.4%
Fractional error	57.6%	63.1%	111.4%

	Isoprene WSU-BEIS 2000	Isoprene WSU-BEIS 2001	Isoprene WSU-BEIS 2002
Mean bias	0.19	1.67	1.22
Mean error	1.50	1.92	1.32
Fractional bias	36.9%	41.0%	33.5%
Fractional error	56.8%	44.2%	38.4%

	Isoprene BEIS3 2000	Isoprene BEIS3 2001	Isoprene BEIS3 2002
Mean bias	-0.98	0.13	0.53
Mean error	1.86	1.18	0.95
Fractional bias	11.9%	12.5%	17.9%
Fractional error	66.3%	33.9%	31.9%

	Isoprene LE correl. 2000	Isoprene LE correl. 2001	Isoprene LE correl. 2002
Mean bias	1.50	0.47	0.34
Mean error	2.67	1.64	0.98
Fractional bias	64.7%	18.6%	14.3%
Fractional error	79.9%	49.2%	36.4%

Table 4.6: Average slope determined from the daily linear regression of estimated isoprene flux vs. estimated H or LE over the period from day of year 175-250 (end of June to early September). Also listed are the standard deviation, the number of days where there was sufficient data, the range of the slope (minimum and maximum), and the average correlation coefficient (R^2).

	2000 WSU-BEIS F_{iso} vs H	2001 WSU-BEIS F_{iso} vs H	2002 WSU-BEIS F_{iso} vs H	2000 WSU-BEIS F_{iso} vs LE	2001 WSU-BEIS F_{iso} vs LE	2002 WSU-BEIS F_{iso} vs LE
Average R^2	0.65	0.65	0.65	0.92	0.93	0.93
Average slope[a]	0.011	0.009	0.009	0.031	0.021	0.018
St. Deviation	0.005	0.004	0.004	0.004	0.002	0.002
Day count (n)	74	72	76	74	74	74
Minimum	~0	~0	~0	0.004	0.006	0.009
Maximum	0.035	0.031	0.033	0.048	0.036	0.027

Notes: [a] Only considered positive correlations

CHAPTER 5

SUMMARY AND CONCLUSIONS

5.1. Summary

The work presented here begins with a description of the importance of biogenics, some of the primary chemical reactions that involve biogenic emissions, a summary of previous isoprene emission work, and a description of the micrometeorological eddy covariance technique and its underlying theory. Following that is a detailed account of the site where measurements were made, and each step involved in acquiring and processing the flux data. Results of the fieldwork and scientific conclusions are presented in the third and fourth chapters, both of which are stand-alone manuscripts that have been submitted to journals for publication.

The first manuscript entitled "Long term isoprene flux measurements above a northern hardwood forest", presents results of the eddy covariance isoprene flux measurements. These data provide one of the longest records of isoprene emissions from any ecosystem, and they provide an invaluable record for studying long-term controls over isoprene emissions. The primary objective for this manuscript was to present the long-term isoprene flux measurements along with the biosphere-atmosphere exchange of energy (momentum, sensible heat, and latent heat flux) and CO_2. Discussions regarding the eddy covariance technique and the inherent uncertainties are presented, along with a brief description of the daily and annual isoprene flux observations. The response of isoprene to temperature, light, and phenology is presented, and the performance of the current U.S. Environmental Protection Agency (USEPA) biogenic emission model is evaluated for isoprene emissions at this site. Because observations of isoprene differ

from the models, and there is variability in isoprene fluxes that cannot be explained with current biogenic emission models, long-term observations may help us to better understand the dynamics of these differences.

Results showed significant variation of isoprene fluxes from one 30-minute period to the next (in some cases by a factor of 5), and from one day to the next. Average midday isoprene fluxes were fairly consistent across each year, 2.8, 3.2, and 2.9 mg C m^{-2} h^{-1} for 2000 through 2002 respectively, and the sum of accumulated isoprene emissions for each year varied by less than 10%. The warmest and driest year, 2001, had the highest average midday isoprene flux (3.2 mg C m^{-2} h^{-1}), but the largest 30-minute isoprene flux occurred in 2000 (25.5 mg C m^{-2} h^{-1}). Last frost was delayed by roughly one month, and full leaf out was delayed by roughly 2.5 weeks in 2002, compared to the other 3 years. Isoprene emissions were fully developed in 1999 roughly 18 days after full leaf out, but in 2000 and 2002 isoprene emissions were fully developed shortly after leaf out (5 days in 2000) or before full leaf out (2002). The time required to reach fully developed isoprene emissions at this site was roughly half of that required at other sites on the east coast (400-500 heating degree-days vs. 1000 heating degree-days). Lastly, we estimated that isoprene represents between 1.7 to 3.1% of the net carbon uptake at this site.

Based on our analysis of the long-term flux data, we found there is variation from day-to-day that current biogenic emission models cannot completely simulate, and the seasonal onset and decline of isoprene emissions is also an important aspect that current models do not predict well. The use of heating degree days to estimate the onset of emissions may improve model estimates; however, as previously pointed out, the

emissions appear to "turn on" at different times, possibly as a function of ecosystem. Model results again show the strong dependence of isoprene on the environmental drivers (temperature and light), but there are obviously additional environmental parameters that affect isoprene emissions. Continued work in this area will improve our understanding of what drives isoprene emissions. Meanwhile, this long-term isoprene flux dataset will be instrumental for verifying canopy scale models that are used to generate emission inventories for regional photochemical models.

The fourth chapter explores the long-term dataset in a little more depth, and presents an observed correlation between the midday isoprene fluxes and the associated energy fluxes. This manuscript is titled "Relationships among canopy scale energy fluxes and isoprene flux derived from long-term, seasonal eddy covariance measurements over a hardwood forest". Given the similarities of the biosphere drivers for both isoprene and energy fluxes, we hypothesized that correlations between these fluxes could be a useful tool both for testing existing canopy emission models and to guide the development of improved isoprene emission models. Correlations were quantified by performing a linear regression between midday isoprene fluxes and either H or LE. Average daily slopes between isoprene fluxes and the associated energy fluxes varied between 0.016 and 0.026 with correlation coefficients (R^2) that averaged 0.82 for isoprene flux vs. H and 0.77 for isoprene flux vs. LE. Isoprene fluxes appear to be linked more directly with LE fluxes, as is evident in the correlation coefficients for seasonally averaged fluxes. During 2000, there was significantly less rainfall than 2001 or 2002, and as a result of this LE fluxes for 2000 were suppressed during the midday periods, and isoprene fluxes were 1.5 times greater compared to the other years.

On a day-to-day basis, as sensible and latent heat fluxes increase, isoprene fluxes increase and there is a positive, linear correlation between them. The magnitude of the slope of isoprene flux vs. energy flux varies from one day to the next. Some of the variation can be explained by comparing the magnitude of the slope with changes in soil moisture. More specifically, under drought conditions, low soil moisture suppresses latent heat flux and reduces the evaporative cooling capabilities of the leaf/canopy. In turn, this results in increased leaf temperatures and increased isoprene emissions. Thus, the magnitude of the daily slope between isoprene flux and latent heat flux is greater when soil moisture is reduced. We hypothesize that the reduced soil moisture and reduced LE fluxes in combination with increased isoprene fluxes explains some of the day-to-day variation in the daily slopes between isoprene fluxes and latent heat fluxes. Links between isoprene emissions and LE fluxes such as this indicate that LE in particular may be a valuable surrogate for modeling isoprene fluxes. The daily rise and fall of latent heat flux mimics the rise and fall of isoprene flux, and the magnitude of the maximum daily latent heat flux is an indicator of water availability and thus, latent heat fluxes also capture the effects of water stress on isoprene emission levels.

The last objective for this manuscript was to determine if the observed daily correlations could be used to evaluate and improve current isoprene emission models. BEIS3, the current EPA biogenic emission model, was run using observational 30-minute meteorological data and detailed biomass data collected from the site. A second model, WSU-BEIS, was developed to directly compare estimated energy fluxes with observational fluxes, and evaluate how well our energy fluxes compare during different isoprene flux conditions. The primary difference between the two models is the number

of layers within the canopy and the estimate of leaf temperature, which ultimately drives the isoprene emission algorithm. BEIS3 assumes one layer, and leaf temperature is equal to above canopy air temperature. WSU-BEIS uses a 15-layer canopy model and energy balance equations for each layer provide an estimate of the leaf temperature for that layer. The fractional error for both models averaged 45% (for all three years) and the average fractional bias was 40% for WSU-BEIS and 14% for BEIS3. In addition to isoprene emissions, H and LE fluxes were compared between modeled (WSU-BEIS) and observed. With predicted H and LE fluxes, the overall performance of the canopy model can be evaluated in order to gauge if isoprene emissions are accurately estimated. For example, in years where H fluxes are over-estimated, the corresponding isoprene fluxes are also over-estimated. Overall if a canopy model predicts accurate H and LE fluxes, then isoprene fluxes in general match observations better. Applying the annual average correlation between isoprene emissions and LE fluxes to the observed LE fluxes yielded estimated isoprene emissions with fractional errors of 80%, 49% and 36% for 2000-2002 respectively. Fractional bias for the simple LE surrogate estimate of isoprene was 65%, 19%, and 14% for years 2000-2002 respectively. Combining all three years yields a fractional error (55%) slightly greater than the fractional error (45%) for both the WSU-BEIS and the BEIS3 models. Future work will determine if different ecosystems have similar slopes between isoprene flux and associated energy fluxes, and if so, then reasonable estimates of isoprene emissions may be possible given surface energy fluxes. It is recommended that future biogenic emission models incorporate energy flux estimates in order to improve our understanding of the relationship between the biosphere-atmosphere exchange of energy and mass.

5.2. Future Work

Where do we go from here? Currently there is some exciting research being done with some of this data by colleagues at the University of Michigan. Concurrent measurements of O_3, NOx, and possibly NOy are being collected from the same location as the isoprene flux measurements. We know there is a potential for biosphere feedbacks involving pollutants such as O_3 and NOx, and this type of research will enable us to look for correlations between isoprene emissions and pollutants. In addition to the data presented in this dissertation, flux measurements have continued through the growing season of 2004. Thus, there are 2 additional years of flux data that need to be processed and analyzed. Additional data will hopefully strengthen the correlation analysis presented in the second manuscript. In terms of making more measurements in 2005, careful analysis of existing data gaps needs to be done in order to determine if additional measurements should be added to the system. For example, sap flow measurements were suggested as one measurement that would strengthen the correlation analysis between isoprene emissions and reduced soil moisture.

The existing dataset is an invaluable resource for "data mining" or exploring new theories for the cause and effect of isoprene emissions. Some additional questions that probably should be addressed in more detail using this dataset include: 1.) Does historical temperature account for some of the variation in isoprene emissions? 2.) What could explain the reduced heating degree days (compared to other sites) for fully developed isoprene emissions? 3.) Do we see similar slopes between isoprene flux and energy fluxes for additional years (i.e., 2003 and 2004) and at different sites? And lastly, 4.) Are there

any other ecological drivers or environmental parameters that could explain why we see such different slopes from one day to the next?

5.3. Personal Thoughts

After stepping back and looking at the finished product, I'm struck by the amount of work that truly goes into obtaining a dataset of this magnitude. I'm not really referring to my work in particular, but more to those that had the foresight to begin this project and to keep it going year after year, often without any funding. There were, and still are so many people involved in this project, from previous WSU students, to REU students, to staff at UMBS, to the AmeriFlux group, to past, present, and future BART students, and to mentors and advisors from all over the country. Then I think about how many more people will be involved in this project by using the dataset for everything from model evaluation, to exploring isoprene emission characteristics, to ground-truthing satellite measurements. True to the magnitude of the task is also the variety of people that have been involved. This type of research touches on so many different areas, that I truly can say I've experienced a multidisciplinary education. I've been exposed to plant physiology, forest dynamics, atmospheric chemistry, instrumentation, the study of turbulence, canopy models, boundary layer meteorology, and the list keeps going. Thus, one of the lessons I've learned in this adventure is to always communicate your plans, ideas, or problems with as many people as possible; because you never know who just might have the suggestion that makes everything work.

After field campaigns there are always "things that we wish we could have done better...". This work is no exception, and I have a list of things that I wish hadn't have happened. But more importantly, learning from those mistakes, I now have a list of

"things to do better the next time". I think at the top of the list should be "Write it down in the logbook!" Our memories aren't that good, and each year things were a little different. Well, after awhile the years all start to run together. Another one for the list is "Look at the data...I mean really look at the data!". Don't wait until the end of the field campaign to work up the numbers and check the program. Even though you might not have time, do it while you are in the field. And again, share your results with others and get their feedback. Sometimes we are so focused on keeping things running that we have the field blinders on, and the quality of the data isn't good enough…but there's quantity!

One of the most challenging aspects of completing this dissertation has been completing the dissertation. There are so many different methods available for processing eddy covariance data, and there are so many different possible analyses to use with this type of dataset, that it's hard to say you are finished. Thus, in some aspects I feel I have merely scratched the surface with exploring the many facets of this dataset, and there is so much more lurking somewhere in the depths. With every new paper I read, some idea is proposed by the author about the possible relationship between isoprene and situation x, that just begs to be explored with a long-term dataset. The same is true with every biogenic emission model that is developed; "How does it perform against this dataset?" So I know there is still more work to be done, however, I also know it's time for others to explore this dataset.